

Iida Kangashaka

**WAYS TO DECREASE THE EFFECT OF
THERMAL DEGRADATION OF WEEE
PLASTICS DURING MECHANICAL
RECYCLING**

Master's Thesis
Faculty of Engineering and Natural Sciences
University Instructor Ilari Jönkkäri
Associate Professor (tenure track) Essi Sarlin
February 2022

ABSTRACT

Iida Kangashaka

Ways to decrease the effect of thermal degradation of WEEE plastics during mechanical recycling

Tampere University

Master's Programme in Materials Engineering

February 2022

As the world moves towards a more circular economy the recyclability of different materials becomes an increasingly pressing issue. The EU has created a strategy that aims to push the European plastic industry towards circularity, and this also includes significantly increasing the recycling rates of all plastic products. However, some plastic fractions are harder to recycle than others. An example of such a plastic fraction are the plastics in waste electrical and electronic equipment. Part of the reason why this material stream is difficult to recycle are those bromine-containing fire retardants, which are harmful, and which have been used in older electrical and electronic equipment, but are no longer allowed in new products, so they must be removed during recycling. Another problem facing plastic recycling is the degradation that occurs during re-processing, which lowers the plastic's molecular weight.

The ALL-IN for Plastics Recycling project, which this thesis is a part of, aims to help actors in the plastic industry to discover better recycling systems for challenging plastic streams, such as plastics from waste electrical and electronic equipment. This thesis aims to find if the effects of the degradation during processing can be prevented by adding certain additives into the bromine-free plastics from waste electrical and electronic equipment, and if the resulting recycled plastics can be used in new electrical and electronic equipment.

The work begins with a literature review section, where the current state of the waste electrical and electronic equipment plastic recycling is mapped. Additionally, the theory of how the polymers degrade during processing, how it affects the properties, and how the additives can be used to prevent this are discussed. The studied plastics are polypropylene, polystyrene, acrylonitrile-butadiene-styrene, and polycarbonate/acrylonitrile-butadiene-styrene recycled from waste electrical and electronic equipment. The chosen additives are antioxidants, chain extenders, and graphene nanoplatelets grafted with maleic anhydride. The antioxidant products are Irganox 1010 and Irganox 1076, the chain extender products are Joncryl ADR 4400 and Joncryl ADR 4468, and the graphene nanoplatelets grafted with maleic anhydride are produced in the laboratory. The study is done by performing tensile tests and by measuring the viscosity curve with rotational rheometer experiments for the plastics with and without the additives. These results are then compared to the section in the literature review, that explained how the changes in the molecular weight affect the properties to see how well the different additives prevent degradation. Additionally, oxidation induction times are determined for the samples with antioxidants to evaluate their ability to prevent oxidation.

Based on this analysis it seems that the additive type that worked the best at preventing degradation for polypropylene are the antioxidants, the most effective additive for polystyrene are the graphene nanoplatelets grafted with maleic anhydride, and the best additive type for acrylonitrile-butadiene-styrene and polycarbonate/acrylonitrile-butadiene-styrene are the chain extenders. The rheological and mechanical properties seem to be quite a reliable way to assess degradation caused by thermal oxidation in plastics. In addition, the mechanical properties of the recycled plastics are high enough to be used in new electrical and electronic equipment.

Keywords: plastic recycling, WEEE, waste electrical and electronic equipment, thermal oxidation, antioxidant, chain extender, graphene nanoplatelets grafted with maleic anhydride

The originality of this thesis has been checked using the Turnitin OriginalityCheck service.

TIIVISTELMÄ

Iida Kangashaka
Keinoja SER-muovien mekaanisen kierrätyksen aikana tapahtuvan termisen hajoamisen vähentämiseen
Tampereen yliopisto
Materiaalitekniikan DI-ohjelma
Helmikuu 2022

Maailman siirtyessä kohti kiertotaloutta materiaalien kierrätettävyydestä on tulossa yhä kiireellisempi kysymys. EU on luonut strategian, jonka tarkoituksena on ohjata Euroopan muoviteollisuus kohti kiertotaloutta, mikä vaatii myös kaikkien muovituotteiden kierrätyksen lisäämistä huomattavasti. Jotkin muovijakeet ovat kuitenkin vaikeampia kierrättää kuin toiset. Esimerkki tästä ovat muovit sähkö- ja elektroniikkalaiteromussa. Osittain tämän materiaalivirran kierrätyksen vaikeus johtuu niistä bromia sisältävistä palonestoaineista, jotka ovat haitallisia, ja joita on käytetty vanhoissa sähkö- ja elektroniikkalaitteissa, mutta joiden käyttö ei ole enää sallittua uusissa tuotteissa, ja jotka on siksi poistettava kierrätyksen yhteydessä. Toinen muovien kierrätykseen liittyvä ongelma on jälleenkäsittelyn aikana tapahtuva hajoaminen, joka alentaa muovin moolimassaa.

ALL-IN for Plastics Recycling -projekti, jonka osa tämä diplomityö on, pyrkii auttamaan muoviteollisuuden toimijoita löytämään parempia kierrätysjärjestelmiä haastaville muovivirroille, kuten esimerkiksi sähkö- ja elektroniikkalaiteromun muovit. Tämän työn tavoitteena on selvittää voiko jälleenkäsittelyn aikana tapahtuvan hajoamisen vaikutuksia estää lisäämällä tiettyjä lisäaineita bromivapaaseen sähkö- ja elektroniikkalaiteromun muoviin, ja voiko tätä muovia käyttää uusissa sähkö- ja elektroniikkalaitteissa.

Työ alkaa kirjallisuuskatsauksella, jossa sähkö- ja elektroniikkalaiteromun muovin nykytilanne on kerrattu. Lisäksi katsauksessa käydään läpi, miten polymeerit hajoavat prosessoinnin aikana, miten se vaikuttaa niiden ominaisuuksiin, ja miten tätä voidaan estää lisäaineilla. Työssä tutkitut muovit ovat polypropeeni, polystyreeni, akryylinitriilibutadieenistyreeni ja polykarbonaatti/akryylinitriilibutadieenistyreeni, jotka on kierrätetty sähkö- ja elektroniikkalaiteromusta. Lisäaineiksi on valittu antioksidantit, ketjunjatkajat ja grafeeni nanohiutaleisiin liitetty maleiininhydridi. Antioksidanttituotteet ovat Irganox 1010 ja Irganox 1076, ketjunjatkajatuotteet ovat Joncryl ADR 4400 ja Joncryl ADR 4468, ja grafeeni nanohiutaleisiin liitetty maleiininhydridi valmistetaan laboratoriossa. Tutkimuksessa lisäaineellisille ja lisäaineettomille muoveille tehdään vetokokeet ja määritetään viskositeettikäyrä rotaatioreometrillä. Tämän jälkeen näitä tuloksia verrataan kirjallisuuskatsauksen osioon, jossa selitettiin miten moolimassan muutokset vaikuttavat ominaisuuksiin, ja vertailun perusteella arvioidaan miten hyvin eri lisäaineet estävät hajoamista. Lisäksi hapettumisajat määritetään antioksidantteja sisältäville muoveille, jotta niiden kykyä estää hapettumista voidaan arvioida.

Tämän analyysin perusteella näyttää siltä, että polypropeenin tapauksessa antioksidantit estävät hajoamista parhaiten, polystyreenille grafeeni nanohiutaleisiin liitetty maleiininhydridi on tehokkain lisäaine, ja akryylinitriilibutadieenistyreenille ja polykarbonaatti/akryylinitriilibutadieenistyreenille ketjunjatkajat ovat paras lisäaineryhmä. Reologiset ja mekaaniset ominaisuudet vaikuttavat varsin luotettavalta tavalta arvioida termisen hapettumisen aiheuttamaa hajoamista muoveissa. Lisäksi kierrätettyjen muovien mekaaniset ominaisuudet ovat tarpeeksi korkeita käytettäväksi uusissa sähkö- ja elektroniikkalaitteissa.

Avainsanat: muovien kierrätys; SER, sähkö- ja elektroniikkalaiteromu, termisen hapettuminen, antioksidantti, ketjunjatkaja grafeeni nanohiutaleisiin liitetty maleiininhydridi

Tämän julkaisun alkuperäisyys on tarkastettu Turnitin OriginalityCheck –ohjelmalla.

PREFACE

This thesis was done for the Plastics and Elastomer Technology research group at Tampere University during the time period 1.3.2021 – 26.2.2022 as a part of the ALL-IN for Plastics Recycling project, Work Package 3, Task 3.1. The responsible supervisor was University Instructor Ilari Jönkkäri. The examiners were University Instructor Ilari Jönkkäri and Associate Professor (tenure track) Essi Sarlin.

I would like to thank Ilari Jönkkäri and Essi Sarlin for all of their valuable support during the writing process of this work. I would also like to thank Ilari Jönkkäri and Postdoctoral Research Fellow Minna Poikelispää for teaching me how to use the equipment I needed for my experiments. Thank you to Visiting Researcher Rama Layek and Research Assistant Karoliina Hopia for helping me with the laboratory work necessary for preparing my additives. I would also like to thank the rest of the members of the research group that helped and supported me with my experiments. Most importantly, I would like to thank Ilari Jönkkäri for providing an exceptionally interesting subject, which allowed me to cultivate my passion for plastic recycling.

Finally, I would like to thank my family and friends for all of their support and encouragement during this process. I meant a lot.

Tampere, 26.2.2022

Iida Kangashaka

TABLE OF CONTENTS

1. INTRODUCTION	1
2. RECYCLING WEEE PLASTIC	4
2.1 Plastic recycling	4
2.1.1 Strategies for plastic management in Finland and the EU	4
2.1.2 Plastic recycling methods	5
2.1.3 Current situation of plastic recycling in Finland	7
2.2 Recycling WEEE plastic	10
2.2.1 Plastics in EEE	10
2.2.2 Directives and regulations affecting WEEE	13
2.2.3 Recycling process for WEEE	15
2.2.4 Quantities of WEEE plastic processed annually	17
3. DEGRADATION AND PROPERTIES OF EEE	19
3.1 Thermo-oxidative degradation mechanisms	19
3.2 Effect of variables on viscosity	24
3.3 Effect of variables on tensile properties	29
3.4 Oxidation induction time	31
3.5 Thermogravimetry	32
4. ADDITIVES FOR RECYCLING WEEE PLASTICS	33
4.1 Antioxidants	33
4.2 Chain extenders	35
4.3 Graphene nanoplatelets grafted with maleic anhydride	37
5. METHODS	39
5.1 Micro compounder and injection moulding machine	39
5.2 Universal testing machine	40
5.3 Rotational rheometer	40
5.4 Simultaneous thermal analyser	41
6. MATERIALS	42
6.1 Recycled plastics	42
6.2 Additives	42
7. TESTING RECYCLED WEEE PLASTICS	45
7.1 Rheological properties	45
7.1.1 Viscosities of additive-free plastics and the effect of fillers	45
7.1.2 Zero-shear viscosities	47
7.1.3 Power-law indices	52
7.2 Thermal properties	55
7.2.1 Oxidation induction times of samples with antioxidants	55
7.2.2 Thermogravimetric analysis of additive-free samples	57
7.3 Mechanical properties	57
7.3.1 Modulus	57

7.3.2 Yield stress and strain.....	61
7.3.3 Break stress and strain	64
8. DISCUSSION.....	69
8.1 Analysing results.....	69
8.2 Can recycled plastics be used in new EEE?	76
8.3 Is recycling WEEE plastics rational?	80
9. CONCLUSIONS.....	81
REFERENCES.....	83
ANNEX A: MATERIAL FLOW OF PLASTIC FROM WEEE IN 2019.....	95
ANNEX B: VISCOSITY RESULTS	96
ANNEX C: PROCEDURE FOR CALCULATING THE POWER-LAW INDICES	105
ANNEX D: TENSILE PROPERTIES.....	107
ANNEX E: VIRGIN POLYMERS	122
ANNEX F: RECYCLED POLYMERS.....	125

LIST OF FIGURES

Figure 1.	<i>Mechanical recycling process [21] [22] [23].</i>	6
Figure 2.	<i>Plastic demand in 2019 divided by segment and plastic type in Europe [24].</i>	8
Figure 3.	<i>Plastic compositions of appliances [34].</i>	11
Figure 4.	<i>The chemical structure of monomers for a) PP [37], b) PS [37], c) ABS (a representative structure) [38], and d) PC (bisphenol A - based) [37].</i>	12
Figure 5.	<i>The symbol indicating that the product is EEE and requires separate collection [40].</i>	13
Figure 6.	<i>The material flow of WEEE plastic in 2019 in Finland.</i>	17
Figure 7.	<i>PS alkoxy radical decomposing into an aldehyde or a ketone, and an alkyl radical. Adapted from [66].</i>	22
Figure 8.	<i>PS hydroperoxide decomposing into a ketone and an alcohol. Adapted from [65] and [67].</i>	22
Figure 9.	<i>The oxidation process of vinyl-1,2-PB. Adapted from [68].</i>	23
Figure 10.	<i>The oxidation process of trans-1,4-PB. Adapted from [68].</i>	23
Figure 11.	<i>The cross-linking processes of the ketones and aldehydes formed during cis- and trans-1,4-PB oxidation. Adapted from [68].</i>	23
Figure 12.	<i>The oxidation and decomposition process of PC. Adapted from [69].</i>	24
Figure 13.	<i>The relationship between MW and the zero-shear viscosity of a polymer. Adapted from [74] and [75].</i>	25
Figure 14.	<i>The effect of the MWD on the shape of the viscosity curve. Adapted from [74], [75], [76], and [77].</i>	27
Figure 15.	<i>The effect of filler content on the zero-shear viscosity. Adapted from [80].</i>	28
Figure 16.	<i>A schematic showing the effects of very small fillers on the viscosity of plastics. Adapted from [79].</i>	28
Figure 17.	<i>The basic relationship between MW and tensile properties. Adapted from [81].</i>	30
Figure 18.	<i>OIT on a heat flow rate-time curve. Adapted from [85].</i>	31
Figure 19.	<i>2,6-di-tert-butyl-4-methylphenol (BHT) [87].</i>	33
Figure 20.	<i>a) Phosphite and hydroperoxide reacting to form phosphate and alcohol. b) Thioester and hydroperoxide reacting to form sulphoxide and alcohol. [87].</i>	34
Figure 21.	<i>A schematic illustration of a multifunctional styrene-acrylic oligomeric epoxy chain extender [91].</i>	35
Figure 22.	<i>The Diels-Alder reaction between butadiene and ethene. Adapted from [101].</i>	38
Figure 23.	<i>The Diels-Alder reaction of graphene and maleic anhydride on the armchair edge. Adapted from [99] and [100].</i>	38
Figure 24.	<i>The micro compounder (left) and the micro injection moulding machine (right) from Xplore Instruments.</i>	39
Figure 25.	<i>A scheme showing the approximate dimensions (in mm) of the tensile test samples produced with the micro compounder. The approximate thickness of the samples was 2 mm.</i>	40
Figure 26.	<i>Examples of the tensile testing samples made with the micro compounder. a and b are PP, c and d are PS, e and f are ABS, and g and h are PC/ABS. a, c, e, and g are examples of the plastics with antioxidants, chain extenders, or without additives. b, d, f, and h are examples of the plastics with graphene nanoplatelets grafted with maleic anhydride.</i>	42

Figure 27.	The molecular structures of the antioxidants a) AO 1, b) AO 2 [126] [127].....	43
Figure 28.	Comparing the viscosity curves measured from the milled plastics (m) and the plastics injection moulded into discs (d).	46
Figure 29.	Comparison of the viscosity curves of samples with and without additives. The subindexes “m” and “d” signify the additive-free samples’ viscosities measured from milled plastic and injection moulded discs, respectively. a) PP, b) PS, c) ABS, d) PC/ABS.....	48
Figure 30.	The viscosity curves of the PS samples with and without additives separated so that the curves are more visible. a) Samples with CEs and GM, b) samples with AOs. Both figures have the additive-free curves.	49
Figure 31.	The DSC curves to determine OITs of a) PP, b) PS, c) ABS, and d) PC/ABS	56
Figure 32.	TGA curves of the additive-free plastics.....	57
Figure 33.	Stress-extensometer strain curves for the studied plastics with and without additives. The curves on the left have the full curve until the removal of the extensometer, and the curves on the right are close-ups of the same curves in the area where the modulus is determined. a) PP, b) PS, c) ABS, d) PC/ABS	59
Figure 34.	Stress-nominal strain curves for the studied plastics with and without additives. a) PP, b) PS, c) ABS, d) PC/ABS.....	65
Figure 35.	The properties of the studied recycled plastics compared to virgin and previous recycled plastics. X = properties of the additive-free samples, black dots = properties of studied recycled plastics with additives, grey dots = properties of virgin plastics, circles = properties of previous recycled plastics. a) modulus, b) yield stress, c) yield strain, d) break stress, e) break strain.....	77

ABBREVIATIONS AND SYMBOLS

ABS	acrylonitrile-butadiene-styrene
AO	antioxidant
BAS	Basic Auto-oxidation Scheme
BHT	2,6-di-tert-butyl-4-methylphenol
CE	chain extender
DSC	differential scanning calorimetry
ECHA	European Chemicals Agency
EEE	electrical and electronic equipment
EEW	epoxy equivalent weight
FTIR	Fourier transform infrared
GM	graphene nanoplatelets grafted with maleic anhydride
HIPS	high-impact polystyrene
MW	molecular weight
MWD	molecular weight distribution
NIR	near-infrared
OIT	oxidation induction time
PB	polybutadiene
PC	polycarbonate
PC/ABS	polycarbonate/acrylonitrile-butadiene-styrene blend
PE-LD	low-density polyethylene
PET	polyethylene terephthalate
PLASTin	ALL-IN for Plastics Recycling
PMDA	pyromellitic dianhydride
PP	polypropylene
PS	polystyrene
PVC	polyvinyl chloride
REACH	a regulation on the registration, evaluation, authorisation, and restriction of chemicals
RoHS	a directive on the restriction of the use of certain hazardous substances
STA	simultaneous thermal analyser
TG	thermogravimetric
WEEE	waste electrical and electronic equipment
XRF	X-ray fluorescence
$\dot{\gamma}$	shear rate
η	viscosity
η_c	calculated viscosity
K	consistency factor
MW_c	critical molecular weight
n	Power-law index

1. INTRODUCTION

Today humanity is consuming beyond the capacity of the planet [1]. It is expected that the global consumption of materials such as biomass, fossil fuels, metals, and minerals will double during the next forty years, and the amount of waste generated is expected to increase by 70 % by 2050 [1]. In efforts to remedy the situation, the European Commission adopted its first circular economy action plan in 2015 [2]. The plan, which was completed in 2019, covered a broad range of subjects from production, through consumption, all the way to waste management in an effort to move the EU closer to a circular economy and to encourage sustainable economic growth [2]. The work was continued when the European Commission adopted the new circular economy action plan in 2020 [1]. Several more detailed plans and strategies related to specific subtopics within circular economy were also adopted during this time. One of them was the European Strategy for Plastics in a Circular Economy published in 2018 [3]. The strategy details a plan to tackle the challenges related to plastics, such as finding more sustainable raw materials for plastics, increasing plastic's recyclability, reducing the amount of harmful substances in plastic, and lessening plastic's harmful effects on the environment [3]. Finland also published its own plan for better plastic management in 2018 called Plastics Roadmap for Finland, which was based on the European plan [4]. Both plans greatly emphasize the importance of increased recycling and the removal of harmful substances from plastics.

This thesis was part of the ALL-IN for Plastics Recycling (PLASTin) project [5]. The aim of the project is to help actors in the plastics industry to develop better recycling systems for demanding plastic streams, such as plastic from liquid packaging board and plastics from waste electrical and electronic equipment (WEEE). This thesis is specifically part of Work Package 3, Task 3.1, which is related to better management of the harmful additives that are used in WEEE. The task aims to find ways to identify pieces of plastic recovered from WEEE that are free of harmful substances, such as fire retardants containing bromine, and to study the properties of the recycled plastics.

Several studies have been done to determine the properties of plastics recycled from WEEE. In many of those studies the methods through which the plastics are recycled are not explicitly described [6] – [13]. Therefore, it is not known whether these plastics are free of harmful substances. Additionally, the recycling method was not described in [14],

but the material stream was known to not contain any fire retardants, such as those containing bromine. A few articles mention the method through which the different polymer types have been separated but say nothing about the removal of harmful substances. In [15] they were separated using near-infrared (NIR) spectroscopy. In [16] and [17] the sorting was done using the resin identification codes on the plastic parts of the products, and in [17] a Fourier transform infrared (FTIR) spectroscopy analysis was also used. In [18] density separation was used. Finally, there were two articles that mentioned both the removal of harmful bromine containing fire retardants and the method through which the polymer types were separated. In [19] a CreaSolv process was used to dissolve the bromine containing substances into the solvent and to remove them from the plastic, and the plastic was sorted through density separation. In [20] the pieces of plastic with bromine in them were identified with a handheld X-ray fluorescence (XRF) scanner and removed, and the plastic was sorted using FTIR.

In many of these studies the mechanical properties of the recycled plastics were determined, with no effort to try to improve them by adding additives [6], [15] – [20]. In some articles compatibilizers were used. Acrylonitrile-butadiene-styrene grafted maleic anhydride was used in [8] and [12], and ethylene-vinyl-acetate grafted maleic anhydride was used in [8] and [13]. Few studies explored impact modifiers, such as styrene-butadiene-styrene copolymer in [12] and methacrylate-butadiene-styrene copolymer in [9] and [14]. Antioxidants were utilized in two studies, in [10] the phenolic antioxidant 1010 was used, and in [9] a phenolic antioxidant Irganox 1076 as well as a metal de-activator Irganox MD1204 were used. Chain extenders were utilized in three studies. Styrene-butadiene-glycidyl methacrylate was used in [11], hydroxyl-terminated polybutadiene in [10], and the styrene-acrylic multifunctional oligomer Joncryl ADR 4370S in [7].

The majority of these studies focused on mechanical properties, and the changes in rheological properties were mostly not examined. In several articles viscosity was not determined at all [6], [8], [9], [12], [14] – [17], [20]. Melt flow rates were studied in [18] and [19]. Complex viscosities were determined in [7], [11], and [13]. One study compared the shear viscosities of samples with different amounts of additives [10].

As can be seen, no studies aim to use a broad selection of additives to improve the properties of recycled WEEE plastics, that are known to be free of bromine fire retardants, and to analyze these improvements by determining both mechanical and rheological properties. This is the objective for the current thesis. The study aims to answer the following questions: which additives work the best at preventing the degradation caused by thermal oxidation, how reliable are the rheological and mechanical properties when used as indicators on the changes to molecular weight and molecular weight distribution

caused by degradation, and are the properties of the recycled plastics good enough to be used in new electrical and electronic equipment (EEE). The studied plastics are chosen based on which plastics from WEEE had the highest yield in the recycling process done by Kuusakoski Oy as part of the PLASTin project. They are also some of the most common plastics in EEE. The additives are chosen based on a literature review. The plastics and additives are compounded and made into samples. Finally, the effects of the additives are studied by way of tensile testing, viscosity measurements, and oxidation induction time measurements. An additional thermogravimetric analysis is done to the additive-free plastics to study their possible filler contents.

The thesis begins with a section on the recycling of WEEE plastics (Chapter 2). This chapter first introduces the European and Finnish plans for circular plastic management and the situation with plastic recycling in general in Finland. Some of the plastics used in EEE and the legislation related to WEEE are introduced, the recycling process is described, and the magnitude of the annual WEEE plastic stream is estimated. Chapter 3 explains the thermo-oxidative degradation mechanism for polymers, as well as how this affects their properties. In Chapter 4 the additive types used in this study are introduced. Chapter 5 describes the methods used to assess the efficiency of the additives in preventing degradation. The plastics and additives studied are introduced in more detail in Chapter 6. Chapter 7 lays out the results of the rheological, thermal, and mechanical experiments. Chapter 8 includes an analysis of the results to see if any of the additives have prevented the degradation more effectively than the others. This chapter also contains an assessment on how well the properties of the plastics recycled in this study compare to the properties of virgin plastics, as well as to the properties of the plastics recycled in the articles discussed earlier in this Introduction to see if recycled plastics can be used in new EEE. Finally, the chapter also includes an estimation on the rationality of recycling WEEE plastics. Chapter 9 contains the conclusions. After this the references are listed, followed by the annexes

2. RECYCLING WEEE PLASTIC

2.1 Plastic recycling

2.1.1 Strategies for plastic management in Finland and the EU

In recent years the discussion around plastics and their harmful effects has become more prevalent. To address this issue the EU published A European Strategy for Plastics in a Circular Economy [3]. The strategy lays out plans for how to manufacture, use, reuse, and recycle plastics in a more sustainable way, and a vision for a new plastics economy in Europe. The vision aims to guide Europe into an era where, for example, plastic products are designed to facilitate reuse and recycling, which brings about a more united value chain for plastics, since the chemical industry and recycling sector can co-operate more. Plastic waste collection is improved, leading to a higher amount of recycled plastic used in products, and less poorly sorted plastic being exported, landfilled, or incinerated. New innovative materials and alternative raw materials will be developed to replace the fossil fuel-based plastics currently dominating the market, and to reduce EU's dependency on fossil fuels. Actions will be taken to reduce littering and the amount of microplastic in the environment. Increased recycling will generate new business opportunities, and the know-how required for it can become a valuable export for European countries, who can then take a leading role in the global efforts for better plastic management. The strategy also includes actions that should be taken to achieve the vision. These include taking into account the recyclability during product design, such as choosing the additives, colours, and polymer combinations that will make sorting and recycling easier, as well as eliminating harmful substances. The value chain of plastics needs to be modified so that it is more unified, and the recycling operations need to be expanded, which will lead to a more reliable material flow, and thus increases the demand for recycled plastics. The systems used for separate collection and sorting of plastics should be developed and standardized to make them more efficient and streamlined. The amount of plastic ending up in the environment will be reduced by limiting the use of single-use plastics and overpackaging, as well as implementing an extended producer responsibility for plastic products. A clear regulatory framework for defining and marking of compostable and biodegradable plastics is needed. The problems related to microplastics are to be addressed by eliminating them from products, where they've been added intentionally, and increasing scientific efforts to better understand the effects of microplastics. Innovation and investment related to finding good solutions to advance circular economy should be promoted. Finally, the issue of better plastic management cannot be solved

by any individual country on its own, so global efforts ought to be utilized to fulfil the vision laid out in the strategy.

The Finnish Ministry of the Environment has also published its own Plastics Roadmap for Finland [4], which is based on the European strategy. The roadmap aims to lay out an action plan that comprises of very specific, practical steps to achieve the better plastic management goals introduced in EU's strategy. The practicality of the steps is intended to make it easier for different actors, such as politicians, product designers, researchers, and recyclers, to get started. The individual steps of the plan are not discussed here in detail, but the goals the plan aims to fulfil include reducing littering and overconsumption, considering the introduction of a plastic tax, making plastic waste collection more efficient, as well as improving the identification of plastics in buildings and their sorting on construction sites. Additionally, the recycling and replacement of agricultural plastics is to be made more efficient, diverse plastic recycling solutions will be adopted, and alternative material solutions will be developed. Plastic management will be fitted into Finland's international agenda, the know-how related to plastic recycling will become an export for Finland, and finally, the harmful effects of plastics on humans and the environment ought to be the subject of further scientific study.

Both the European strategy and the Finnish roadmap put great emphasis on the efforts to increase plastic recycling rates in all fields plastics are used. This is the case especially for plastics in applications that are harder to recycle. Another important topic is the removal of harmful substances from plastics, which, in the worst-case scenario, might completely prevent the recycling of a plastic product.

2.1.2 Plastic recycling methods

There are many techniques for recycling plastics. They are divided into four categories: primary, secondary, tertiary, and quaternary recycling. The first two involve mechanical recycling, where the polymer chains are separated through physical means, i.e., melting, and the other two involve chemical reactions, where the polymer chains are broken into chemical compounds. [21] [22] Recycling methods can also be classified based on whether they are closed or open loop processes. In a closed-loop process the recycled material is used to produce the same product it was originally recovered from, and in an open loop process the material is used to make something other than the original product. [23]

Primary recycling means the mechanical recycling of clean, single-type plastic free of contaminants. It usually occurs in factories, where scrap material can easily be recycled

directly. Primary recycling is a simple, low cost, closed-loop process resulting in recycled material with properties very close to those of virgin plastics. [21] [22]

Secondary recycling differs from primary recycling in the sense that secondary recycling is an open loop process, and the recycled waste has often been contaminated and degraded during use. The degradation as well as the heterogeneity of the waste are the biggest challenges in secondary recycling. Since the composition of the waste is more complex, the process of secondary recycling will also have more steps compared to primary recycling. [21] [22] [23] The recycling process described in [21], [22], and [23] is summarised in Figure 1.

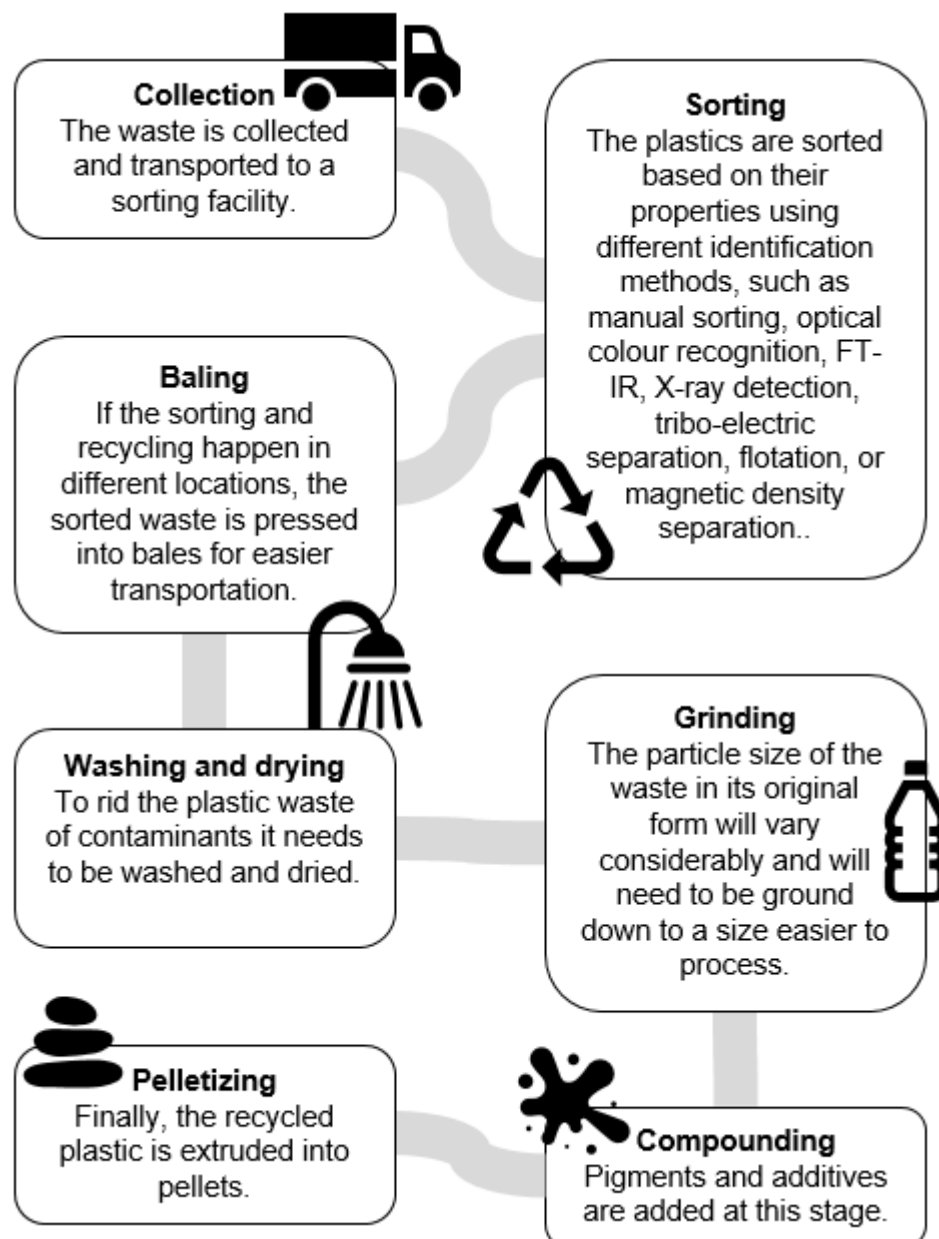


Figure 1. Mechanical recycling process [21] [22] [23].

Tertiary recycling is also known as chemical recycling. It is the process of depolymerizing the polymer chains to monomers, oligomers, or other chemical substances. These are then used as inputs in the production of new polymers or petrochemicals. This recycling method can better handle contaminated and degraded plastic waste, which is why it is a good option for plastics that are not suitable for mechanical recycling. Some of the possible processes for chemical recycling include pyrolysis, gasification, glycolysis, and methanolysis. [21] [22] [23]

Quaternary recycling is the option for materials, that are not suitable for recycling with any of the previously mentioned methods. With this method the material is disposed of via combustion and the energy content is recovered. This significantly reduces the volume of the waste, and the rest is made inert, and can be placed at a landfill. However, combustion generates harmful emissions, such as CO₂, NO_x, and SO_x, which is undesirable. Additionally, energy recovery does not contribute to the circulation of material, since the result of the process is the recovered energy. This method therefore does not support circular economy. [21] [22]

2.1.3 Current situation of plastic recycling in Finland

Plastic products can be divided into the following categories of application: packaging, building and construction, automotive, electrical and electronic equipment, agriculture, as well as household, leisure and sports, and others (e.g., appliances, mechanical engineering, furniture, medical) [24]. The demand of different plastic types in these segments in Europe in 2019 can be seen in Figure 2. In the figure the demand is divided according to plastic type along the x-axis and according to application along the y-axis. The size of the circles represents the magnitudes of the demand of each plastic type for each application. From the figure it can be seen that packaging is the most significant application for plastics, and low-density polyethylene (PE-LD) is the most used plastic type. The current recycling situation in Finland for the plastics used in these categories is described in the following.

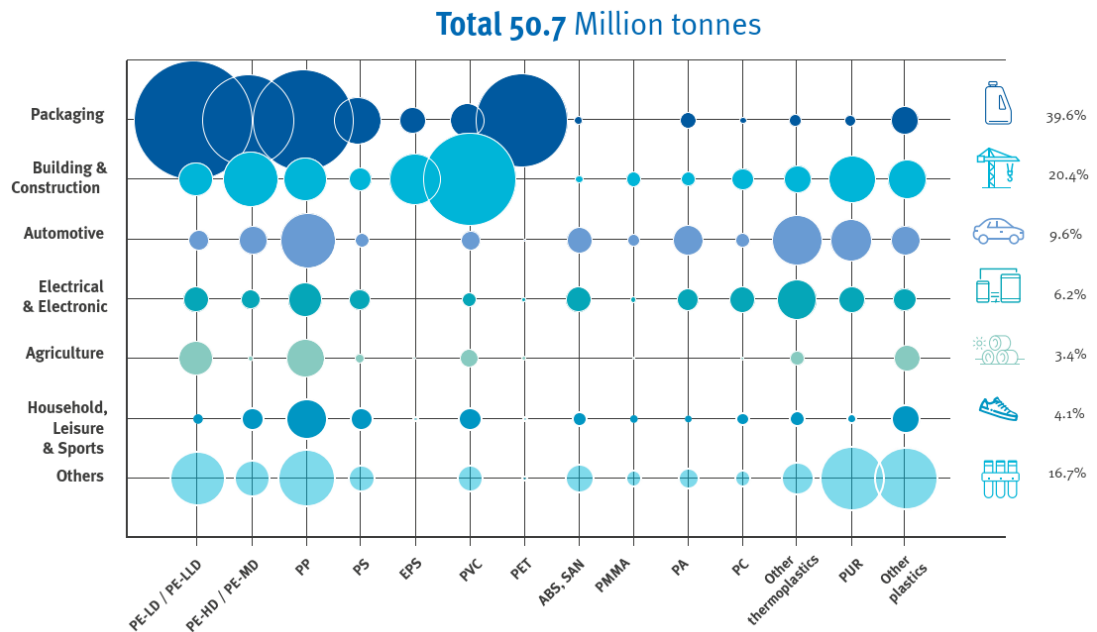


Figure 2. Plastic demand in 2019 divided by segment and plastic type in Europe [24].

As can be seen in Figure 2, packaging is clearly the application with the highest demand for plastics as a whole, with building and construction not far behind. However, even though packaging is such a big portion of plastic waste, the recycling of packaging plastic is doing quite poorly in Finland. In 2018 the plastic packaging recycling rate in Finland was the lowest in Europe (26 %) [24]. As is described in [25], the separate collection of packaging plastic based on producer responsibility began in 2016 in Finland. The collection is done by municipal and private waste management companies through Rinki Ltd.'s waste collection points. Rinki Ltd. is financed by the companies with producer responsibility. After collection, the plastic is recycled mechanically. Currently all Finnish plastic packaging waste is processed in Fortum's recycling plants in Riihimäki. Some industrial and agricultural plastic wastes are also processed there.

However, unlike with general plastic packaging, the recycling rate of plastic beverage packaging is very high in Finland (92 % in 2020). The recycling of beverage bottles and cans is based on a deposit added to the price of the beverage, which will be paid back to the consumer when they return their bottle or can to a returning point. The beverage packages are sorted into cans, plastic polyethylene terephthalate (PET) bottles, recyclable glass bottles, and re-fillable glass bottles, and are then transported to processing plants. At the plant for processing plastic bottles, they are recycled mechanically, which includes sorting by colour. Clear PET can be used as the raw material for new bottles, and colourful PET can be used to make e.g., other packaging and textiles. [26]

Construction is the second largest application for plastics after packaging. It uses about 20 % of all plastics used in Europe. This does not include the plastic used in construction sites coming from packaging and weather protection, nor the furniture and equipment in buildings. However, on most construction sites plastic is not recycled, and instead it is burned for energy. Although, on some construction sites with higher environmental standards, a large portion of films are recycled, but the rest of the plastic (hard plastic, pipes, polyvinyl chloride) are still disposed of as energy waste. Currently the collected plastic films are recycled mechanically in Fortum's recycling plants in Riihimäki. Additionally, Remeo Oy is in the process of building a new recycling plant in Vantaa, which will be able to mechanically process about 120 000 tonnes of construction waste and 60 000 tonnes of commercial and industrial packaging materials. [27]

Since 2015 at least 85 w-% of the materials used in cars in Europe have to be such that they can be re-used as parts or recycled as material, and a maximum of 10 w-% can be burned for energy [28]. In Finland in 2019 84,7 w-% of materials used in cars were recycled as parts or material, and 10,5 w-% was burned as energy [29].

The tyres of vehicles and working machinery are also collected based on a producer responsibility. Finnish Tyre Recycling Ltd was founded in 1995 to take care of the recycling obligation. The collection and transportation of waste tyres is done by their contracting party Kuusakoski Oy. Old tyres can be taken to a collection point, from where they will be taken to recycling. In Finland almost all tyres are recycled, and thus the recycling goal of 95 % is reached. Rubber cannot be thermoformed due to the chemical cross-linking and so it cannot be recycled mechanically. However, it can be used in infrastructure construction as filler material in soil structures, in different shields and barriers such as noise and flood barriers, in pavements such as rubber asphalt and safety surfaces in playgrounds, and in water purification. Additionally, tyres can be refined into new products through pyrolysis, which produces gas, oil, and charcoal. The oil can be utilized as a fuel, the gas is reminiscent of natural gas, and the charcoal can be used at the wastewater treatment plant, as a filler in the plastic and rubber industries, or as a pigment. Tyres are also burned for energy. [30]

The collection and waste management of WEEE is also handled via producer responsibility in Finland. There are five producer responsibility organisations for EEE in Finland: SERTY ry, ERP Finland, SELT Association, ICT Producer Co-operative, and FLIP Association. Together they organize the waste management of WEEE through the use of waste collection points. [31] EEE tends to comprise of many different difficult-to-separate materials. Especially troublesome is the kind of WEEE that contains multiple different types of plastics, and the resulting mix of plastics is rarely recyclable, and thus is burned

for energy. Some plastic fractions, however, are pure enough, and can be recycled mechanically as material. [32]

Farms generate two types of plastic waste, plastic packaging, that falls under the producer responsibility for packaging, and other plastics, such as plastic films, netting, and cloth, as well as trickle tubes. Only about a fifth of agricultural plastic waste is recycled mechanically as material, the rest is burned for energy or disposed of through other methods. The collection is done by one national and several local waste collectors. Forum Waste Solutions Oy, which is the only national collector, collects all agricultural plastic packaging and protective material (except for plastic netting) from farms for a price. [33]

2.2 Recycling WEEE plastic

2.2.1 Plastics in EEE

Plenty of plastics are used in the manufacturing of EEE. The plastic compositions used in different equipment vary significantly, as can be seen in Figure 3, but the most important ones stay roughly the same regardless of application. Figure 3 is from a study done on the composition of plastics in EEE by Martinho, G. in 2012 [34]. The composition of EEE was determined from 3417 appliances collected from a recycling unit in Portugal. Based on the results the most common plastics in WEEE are polypropylene (PP), polystyrene (PS), acrylonitrile-butadiene-styrene (ABS), polycarbonate/acrylonitrile-butadiene-styrene blend (PC/ABS), high-impact polystyrene (HIPS), polycarbonate (PC), and polyvinyl chloride (PVC). The recycled plastics chosen for the current study were PP, PS, ABS, and PC/ABS.

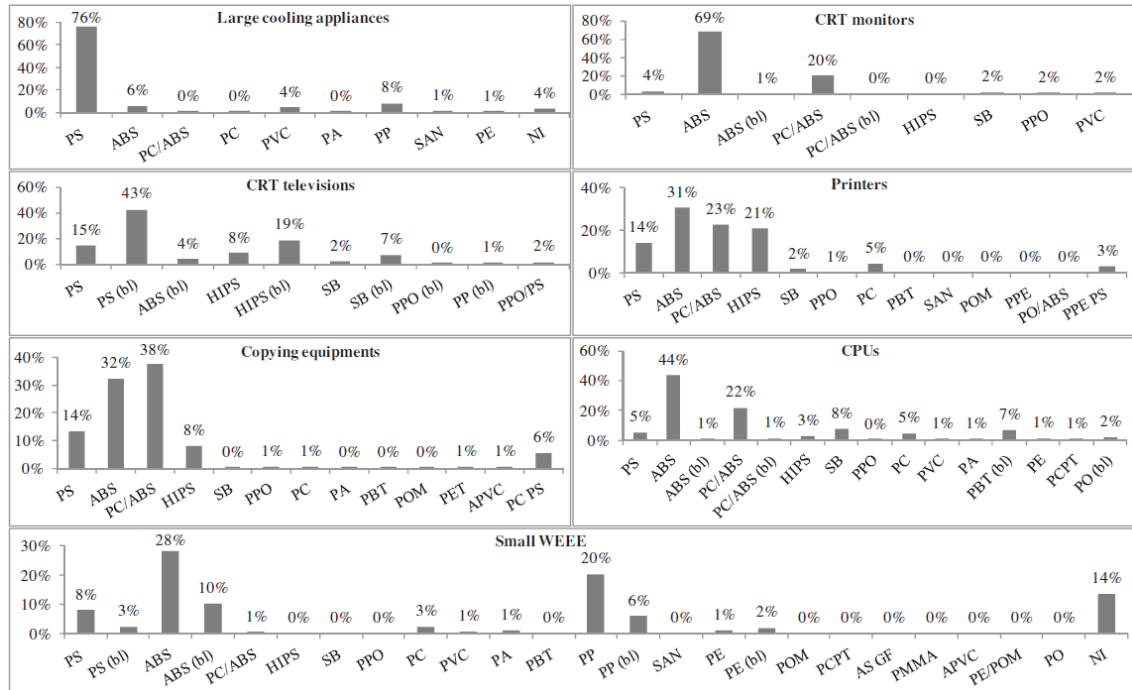


Figure 3. Plastic compositions of appliances [34].

PP is a polyolefin polymerized from propylene (Figure 4). Ziegler-Natta catalyst with titanium as the transition metal is the most common method of polymerizing PP. PP's crystallinity depends on its tacticity. Isotactic and syndiotactic PP have high crystallinity, whereas atactic PP is amorphous. Isotactic PP is the most common form of PP. [35]

PS (Figure 4) is a styrenic polymer. Commercially it is polymerized through radical polymerization with either thermal or peroxide initiation. PS as such is often called general purpose polystyrene and is very brittle. The impact properties of PS can be improved by adding polybutadiene (PB) in two steps. In the first step styrene is pre-polymerized in the presence of PB and in the second step PS is polymerized and the PB/styrene phase particles are blended into it. This type of PS is called high-impact polystyrene. PS is an amorphous polymer. [36]

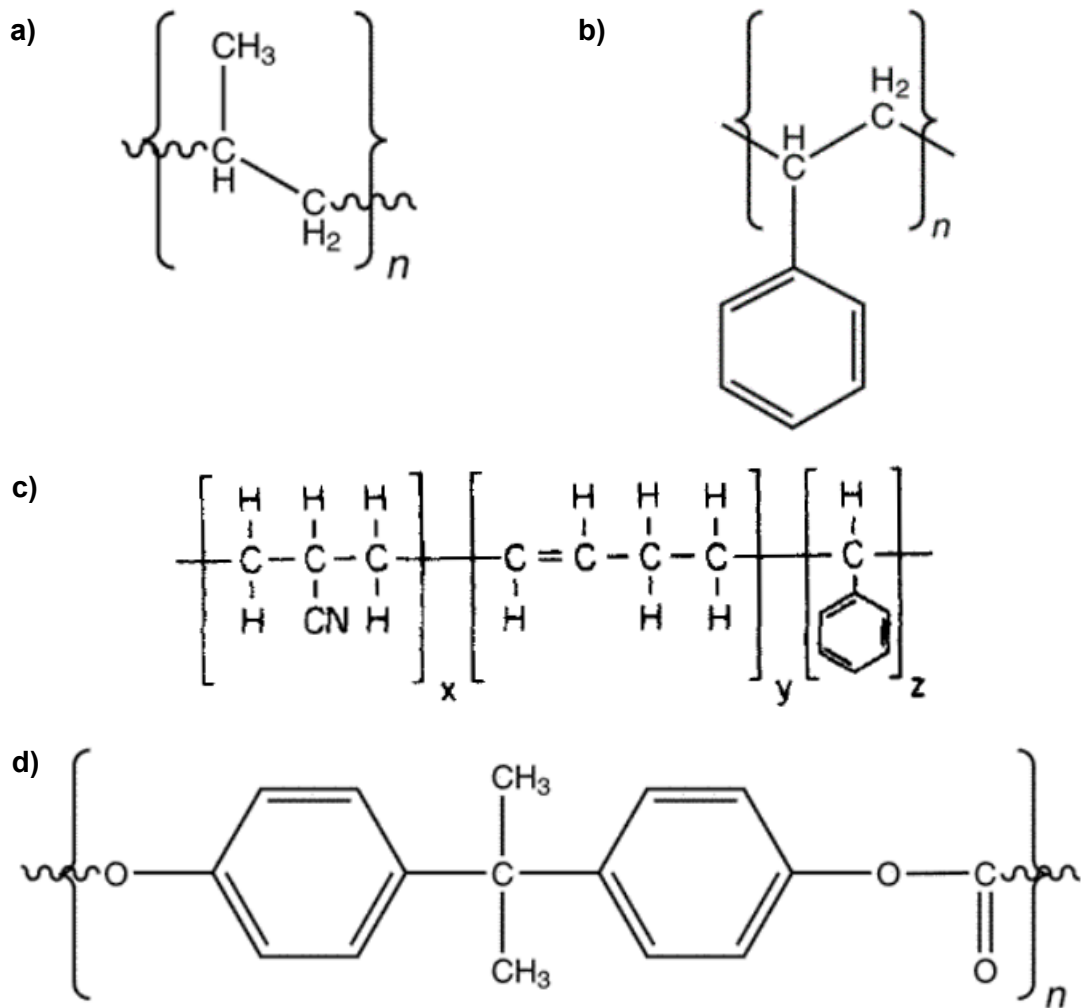


Figure 4. The chemical structure of monomers for a) PP [37], b) PS [37], c) ABS (a representative structure) [38], and d) PC (bisphenol A -based) [37].

ABS is defined as a styrenic terpolymer. It comprises of three monomers, acrylonitrile, butadiene, and styrene (Figure 4). The composition of different monomers in the polymer is approximately 21 – 27 % of acrylonitrile, 12 – 25 % of butadiene, and 54 – 63 % of styrene. Emulsion polymerization is the most common method for polymerizing ABS. The structure of ABS is polybutadiene particles dispersed in a styrene-acrylonitrile copolymer matrix. [39]

Bisphenol A polycarbonate (Figure 4) is the most common form of PC. It is an amorphous polymer. The polymerization method most commonly used for bisphenol A polycarbonate is an interfacial polymerization process, which involves the condensation of bisphenol A with phosgene. PC and ABS are often used together as a blend. [39]

2.2.2 Directives and regulations affecting WEEE

The management of WEEE is discussed in Directive 2012/19/EU (a recast of Directive 2002/96/EC, which entered into force in 2003) on WEEE, which aims to protect the environment and human health, as well as to preserve natural resources. The directive calls for the implementation of producer responsibility. Producers are responsible for organizing an efficient separate collection system for WEEE with a high collection rate, especially for cooling and freezing equipment that contain ozone-depleting substances and fluorinated greenhouse gases. The disposal of WEEE as unsorted municipal waste should be avoided. The producer is also responsible for adding adequate material and component information to their products to facilitate easier sorting, and for printing the symbol marking EEE shown in Figure 5 on the products. The producers are encouraged to design their products so, that they are easy to re-use or recycle. The amount of hazardous substances ought to be limited. The collection system needs to allow the return of large waste appliances free of charge when purchasing an equivalent product, or with no obligation for a new purchase in the case of small EEE (all external dimensions below 25 cm). Citizens should be given the necessary information on where and how to dispose of WEEE, and their role in recovery of WEEE. The treatment of WEEE is to be done using the best available technologies. Finally, Member States are to gather information on the collected and recycled WEEE. The products this directive does and does not apply to are shown in Table 1. [40]



Figure 5. The symbol indicating that the product is EEE and requires separate collection [40].

Table 1. The product categories that Directives 2012/19/EU [40] and 2011/65/EU [41] do and do not apply to. * Only listed in Directive 2012/19/EU, ** Only listed in Directive 2011/65/EU.

2012/19/EU (WEEE) applies to	2011/65/EU (RoHS) applies to	Directives do not apply to
<ul style="list-style-type: none"> • Temperature exchange equipment • Screens/monitors over 100 cm² • Lamps • Large equipment, over 50 cm • Small equipment, under 50 cm • Small IT and telecommunication equipment 	<ul style="list-style-type: none"> • Large household appliances • Small household appliances • IT and telecommunications equipment • Consumer equipment • Lighting equipment • Electrical and electronic tools • Toys, leisure and sports equipment • Medical devices • Monitoring and control instruments • Automatic dispensers • Other EEE not covered by any of the categories above 	<ul style="list-style-type: none"> • Military equipment • Equipment designed to be used as part of another equipment, that this directive does not apply to • Filament bulbs * • Space equipment • Large-scale stationary industrial tools • Large-scale fixed installations • Means of transport (excluding not type-approved electric two-wheel vehicles) • Non-road mobile machinery for professional use • Equipment for research and development • Active implantable medical devices • Photovoltaic panels ** • Pipe organs **

The actions to restrict the use of hazardous substances are further discussed in Directive 2011/65/EU (a recast of Directive 2002/95/EC, which entered into force in 2003) on the restriction of the use of certain hazardous substances (RoHS) in EEE to protect the environment and human health. Member States are to make sure there are no hazardous substances in new EEE placed on the market, spare parts made available for repairable EEE, or parts used as upgrades. The aim is to slowly phase out all such substances. The directive gives maximum acceptable concentrations for each substance. The list of restricted substances is periodically assessed and amended. The obligation of the manufacturer is to make sure the product is designed and produced in accordance with the directive, and all the related documentation is in order. Importers and manufacturers are to make sure that they keep a registry of previous non-conforming products and recalls

and indicate their contact details on the product or accompanying documentation. In case the manufacturers, importers or distributors have reason to believe the product is not in conformity, they should either bring it to conformity, recall it, or in the case of importers and distributors, not bring it on the market. All three operators are also required to give information and documentation related to the conformity of the product to competent national authorities, if asked. The EEE this directive does and does not apply to are shown in Table 1. The restricted substances are as follows:

- Lead
- Mercury
- Cadmium
- Hexavalent chromium
- Polybrominated biphenyls
- Polybrominated diphenyl ethers
- Bis(2-ethylhexyl) phthalate
- Butyl benzyl phthalate
- Dibutyl phthalate
- Diisobutyl phthalate [41]

The restrictions listed in Regulation No 1907/2006 on the registration, evaluation, authorisation, and restriction of chemicals (REACH) also apply to EEE. This regulation aims to protect human health and the health of the environment through better management and oversight of chemicals. The regulation requires the manufacturers and importers of chemicals to examine the risks related to each chemical. This information is then submitted to the European Chemicals Agency (ECHA), which was founded along the publication of REACH. The aim is to eventually replace the harmful chemicals with substances and technologies that are less dangerous. [42]

2.2.3 Recycling process for WEEE

EEE generally consists of a highly varied group of materials, which are joined together in a complex structure. This causes the recycling process for WEEE to be quite complicated. The process can also change slightly depending on the situation, the desired outcome, and the operator. The process used to acquire the samples for this study is described here. The WEEE originated from post-consumer collection points around Finland. The initial sorting happens at the collection point, where appliances are sorted into categories, since different types of appliances might have different recycling needs. The

sorting logic might vary a little with the operator, but it mainly follows the product categories listed in the Directive 2012/19/EU on WEEE shown in Table 1. The plastic in the current study came primarily from small household appliances. [43]

After the collection point the waste is handed over to a recycling operator, Kuusakoski Oy in this case. Manual sorting is the first step. In this step at least the minimum list of substances and components listed in Annex 7 of the WEEE directive are removed, as well as any components made of valuable materials, so as to not lose them during the further recycling steps. Over 20 separate fractions are removed in this step. [43]

Next, the waste, which consists of mainly intact equipment with plastic shells, is taken to a pre-breaker. Here the appliances are broken down slightly to make further separation easier, even though the pieces are still very large and there are plenty of different materials attached to each other. Any magnetic metals that have come loose are collected with magnets at this point. The pieces are then taken to a crusher, where they are crushed to a size, where the final separation of materials is possible. Once again, loose magnetic metals are collected with magnets. As a result, a plastic rich fraction is obtained, which consists mainly of plastic, but also other materials such as metals, paper, and textiles, and has a broad particle size distribution. After this, the material is screened to separate it by size. The finer particles are removed and taken to their own refining process. The larger pieces are separated into two size fractions, large and medium. [43]

Next, the plastic rich fractions are taken to a reject unit, where the lightweight materials (paper and textiles) are removed using an air elutriator, and metals are removed and collected using magnets and an eddy current separator. The aim is for the resulting plastic fraction to be free of metals and lightweight materials, and in this case the sorting was very successful. [43]

The plastic is then taken through an XRF line where the pieces containing bromine are identified and removed. The line has a sensor that scans every piece, and if it finds bromine, it signals to the blower further down the line to blow the piece off of the line. The method does not recognize what kind of compound the bromine is in, and thus removes them all, even the harmless ones. The earlier sorting of the plastic rich fraction into different size groups was done, because the XRF separation requires a narrow size distribution. This is so that the blower strength can be optimized to the weight of the pieces more accurately, and so that the smaller pieces cannot hide under the larger ones as easily. [43]

Finally, the bromine-free plastic is taken to a NIR spectroscopy line, which works the same way as the XRF line, but the radiation used is near-infrared instead of X-ray. In

this step the plastic is sorted based on the polymer type, after which it goes through the basic mechanical recycling process described in Chapter 2.1.2. Any plastics that cannot be identified by NIR (e.g., black plastic), or that does not have suitable applications after recycling will be burned for energy. [43]

2.2.4 Quantities of WEEE plastic processed annually

As stated in Directive 2012/19/EU on WEEE, the Member States of the EU are to collect and report information on the amounts of collected and recycled WEEE. In Finland the reporting is done by the Centre for Economic Development, Transport and the Environment of Pirkanmaa. The latest information available is from 2019 [44]. Figure 6 depicts the flow of the plastics in WEEE. The information in the figure is based on the data collected by the Centre for Economic Development, Transport and the Environment [44], as well as a selection of articles describing the plastic content in different types of WEEE [34] [45] – [48]. The amounts of circulating plastic in the figure were calculated by multiplying the amounts of collected WEEE in the data by the plastic content percentages in the articles. A table showing the full data can be found in Annex A.

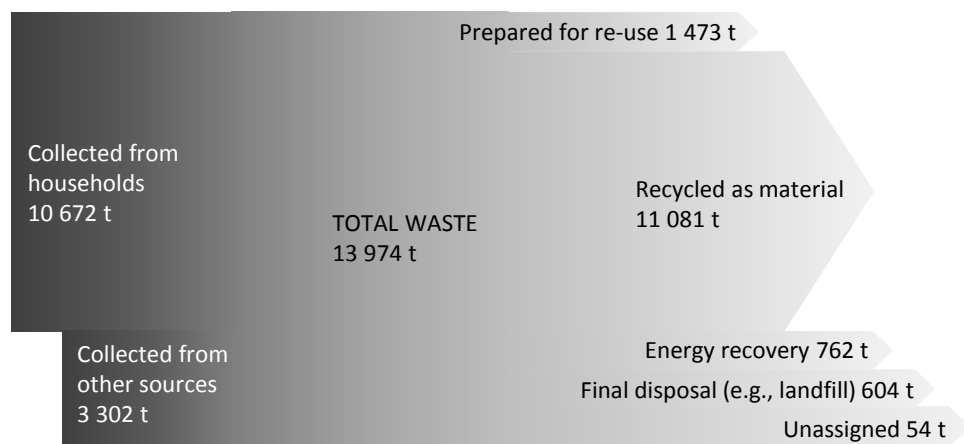


Figure 6. The material flow of WEEE plastic in 2019 in Finland.

Figure 6 shows the amount of collected WEEE plastic in 2019, and how they were disposed of. The majority of the waste was collected from households, about 76,4 %. The rest was collected from other sources. Only 10,5 % of all collected plastic was in equipment that was prepared for re-use. The majority of the waste (79,3 %) was recycled as material. The rest was either burned for energy (5,5 %), or disposed of through other methods, such as landfilling (4,3 %). Finally, the amount of collected plastic and the amount of disposed plastic did not quite match in the data, and the left-over waste is shown in the figure as Unassigned (0,4 %). Since the data only gives information on the waste that enters the management system (left side in the figure), and the waste that

leaves it (right side) during a certain year, the unassigned plastic is simply material that has not been processed yet.

There is, however, very likely quite a significant error in the amount of WEEE plastic recycled as material. The information Figure 6 is based on does not differentiate the waste based on the type of material. Therefore, the distribution of different materials in the disposal categories (re-use, recycled, energy recovery, final disposal, and unassigned) are not necessarily the same. As recycled WEEE plastics are not used as material for new EEE, but metals are, it is likely the information in the figure is not correct [49] [50]. This means it is more likely that the majority of the recycled material from WEEE are metals, and the amount of plastic shown in the figure to be recycled as material would in fact be recovered as energy, which would make the total amount of energy recovered WEEE plastic to be 11842 t, about 84,7 % of the total waste plastic amount.

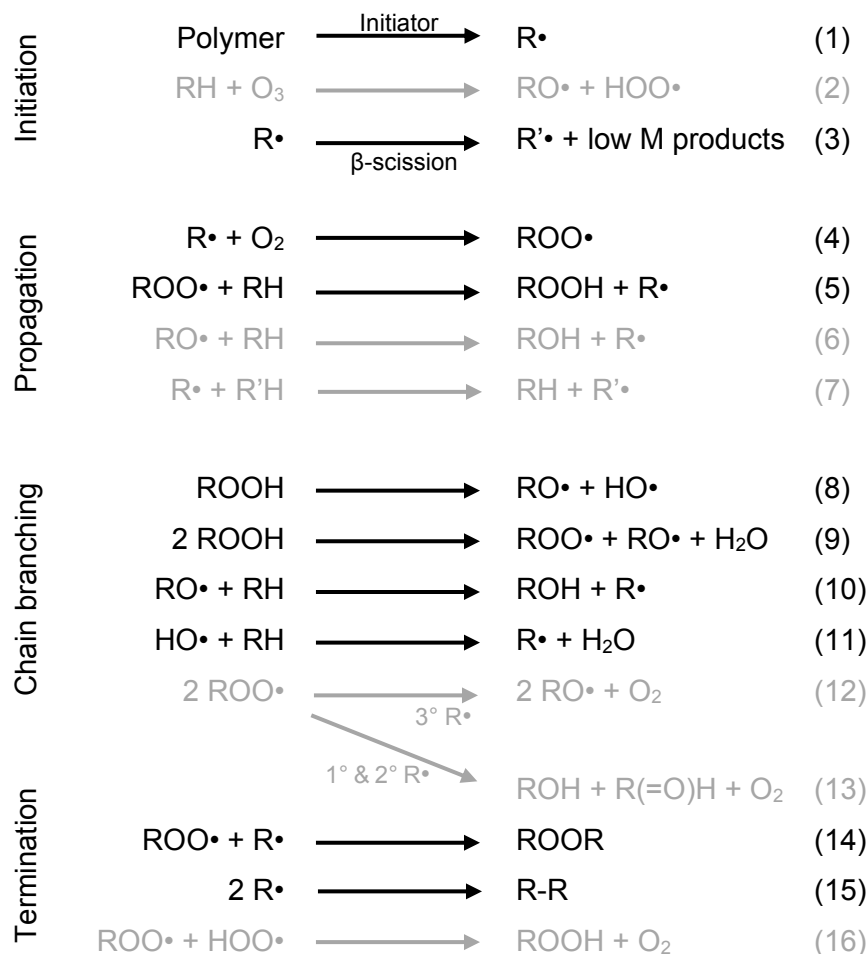
3. DEGRADATION AND PROPERTIES OF EEE

Plastics can be subjected to harsh environments during both processing and service. These environments can include exposure to mechanical loading, high temperatures, oxygen, and moisture. Additionally, they can be subjected to light, radiation, and chemical reactions during use. All of these variables can cause degradation in the polymer. Thermal oxidation is one of the most significant causes of degradation. There usually is an abundance of oxygen available during a product's service life, but the amount of oxygen available during processing is also sufficient for oxidation. [51]

3.1 Thermo-oxidative degradation mechanisms

Polymers are generally thought to oxidize according to the Basic Auto-oxidation Scheme (BAS). BAS is divided into four steps: initiation, propagation, chain branching, and termination. Initiation is the step where alkyl radicals are originally formed. During propagation the radicals react with oxygen to form peroxy radicals, which can then abstract hydrogen to form hydroperoxides. The peroxides decompose during chain branching and form more radicals. During termination the radicals combine into non-radical molecules. [52] [53]

BAS was developed by Bolland and Gee in the 1940s (shown in black in Scheme 1) [54] – [59]. It was originally suggested only for rubbers and lipids but has been widely used to explain the oxidation of other polymers as well. However, in 2010 Gryn'ova et al. [52] discovered that the bond dissociation energy for the R-H bond is higher than the energy of the ROO-H bond for most common polymers. This makes reaction (5) thermodynamically unfavoured, and thus very unlikely. Since oxidation still occurs and hydroperoxides are formed in these polymers, there must be some other process responsible for it. Gryn'ova et al. suggested that the defects in the polymer chains might be what is propagating the oxidation. They also pointed out that for some polymers and in some conditions, BAS is not the only possible auto-oxidation route, and other options are also available. In 2018 the research was developed further by Smith et al. [53] who suggested alternative propagation reactions instead (shown in grey in Scheme 1).



Scheme 1. Basic Auto-oxidation Scheme for polymers. The reactions written in black are the original BAS by Bolland and Gee, and the reactions in grey are the additions suggested by Smith et al.

Adapted from [52] and [53].

Initiation occurs either by hydrogen abstraction or by chain scission according to reactions (1) and (3) and creates alkyl radicals (R•). The chain scission reaction can also form low molecular weight products. Polymers can also oxidize non-radically when they react with ozone (2). The traditional propagation route is for an alkyl radical to react with oxygen to form a peroxy radical (ROO•) according to (4), which can then abstract a hydrogen atom from a pristine polymer chain (RH) to form a hydroperoxide (ROOH) according to (5). In the alternative propagation reactions either an alkoxy radical (RO•, reaction 6) or an alkyl radical (7) abstracts the hydrogen atom, and forms either an alcohol (ROH) or a pristine polymer chain, respectively. During chain branching the peroxide decomposes to create either an alkoxy and a hydroxyl radical (8), or a peroxy and an alkoxy radical, as well as a molecule of water (9). The alkoxy (10) and hydroxyl (11) radicals can then react further by abstracting hydrogen atoms from pristine polymer

chains. The result of the bimolecular combination of peroxy radicals depends on what type of alkyl radical it was originally formed from. If $R\cdot$ was tertiary, the reaction is a chain branching reaction and it produces alkoxy radicals and oxygen (12). If $R\cdot$ was a primary or a secondary radical, it is a termination reaction, which produces an alcohol, an aldehyde ($R(=O)$), and an oxygen molecule (13). The other termination reactions are bimolecular combinations of peroxy and alkyl radicals that form ROOR or R-R (14) (15). Hydroperoxy radicals can also offer an alternative hydrogen source for peroxy radicals to form hydroperoxide (16). [53]

PP thermal oxidation generally initiates through the hydrogen abstraction at the tertiary carbon [60] [61] [62] [63]. The radical then reacts with oxygen according to reaction (4) [60] [61] [62] [63]. PP is capable of intramolecular hydrogen abstraction, where a radical abstracts a hydrogen from a tertiary carbon on the same polymer chain to propagate oxidation [60] [62]. According to [60] and [62] the abstraction is done by a peroxy radical, but according to Gryn'ova et al. [52] and Smith et al. [53] this is not possible for PP as a whole, except for around certain chain end defects. Alternatively, it would be possible for the peroxy to decompose to an alkoxy radical, which can then abstract the hydrogen (reactions 12 and 6). Reaction (16) could account for the formation of hydroperoxides. Adams [60] has shown several different termination pathways for PP, which yield γ -lactones, aldehydes, ketones, acids, and esters.

The thermal oxidation of PS also initiates through hydrogen abstraction at the tertiary carbon according to [64] and [65], although according to [66] abstraction can also occur at the secondary carbon. As mentioned, the propagation can happen either at defects according to the original BAS by Bolland and Gee, as mentioned in [52], or elsewhere on the chain according to the updated BAS according to [53]. According to [64] and [66] the alkyl radical then reacts with oxygen to form a peroxy radical. According to [64] the next step is for the peroxy to decompose according to reaction (12), but according to [66] the next step is hydroperoxidation (reaction 5 or 16) and hydroperoxide decomposition (reaction 8 or 9). Nonetheless, both paths lead to alkoxy radicals. Through chain scission the alkoxy radical then breaks into an aldehyde and an alkyl radical, if the alkoxy radical was formed on a secondary carbon, or a ketone and an alkyl radical, if the carbon was tertiary (Figure 7) [66]. Alternatively, according to [65] and [67] a hydroperoxide forms on a tertiary carbon, does not decompose, and instead breaks through chain scission into a ketone and an alcohol (Figure 8). According to [66] and [67] the oxidation of PS will yield ketones and aldehydes, even though the possibility of a radical being formed on the secondary carbon is not mentioned by [67]. Conversely, according to [64] PS oxidation does not yield aldehydes, only ketones and alcohols.

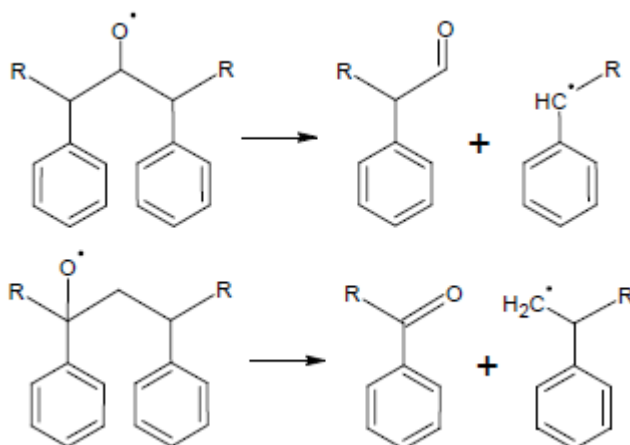


Figure 7. PS alkoxy radical decomposing into an aldehyde or a ketone, and an alkyl radical. Adapted from [66].

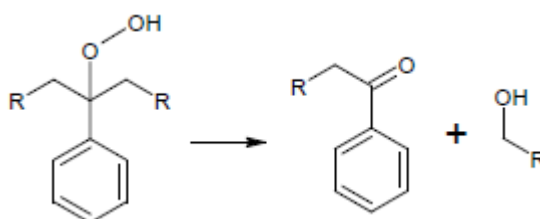
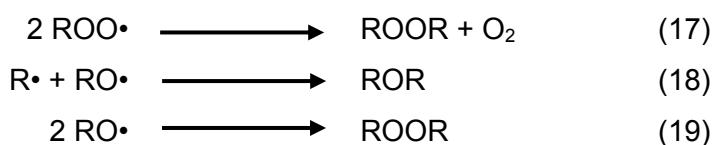


Figure 8. PS hydroperoxide decomposing into a ketone and an alcohol. Adapted from [65] and [67].

ABS contains polybutadiene (PB), which is a rubber, and so the original BAS by Bolland and Gee applies to it. It has been shown that the PB phase is where the oxidation of ABS mainly occurs, and styrene and acrylonitrile oxidize very little. For vinyl-1,2-PB the process initiates through hydrogen abstraction at the tertiary carbon (Figure 9), which then reacts with oxygen (4) and creates a hydroperoxide (5). The hydroperoxide decomposes into an alkoxy radical (reaction 8 or 9), which abstracts a hydrogen atom from a pristine polymer chain and forms an alcohol (10). The alkoxy radicals can also fragment and rearrange into ketones, which causes chain scission. Termination can occur through reactions (14) and (15), or through reactions (17), (18) and (19) given below to cause crosslinking:



Initiation on cis- and trans-1,4-PB happens on one of the carbons not contributing to a double bond (Figure 10). After this, the hydroperoxide formation and decomposition occurs according to reactions (4), (5), (8) or (9), and (10). Instead of alcohol (according to reaction 10) the alkoxy radicals can form ketones and aldehydes. For 1,4-PB crosslinking

happens through the opening of double bonds on adjacent ketones or aldehydes (Figure 11). The graft bond between the PB and styrene-acrylonitrile phases is also targeted by oxidation and broken through chain scission. [68]

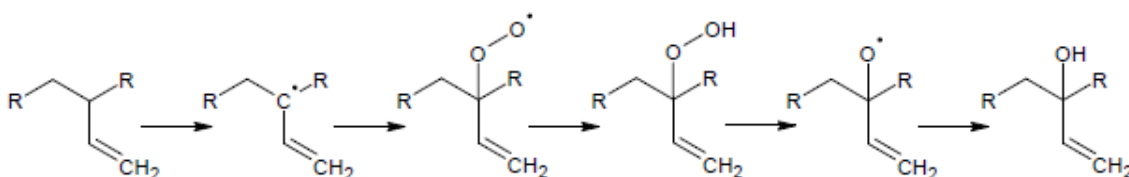


Figure 9. The oxidation process of vinyl-1,2-PB. Adapted from [68].

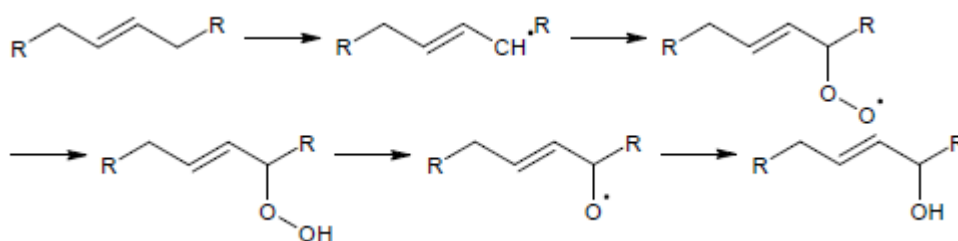


Figure 10. The oxidation process of trans-1,4-PB. Adapted from [68].

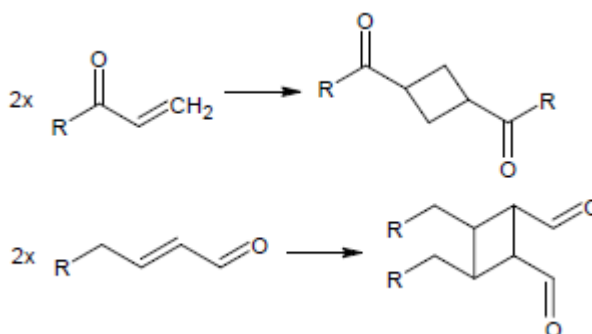


Figure 11. The cross-linking processes of the ketones and aldehydes formed during cis- and trans-1,4-PB oxidation. Adapted from [68].

The oxidation of the most common PC (bisphenol A polycarbonate) initiates at one of the methyl groups through hydrogen abstraction. The alkyl radical then reacts with oxygen to create a peroxy radical (4). The peroxy then isomerizes according to Figure 12 (path a), after which the O-O bond ruptures (path b). One of the formed alkoxy radicals then abstracts hydrogen (path c), and then decomposes into formaldehyde and an alkyl radical (path d). The other alkoxy radical forms a phenol derivative (path e). The alkyl radical formed through path d oxidizes further into an aldehyde and an alkoxy radical (path f-h), which then abstracts hydrogen to form methanol (path i). The formaldehyde decomposes into hydrogen and carbon monoxide (path j). As oxidation progresses, the concentration of aldehyde and hydroxyl groups increases over time. [69]

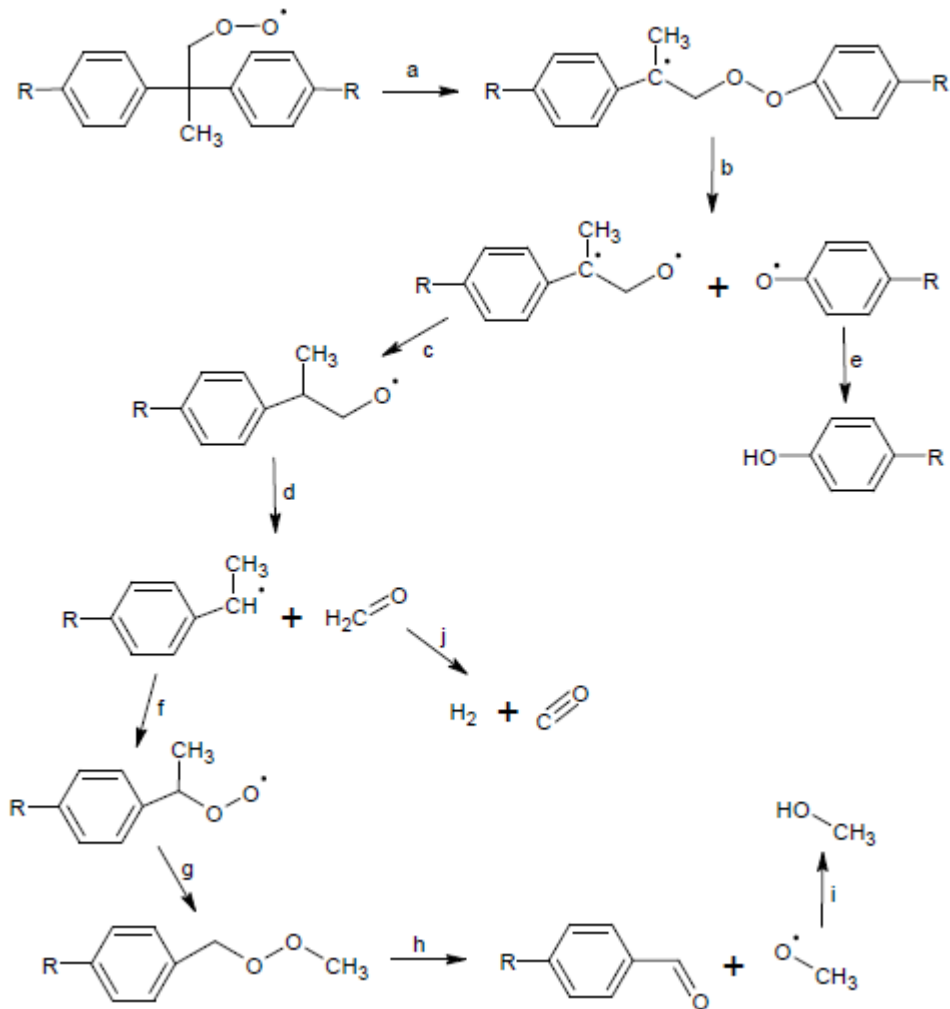


Figure 12. The oxidation and decomposition process of PC. Adapted from [69].

The scission caused by oxidation leads to the molecular weight (MW) of the decreasing as the chains break into shorter segments. As the MW decreases, this means that the molecular weight distribution (MWD) curve as a whole also moves to lower MW values. In addition to this, the degradation causes the MWD to become broader, as the number of shorter chains increases while some of the original longer chains still remain. [70] [71] [72] [73]

3.2 Effect of variables on viscosity

Many variables affect the viscosity of a polymer melt. These include temperature, pressure, type of polymer (chain chemistry and architecture), MW, and MWD [74] [75]. The viscosity is also affected by the filler or plasticizer concentration [74]. However, in this study the temperature, pressure, and type of polymer stayed the same during the experiments, so this section only focuses on the effects of MW, MWD, and filler/plasticizer concentration on viscosity.

The viscosity curve of a shear-thinning material has three sections, the lower Newtonian plateau at low shear rates, the shear-thinning region at higher shear rates, and the upper Newtonian plateau at very high shear rates. The upper plateau is generally not measurable for polymeric melts. For this reason, the viscosity curve of a polymer usually only shows the lower Newtonian plateau and the shear-thinning region. The shape of this curve can be described quite well with three quantities: the zero-shear viscosity, the characteristic shear rate, and the slope of the shear thinning region. [75]

Zero-shear viscosity is the viscosity at zero shear, and since the viscosity in the Newtonian region is independent of the shear rate, it can be used to describe the whole Newtonian plateau. The zero-shear viscosity is found to be dependent on the MW of the polymer. When plotting zero-shear viscosity as a function of MW on a logarithmic scale (Figure 13) the curve is clearly divided into two sections. The dependence is linear in both cases, but the slope changes at a critical molecular weight (MW_C) from 1 to about 3,4. MW_C is thought to be the point where the polymer chains are long enough to form entanglements. [74] [75] MW_C is approximately 2 or 3 times the length of polymer between entanglements [75]. Viscosity of polymers is made up of two components, the first being the localized friction between chain segments, and the second being caused by the entanglements. Both the amount of friction and the number of entanglements increase with MW, and thus both increase viscosity. This is also why the slope of the curve in Figure 13 changes at MW_C , since this is where the effect of the entanglements begins. Commercial polymers are usually significantly above their MW_C . [74]

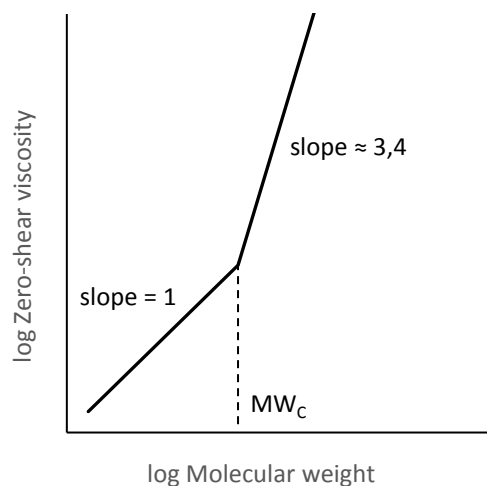


Figure 13. *The relationship between MW and the zero-shear viscosity of a polymer. Adapted from [74] and [75].*

The characteristic shear rate marks the shear rate at which the Newtonian plateau ends, and the shear-thinning region begins. The location of the characteristic shear rate is affected by the MW. When the material is at rest the polymer chains achieve an equilibrium state. When the material is deformed, small local stresses are formed. If the material is given enough time, the stresses relax during what is called a relaxation time. If the material is deformed slowly and the relaxation time is short enough, the stresses have plenty of time to relax. This means entanglements are destroyed and formed at an equal pace as the chains flow in and out of each other's sphere of influence. This causes the entanglement density to remain constant and the structure of the melt is maintained. If the shear rate is too fast in relation to the relaxation time the stresses do not have time to relax, and the flow pulls the chains so that they become more aligned. This means more entanglements are destroyed than are formed, causing the entanglement density to decrease, which lowers the resistance to flow and thus viscosity. The relaxation time decreases as the number of entanglements on a chain increases, which again increases with the MW. In other words, the longer the chains are, the longer it takes for them to relax. This means that for a polymer with a high MW the relaxation time will be too long compared to the shear rate earlier than for a polymer with a low MW, and the shear-thinning region will begin earlier. [74]

As the curve transitions from the Newtonian plateau into the shear-thinning region, a knee is formed on the curve. The shape of this knee is affected by the MWD. A narrower MWD will result in a sharper knee than a broader MWD (Figure 14). For a broad MWD the deviation from the Newtonian plateau will begin earlier than for a narrow MWD, and the transition from Newtonian to shear-thinning behaviour will occur over a larger range of shear rates. [74] [75] [76] [77] This is caused by the wider range of relaxation times that a polymer with a broader MWD will have. The relaxation times of the longer chains will become too long in relation to the shear rate earlier and these chains will start to lose entanglements, while the shorter chains can still maintain their structure. Slowly more and more chains will no longer have time to relax, until all chains are in the shear-thinning region. For a narrower MWD the range of shear rates at which the chains can no longer relax properly is much smaller, and thus the knee is sharper. [74]

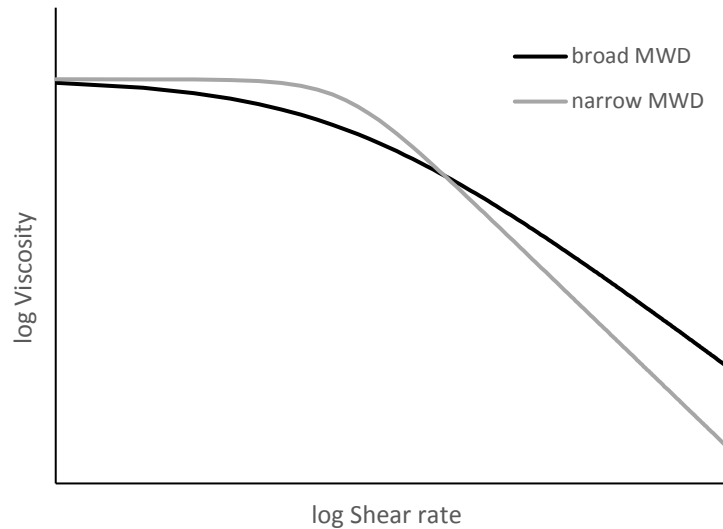


Figure 14. *The effect of the MWD on the shape of the viscosity curve. Adapted from [74], [75], [76], and [77].*

Finally, the slope of the curve in the shear-thinning region describes how dependent the viscosity is on the shear rate. As shear-thinning is caused by the net decrease in entanglements, the slope of the shear-thinning region indicates how easily disentanglement happens as a consequence of a higher shear rate. How easily disentanglement happens, and how steep the slope of the shear-thinning region is, depends on the MWD, as can be seen in Figure 14. A broader MWD will cause the slope to be smaller. [74] [76] [77] However, considerable controversy surrounds the question of the molecular mechanism that causes this change in the shear-thinning region [76].

As mentioned, the plasticizer and filler contents of the plastics also affect the viscosity. Plasticizer lowers the viscosity, whereas fillers increase it [78]. Since the materials will stay the same during the experiments, this will not affect the results. However, fillers can also affect the shape of the viscosity curve, which would be visible in the results even without a comparison curve of a sample without fillers. According to Shenoy [79], larger fillers would only increase the zero-shear viscosity of the curve due to hydrodynamic interactions between the particles and the polymer (Figure 15). Very small fillers also increase the zero-shear viscosity, but they have the additional effect of causing the Newtonian plateau to no longer be horizontal, and instead it slopes slightly. This is caused by the particle-particle interactions when the fine particles temporarily link together to form a network of finite strength. This effect is the strongest at very low shear rates where the shear stress is lower and declines towards higher stresses as the network is broken. This effect is shown in Figure 16.

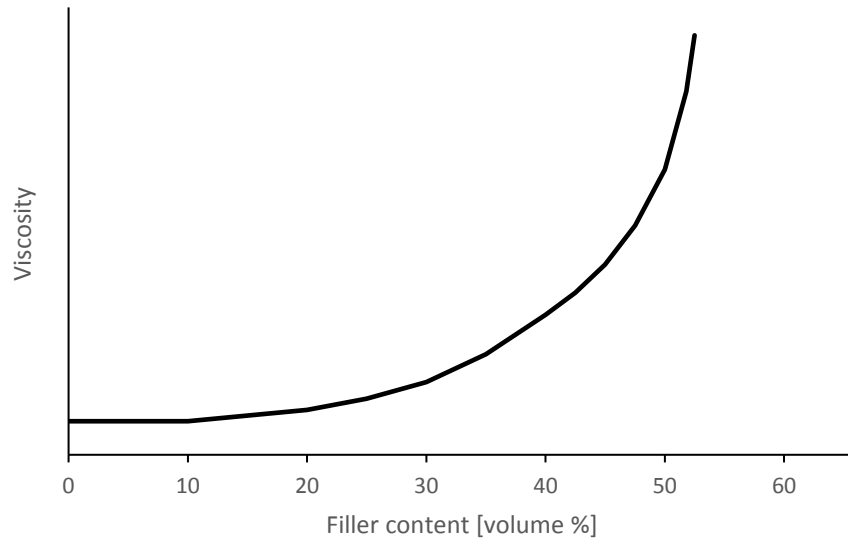


Figure 15. *The effect of filler content on the zero-shear viscosity. Adapted from [80].*

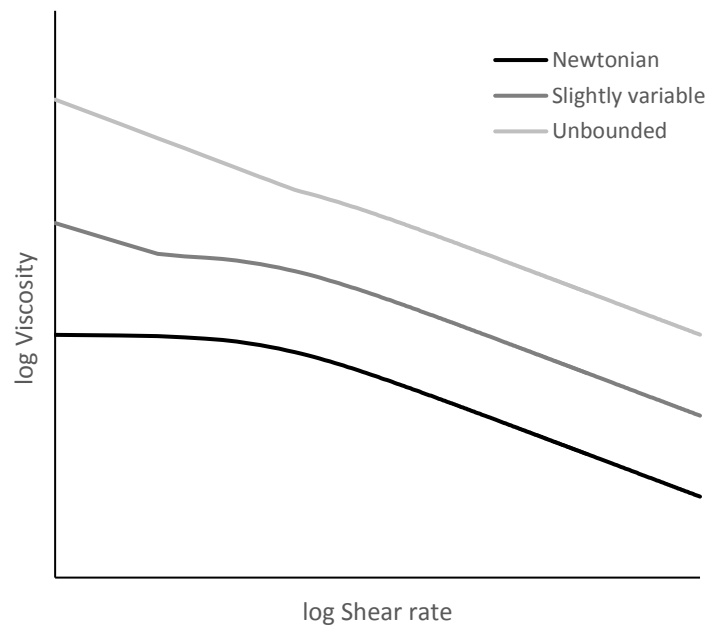


Figure 16. *A schematic showing the effects of very small fillers on the viscosity of plastics. Adapted from [79].*

The effects of fillers are divided into three categories: Newtonian, slightly variable, and unbounded. For the Newtonian curve the fillers do not have any visible effect on the shape of the curve. For the slightly variable curve the effect is obvious, but the beginning of the shear-thinning region is still visible. For the unbounded curve the effect of the filler covers the beginning of the shear-thinning region and hides it. [79]

3.3 Effect of variables on tensile properties

Many variables affect the tensile properties of a polymer. The internal variables include MW, MWD, crystallinity, crystal morphology, crosslinking, branching, copolymerization, plasticization, molecular orientation, and residual stresses [81] [82]. Additionally, the filler-content can have an effect on the properties [83]. The conditions external to the polymer influencing the tensile properties are temperature, speed of testing, type of deformation, pressure, stress and strain amplitude, thermal history, and surrounding atmosphere [81]. As mentioned in the previous section, the sample and testing conditions will remain the same between experiments, so the majority of these variables will not change significantly, except for MW and MWD. In addition to direct effects, MW can affect properties indirectly through crystallinity, since it decreases as MW increases [82] [84]. Additionally, orientation can affect properties, and it increases with MW [82]. Therefore, only the effects of MW and MWD on properties will be discussed here.

The basic relationship between MW and any of the tensile properties is the same (Figure 17). At very low MWs where the chains are not long enough to form entanglements the properties are independent of MW. The properties in this region also have very low values, since the chains being incapable of entangling means the polymer cannot carry a load, and thus has very low strength and elongation values. As the MW increases and entanglements start to form the properties start to increase with the MW, and it becomes possible to measure the properties. This happens because the entanglement density increases as the chain length available for entangling increases. The increasing number of entanglements causes there to be more resistance to flow, which increases the strength, and the stronger the polymer is the further it can strain before fracture. At some point the entanglement density becomes independent of the MW. This is also the point at which the tensile properties become independent of MW. Sometimes secondary processes can start to decrease the tensile properties again at very high MWs. [81]

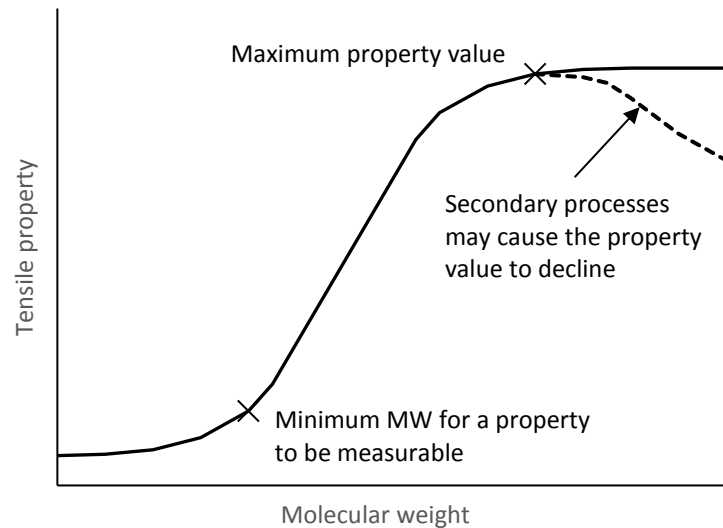


Figure 17. *The basic relationship between MW and tensile properties. Adapted from [81].*

For semicrystalline polymers the MW dependence of tensile properties is slightly more complicated. The crystalline regions also help keep the material intact due to the stronger interchain interactions. However, as mentioned, increasing the MW decreases crystallinity. So as the MW increases the source of strength in a semicrystalline polymer slowly switches from crystallites to entanglements. Still, the entanglement density, and thus MW, nonetheless affects the properties due to the amorphous polymer between the crystallites. The longer chains tend to crystallize first and the shorter chains accumulate at the edges of the crystallites. The shorter chains are therefore the ones that form the tie chains between the crystallites. The tie chains resist the crystallites slipping past each other during deformation, hence increasing the strength. Lowering the MW will decrease the number of tie chains, which will lower the strength of the material and tends to make it brittle. [81] [84]

Stress at yield and break, and strain at yield and break all mainly follow the basic relationship between MW and tensile properties, although this was not the case for all studies presented in [82] and [84]. Additionally, narrowing the MWD tends to increase these properties. However, the Young's modulus is significantly less dependent on MW and MWD directly. The modulus is either independent of MW and MWD, or the dependence might be small enough to be insignificant. Whether modulus increases or decreases with MW and MWD varies greatly. The degree of crystallinity in semicrystalline polymers is a more important factor, as modulus increases with crystallinity. [82] [84] In amorphous polymers where crystallinity is not a variable, orientation has been shown to affect modulus, which increases as the orientation increases [82].

The effect of fillers on the properties of the polymer depends very strongly on the polymer matrix. The reinforcing effect of fillers increases as the modulus of the polymer matrix decreases. For thermoplastics an increasing filler-content will usually decrease the strength and elongation, although in some cases fillers can reinforce the material, and cause the strength to increase. Fillers increase the modulus of the polymer. Fillers can also act as a nucleating agent, which will increase the crystallinity of the polymer. This will also increase the modulus, as was mentioned. [83]

3.4 Oxidation induction time

As a polymer is heated in the presence of oxygen, it will begin to oxidize after some time. This reaction is visible in the amount of heat needed to maintain the high temperature the polymer has been heated to. This can be used to determine the time it takes for a polymer to oxidise. This time is called the oxidation induction time (OIT). The experiment is done using a differential scanning calorimeter. OIT is determined by placing a sample and a reference material into an oven and heating them to a desired temperature in an inert atmosphere. Once the desired temperature is reached, the atmosphere is changed to air or oxygen. The atmosphere and temperature are then held steady. During this process the heat flow rate to the sample is measured constantly and plotted as a function of time. This is called the differential scanning calorimetry (DSC) curve. The experiment is continued until the dip caused by the oxidative reaction shows on the curve. OIT is measured as the time from the change in the atmosphere to the onset of the oxidative reaction (Figure 18). OIT is determined according to standard ISO 11357-6:2018. [85]

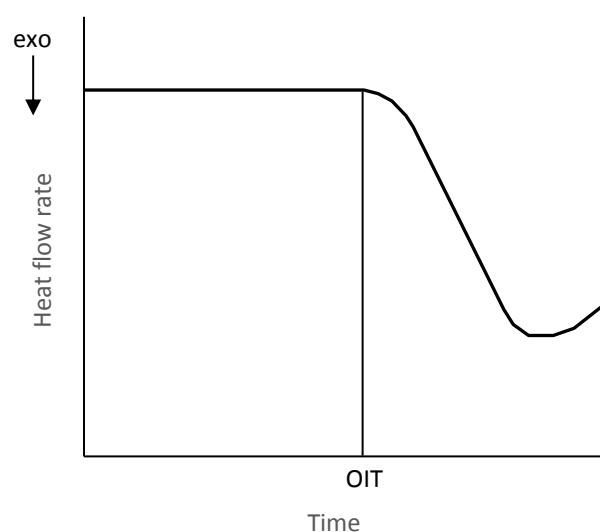


Figure 18. OIT on a heat flow rate-time curve. Adapted from [85].

3.5 Thermogravimetry

As a polymer is heated to very high temperatures in an inert atmosphere, thermal degradation will occur. Its weight will decrease as a result. If the change in weight is plotted as a function of temperature, the temperatures at which the different components of the sample will degrade can be studied, as well as the weight of the components and the unreacted residue at the end of the test. This is called a thermogravimetric (TG) analysis. The test is done by heating up the sample according to a desired temperature programme, and simultaneously weighing the sample in an inert atmosphere. [86]

4. ADDITIVES FOR RECYCLING WEEE PLASTICS

4.1 Antioxidants

Antioxidants are used in plastics to try to prevent the thermo-oxidative degradation during processing, and the oxidation occurring during the lifetime of the product. They are divided into primary and secondary antioxidants depending on the mechanism they use to limit oxidation. Primary and secondary antioxidants are often used together to provide most efficient protection. [87] [88] [89]

Primary antioxidants aim to stop the oxidation cycle by donating a hydrogen atom to the peroxy radical, thus creating a hydroperoxide without the need for the surrounding polymer chains to lose a hydrogen atom. Since a chain has no need to donate a hydrogen atom, no new free radical is formed, and the oxidation cycle stops. This reaction creates a hydroperoxide as well as turns the antioxidant into a radical, but both of these are significantly less reactive than the peroxy radical. The most common primary antioxidants are hindered phenols and aromatic amines. [87] [88] [89]

Hindered phenols consist of a phenol with side groups. The groups adjacent to the reactive OH-group shelter it slightly. This steric hindrance slows down the reactions the antioxidant partakes in. [87] [89] One of the first and simplest hindered phenols was 2,6-di-tert-butyl-4-methylphenol (BHT), shown in Figure 19. One of BHT's deficiencies is that it is very volatile due to its small size. The hindered phenols developed later are based on BHT-like structures. These later phenols have longer hydrocarbons as side groups to improve compatibility with polymers, and some phenols are multifunctional, which reduces volatility, since there are more reactive phenols in one larger molecule. [87] [88]

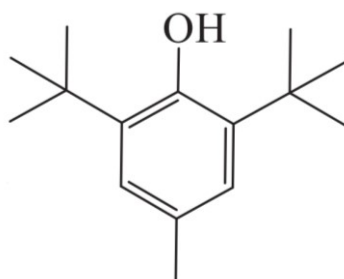


Figure 19. 2,6-di-tert-butyl-4-methylphenol (BHT) [87].

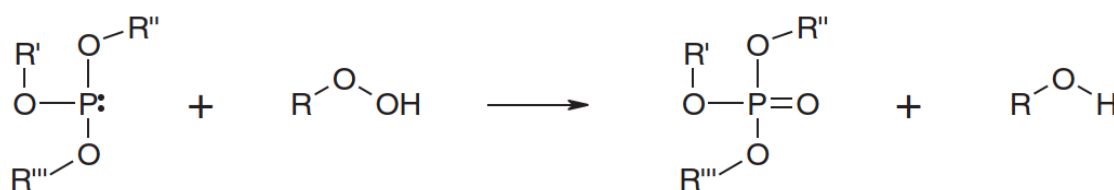
Aromatic amines donate a hydrogen atom from the NH-group of the molecule to eliminate the radical. They give a stronger protection against oxidation at higher temperatures

when compared to hindered phenols. However, they cause the plastic to discolour, which is why they are mainly used in applications, where the colour of the part is not important, or where it can be covered with a dark pigment. Most aromatic amines are not approved for food contact applications. They are mostly used in the rubber industry. [87]

Secondary antioxidants prevent oxidation by decomposing hydroperoxides into less reactive alcohols before the hydroperoxides can decompose into radicals, thus interrupting the oxidation cycle. As mentioned, secondary antioxidants work well in combination with primary antioxidants, since they further neutralize the hydroperoxides formed in the primary antioxidant reactions. The most common secondary antioxidants are phosphites and thioesters. [87] [88] [89]

Phosphites consist of a central phosphorus atom onto which three side groups are attached via oxygen atoms (Figure 20a). The phosphite reduces a hydroperoxide into an alcohol by allowing itself to be oxidized into a phosphate. Phosphites are susceptible to hydrolysis, which can be partially avoided by having bulkier side groups, since they will hinder the reaction. [87] [89]

a)



b)

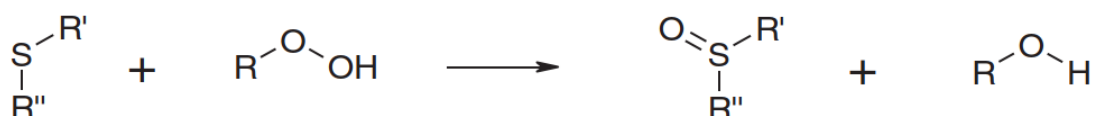


Figure 20. a) Phosphite and hydroperoxide reacting to form phosphate and alcohol. b) Thioester and hydroperoxide reacting to form sulphoxide and alcohol. [87]

Thioesters have a similar structure to phosphites, but the central atom is sulphur, and there are only two side groups (Figure 20b). Similarly to phosphites, thioesters are oxidized in the reaction to reduce hydroperoxides into alcohols. A disadvantage of thioesters is that they create odours, which will transfer onto the plastic. This restricts the applications it can be used in. [87] [89]

4.2 Chain extenders

Chain extenders are chemicals used to increase the MW of polymers, and thus adjust the rheological properties. They are divided into two groups depending on the type of reaction that causes the chain extension. The first group includes chemicals with a reactive functional group that reacts with a hydroxyl or carboxyl group of the polymer. These include epoxy-based chain extenders, isocyanates, anhydrides, oxazolines, imides, and phosphites. The second type causes chain extension by cross-linking through free-radical reactions. Peroxides are used in this manner. Another way to categorize chain extenders is by their functionality, and the polymer structure it enables. Bifunctional chain extenders only allow linear extension, and with multifunctional extenders branching is possible. [90]

Epoxy groups can react with both carboxyl and hydroxyl groups (Table 2) but the reaction with carboxyl groups is more efficient. The earlier epoxy-based chain extenders were tri-, tetra-, or octo-functional. Studies with these extenders established the higher efficiency of the carboxyl reaction. Later, multifunctional styrene-acrylic oligomeric epoxy chain extenders (Figure 21) were developed. These extenders can have a very high functionality, the number of reactive sites can be up to 20. In addition to increasing the MW, epoxy-based chain extenders are known to broaden the MWD. [90]

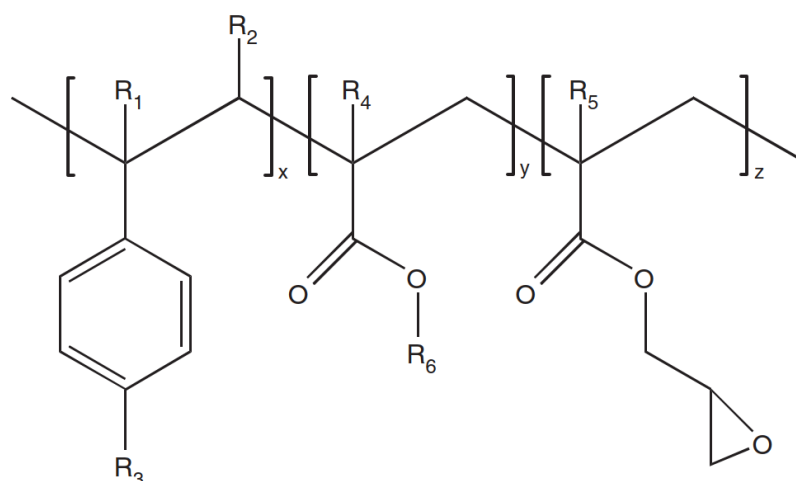
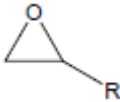
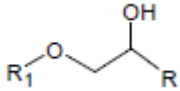
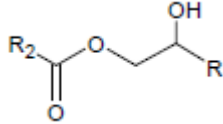
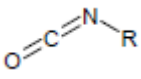
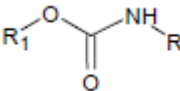
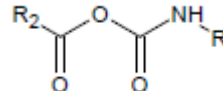
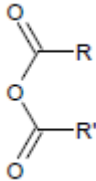
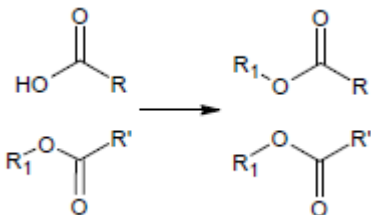
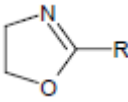
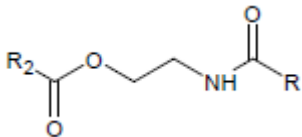
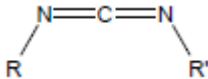
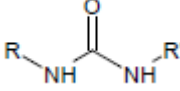
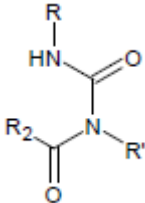
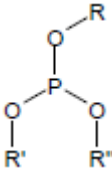
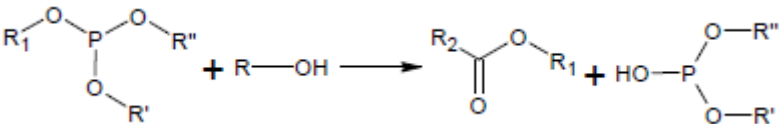


Figure 21. A schematic illustration of a multifunctional styrene-acrylic oligomeric epoxy chain extender [91].

Table 2. Reactions of the chain extenders with the hydroxyl and carboxyl groups on the polymer. Adapted from [90], [92], [88], [94], [95], [96], [97], and [98].

Chain extender	Reaction with the hydroxyl group	Reaction with the carboxyl group
	R_1-OH	$R_2-C(=O)OH$
 Epoxy group [90]		
 Isocyanate [92]		
 Anhydride group [93]		-
 Oxazoline group [94]	-	
 Carbodiimide [95] [96]		
 Phosphite [97] [98]		

Isocyanates are another very reactive chain extender group. The isocyanate group can react with both carboxyl and hydroxyl groups (Table 2). The reactions with hydroxyl

groups lead to the formation of urethane linkages, and the reactions with carboxyl groups create mixed anhydrides. The reaction with a hydroxyl group is more efficient. [90] [92]

Anhydrides can form reactive groups via ring-opening of the anhydride group. The reactive groups can react with hydroxyl groups (Table 2), but the reactivity is rather low. Pyromellitic dianhydride (PMDA) is the most common anhydride used as a chain extender. However, PMDA is hygroscopic and can thus absorb water. This can lead to hydrolysis and degradation of the polymer during processing. [90] The chain extension reaction happens in two steps. The ring-opening happens in the first step, where one half of the ring joins with a hydroxyl group, and the other forms a carboxyl group. In the second step the formed carboxyl group reacts with another hydroxyl group. PMDA is also known to broaden the MWD. [93]

Oxazolines can react with carboxyl groups through ring-opening reactions, forming ester-amide linkages (Table 2). They are usually used to modify oligomers during solution reaction, but they can also be used during melt processing. [90]

Carbodiimides can react with carboxyl groups (Table 2). Carbodiimides can also react with water and can thus reduce hydrolysis. The result of carbodiimide reacting with the hydroxyl group of water is shown in the table as the product of the reaction with hydroxyl. [95] [96]

In addition to acting as antioxidants, phosphites can also play the part of a chain extender. They can react with both carboxyl and hydroxyl groups (Table 2). Phosphites can cause both linear and branched extended chains. [90] The phosphite first reacts with a hydroxyl group, forming a phosphited polymer chain end and ROH. The phosphited chain end can then react with the carboxyl group of another chain. [97] [98]

Peroxides mainly lead to crosslinking between polymer chains. The peroxides decompose to peroxy radicals, which then abstract a hydrogen atom from the chain of a polymer. When two macroradicals meet they can combine, creating a C-C bond. The degree of crosslinking depends on the type and concentration of the peroxide, as well as the reaction conditions. Since the hydrogen abstraction can happen anywhere on the chain, the location of the bond is much more random compared to the bonds created by reactive functional groups. [90]

4.3 Graphene nanoplatelets grafted with maleic anhydride

Due to graphene's aromatic network, it is very stable, and thus difficult to functionalize. Several methods have been developed to overcome this hurdle, one of the most viable methods being the Diels-Alder reaction. [99] [100] The Diels-Alder reaction is the reaction

between a diene and an alkene (also called a dienophile) to form a cyclohexene derivative. The simplest example of this is the reaction between an ethene and a butadiene, shown in Figure 22. [101]

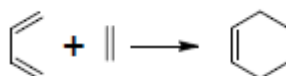


Figure 22. The Diels-Alder reaction between butadiene and ethene. Adapted from [101].

Graphene can fulfil both the diene and dienophile roles [102]. Maleic anhydride, however, can only act as dienophile. The functionalization process causes the delamination of graphite into graphene nanoplatelets. The functionalization reaction happens at the edges of the nanoplatelets, specifically on the armchair edges, instead of the zigzag edges (Figure 23). The maleic anhydride then hydrolyses into carboxyl groups. This improves graphene's dispersity in polar solvents. [99] [100]

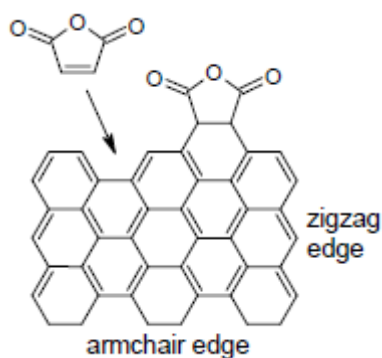


Figure 23. The Diels-Alder reaction of graphene and maleic anhydride on the armchair edge. Adapted from [99] and [100].

In addition to the filler properties of the graphene nanoplatelets, with maleic anhydride grafted onto the surface they can also function as chain extenders. The reaction through which the anhydride group reacts with the polymer is already shown in Table 2.

5. METHODS

5.1 Micro compounder and injection moulding machine

To injection mould the samples, the plastics were milled. They were first washed and dried, and then milled to a particle size of 2 mm. A Micro 5cc Twin Screw Compounder and a Micro 4 cc Injection Moulding Machine (Figure 24) from Xplore Instruments BV were used to make the tensile test samples and some of the rotational rheometer samples. The compounder has two conical, fully intermeshing screws. The temperature of the barrel can be controlled in 6 separate heating zones (3 zones on either side), and cooling is done either with air or water. The balance used to weigh the materials before processing was PB303-S/PH from Mettler Toledo LLC.



Figure 24. *The micro compounder (left) and the micro injection moulding machine (right) from Xplore Instruments.*

The rotating speed of the screws was 100 rpm for all samples, and the processing time was 2 minutes. The barrel was heated uniformly. Five samples of each plastic were produced for each sample set for tensile tests. The approximate dimensions of the samples are presented in Figure 25. Two to three rheometer samples were produced for each plastic-additive combination. They were approximately 25 mm in diameter and the thickness was 2 mm. The temperatures at which the plastics were processed are presented in Table 3.

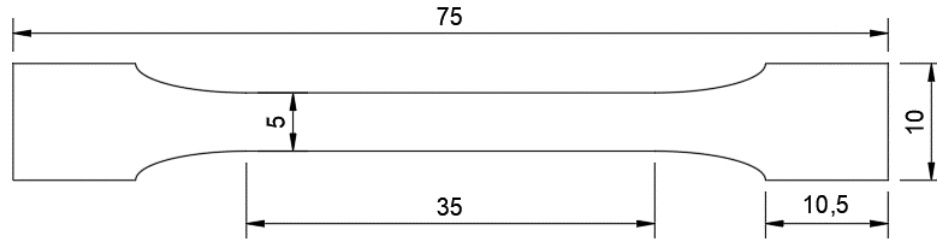


Figure 25. A scheme showing the approximate dimensions (in mm) of the tensile test samples produced with the micro compounder. The approximate thickness of the samples was 2 mm.

Table 3. The barrel and mould temperatures used in processing.

	Barrel temperature (°C)	Mould temperature (°C)
PP	190	40
PS	200	40
ABS	220	50
PC/ABS	265	60

As mentioned in Chapter 3, mechanical loading can cause degradation. The shear stresses in a micro compounder are higher than those in a full-sized injection moulding machine, and thus it will cause more degradation in addition to the oxidative degradation. However, the micro compounder was chosen as the method for processing the samples, because the amounts of recycled plastics available for the study were quite small, and the micro compounder requires a smaller amount of material.

5.2 Universal testing machine

Tensile testing of the samples was done according to the ISO 527-1 standard [103]. The tests were done using an Instron 5967 universal testing machine. A 2 kN load cell was used. An extensometer was used until strain 0,05 mm/mm. The stress was measured both as a function of the extensometer strain and the strain calculated using the original gauge length and the extension measured by the universal testing machine. The strains will from here on out be called extensometer strain and nominal strain. The loading speed was 10 mm/min.

5.3 Rotational rheometer

The viscosities of the materials were measured with the Physica MCR 301 rotational rheometer from Anton Paar. The measuring head used was CP25-4-SN3012, a conical

head with a diameter of 24,936 mm and a cone angle of 4,008°. The first measuring point lasted for 100 s, and the shear rate was 0,01 1/s. The last measuring point lasted for 2 s, and the shear rate was 100 1/s. The shear rate was increased in logarithmic steps (5 points/decade). There were 21 measuring points in total. Since the milled plastics appeared to be quite heterogeneous, more than one adjacent sample was tested for each plastic-additive combination to make sure the results would be accurate.

The testing temperature for PP was 210 °C, PS and ABS were tested at 230 °C, and PC/ABS was tested at 240 °C. The viscosities of plastics with additives were measured with discs injection moulded with the micro compounder. The viscosities of the plastics without additives were measured both directly from the milled plastics, and from injection moulded discs.

5.4 Simultaneous thermal analyser

A simultaneous thermal analyser (STA) was used to determine the OIT and to do a TG analysis. The equipment used was STA 449 F3 Jupiter from NETZSCH-Gerätebau GmbH. The samples were cut from the tensile testing samples after the tensile tests had been done.

The OIT was determined according to ISO 11357-6:2018. It was studied for the plastics without additives and the plastics with antioxidants. The tests began from 30 °C and the heating rate was 20 K/min. The samples were heated to 200 °C. The atmosphere was changed from nitrogen to oxygen at 18,5 min. The samples were held at the high temperature in the oxygen atmosphere for 60 minutes. The flow rate was 50 ml/min for all gases.

The TG analysis was done on the plastics without added additives according to standard ISO 11358-1:2014. The test temperature programme was the same for all plastics, and was such that it increased from 30 °C to 700 °C. The inert atmosphere was nitrogen, whose flow rate was 50 ml/min.

6. MATERIALS

6.1 Recycled plastics

The plastics studied in this thesis were PP, PS, ABS, and PC/ABS recycled from WEEE. As mentioned earlier in Chapter 2.2.3, the studied plastics were supplied by Kuusakoski Oy. They came in small pieces, the size varying between approximately 5 and 15 cm. They were milled as mentioned in Chapter 5.1. All black plastic or plastic containing bromine had been removed previously, leaving rather lightly coloured plastic fractions free from harmful, bromine containing fire retardants. Examples of the tensile samples made with the micro injection moulding machine are shown in Figure 26. The samples with antioxidants, chain extenders, or without additives all looked the same for a plastic type, so they are not shown individually.

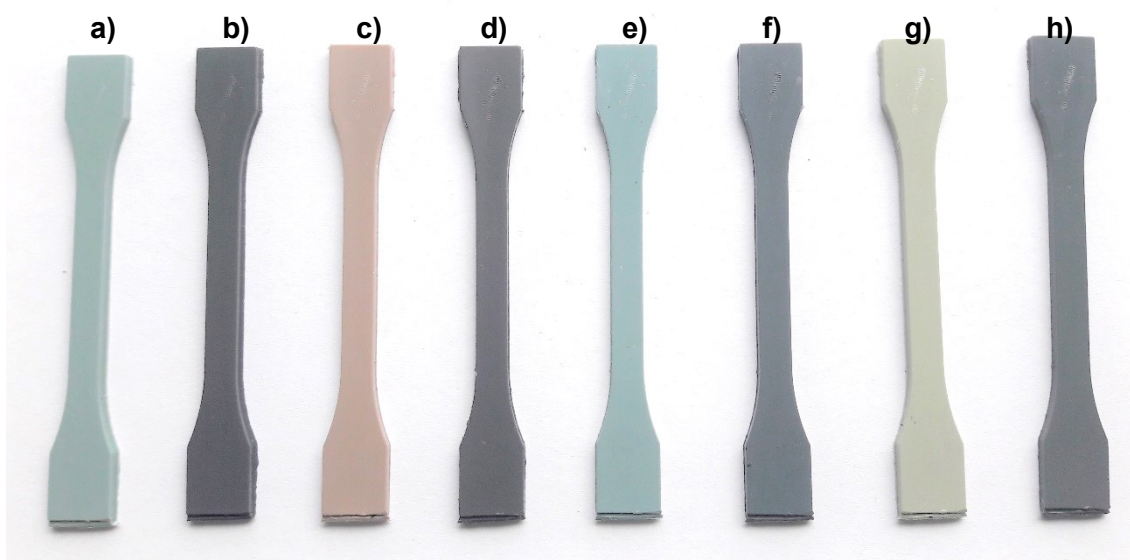


Figure 26. *Examples of the tensile testing samples made with the micro compounder. a and b are PP, c and d are PS, e and f are ABS, and g and h are PC/ABS. a, c, e, and g are examples of the plastics with antioxidants, chain extenders, or without additives. b, d, f, and h are examples of the plastics with graphene nanoplatelets grafted with maleic anhydride.*

6.2 Additives

Additives were used to try to decrease the effects of thermo-oxidative degradation during processing on the properties of the plastics. Three types of additives were studied, antioxidants (AO), chain extenders (CE), and graphene nanoplatelets grafted with maleic anhydride (GM). The AO and CE products were chosen based on a literature review. The AOs chosen were Irganox 1010 (AO 1) [104] – [113] and Irganox 1076 (AO 2)

[112] – [120]. The CEs originally chosen based on the review were Joncryl ADR 4370S [121] – [123] and Joncryl ADR 4368 [123] – [125], but they are not available in Europe, so Joncryl ADR 4400 (CE 1) and Joncryl ADR 4468 (CE 2) were chosen instead. Samples of these additives were kindly supplied by BASF Oy, and they were used as such without any further modification. GM was produced in the laboratory.

The AOs used are both sterically hindered primary phenolic AOs. Their structures are shown in Figure 27. AO 1 has four hindered phenolic groups in one molecule that can donate a hydrogen atom, whereas AO 2 only has one per molecule. As mentioned earlier in Chapter 4.1, the larger size of the AO 1 molecule decreases its volatility, which allows more of it to be of use during oxidation. Additionally, the long hydrocarbon tail of AO 2 improves its compatibility with the polymers. Both AOs are recommended to be used with a broad collection of polymers. Some physical properties of the antioxidants are shown in Table 4. [126] [127]

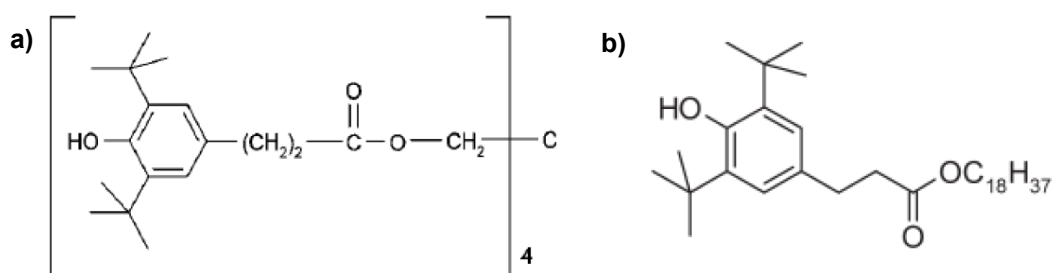


Figure 27. The molecular structures of the antioxidants a) AO 1, b) AO 2 [126] [127].

Table 4. Properties of the antioxidants [126] [127].

		AO 1	AO 2
Molecular weight	g/mol	1178	531
Melting range	°C	110-125	50-55

Both CEs were multi-functional reactive polymers. A schematic picture of their molecular structure has been shown in Chapter 4.2. They are recommended to be used with polycondensation polymers, but they can also be used with other thermoplastics. Their properties are shown in Table 5, including the epoxy equivalent weights (EEW), which depict how many reactive epoxy groups there are on a chain. CE 1 has a medium EEW, which correlates with a medium number of epoxy groups on a chain, whereas CE 2 has a low EEW, meaning the number of epoxy groups is high. Since the MW of CE 2 is also higher, this indicates CE 2 will create more cross-linking as more polymers can attach onto one chain. Table 5 also shows the properties of Joncryl ADR 4370S and Joncryl ADR 4368, which were not chosen for this study, for comparison. As can be seen, the chosen CEs both had significantly higher EEWs than Joncryl ADR 4370S and 4368 do. This is likely

due to the chosen CEs also having significantly higher MWs, meaning there is more space on the chain for epoxy groups. [128] [129] [130]

Table 5. *Properties of the chain extenders [128] [129] [130].*

		CE 1	CE 2	4370S	4368
Molecular weight	g/mol	7100	7250	6800	6800
Glass transition temperature	°C	65	59	54	54
Epoxy equivalent weight	g/mol	485	310	285	285

GM was produced by first measuring 2 g of graphene nanoplatelets (from Sigma-Aldrich, grade C-300) and 6 g of maleic anhydride (from VWR International LLC). The materials were ground into a fine powder and mixed together. Next, the mixture was heated in 180 °C for 3 hours. After this the powder was mixed into 500 ml of de-ionized water. The mixture was sonicated (Q700 sonicator from Qsonica) at 25 °C temperature, at an amplitude of 50 % (corresponding to about 40 W of power) for 75 minutes, which made the total energy added into the mixture 180 000 J. The mixture was then centrifuged (CompactStar CS4 centrifuge from VWR) at 6500 rpm for 10 minutes. This was done to rinse off the excess maleic anhydride, and to separate the GM from the maleic anhydride-rich water. After removing the separated water, its pH was measured, new de-ionized water was mixed into the GM, and it was centrifuged again. This was done repeatedly until the pH of the separated water was the same as the pH of the pure deionized water added to the GM. Finally, the remaining water was evaporated in an oven at 50 °C.

The amounts of additives used in this study were based on a literature survey. The previous literature reviewed to decide the amounts of AOs used was [104] – [120]. The literature survey to decide the CE quantities was divided into two parts. First, the articles where Joncryl ADR 4370S and Joncryl ADR 4368 were used with PP, PS, ABS, and PC/ABS were reviewed [121] – [125], and then a handful of articles was surveyed, where Joncryl ADR 4400 and Joncryl ADR 4468 were used with a variety of polymers (mainly PLA, PET, and PBT) [131] – [142]. No articles were found where Joncryl ADR 4400 and Joncryl ADR 4468 were used with PP, PS, ABS, or PC/ABS. Based on this review two quantities were chosen to be used in the experiments, 0,5 w% and 1 w%. These quantities were used for both the AOs and the CEs. For GM only one quantity was studied, 0,5 w%.

7. TESTING RECYCLED WEEE PLASTICS

The properties of the samples were tested from both the recycled plastics without additives and the recycled plastics with additives. The results of the samples with additives were then compared to the results of the samples without additives to see how they affect the properties.

7.1 Rheological properties

As mentioned in Chapter 3.2, changes in MW and MWD would cause changes in the zero-shear viscosity, the slope of the shear-thinning region, and the shape of the knee between the Newtonian plateau and the shear-thinning region. This study focuses on the differences in the zero-shear viscosity and the Power-law index, which describes the slope of the shear-thinning region.

7.1.1 Viscosities of additive-free plastics and the effect of fillers

The viscosities of the plastics with additives had to be measured from injection moulded discs in order to mix in the additives, but the viscosities of the additive-free samples could be also measured directly from the milled plastics. This was done to see how the processing would affect the viscosities, since the discs would be processed one time more than the milled plastics are. The comparisons are shown in Figure 28. Only one curve of the adjacent samples for each material is shown in the figure, which shows the curves that best describe each material in order to reduce visual clutter. All viscosity results can be seen in Annex B.

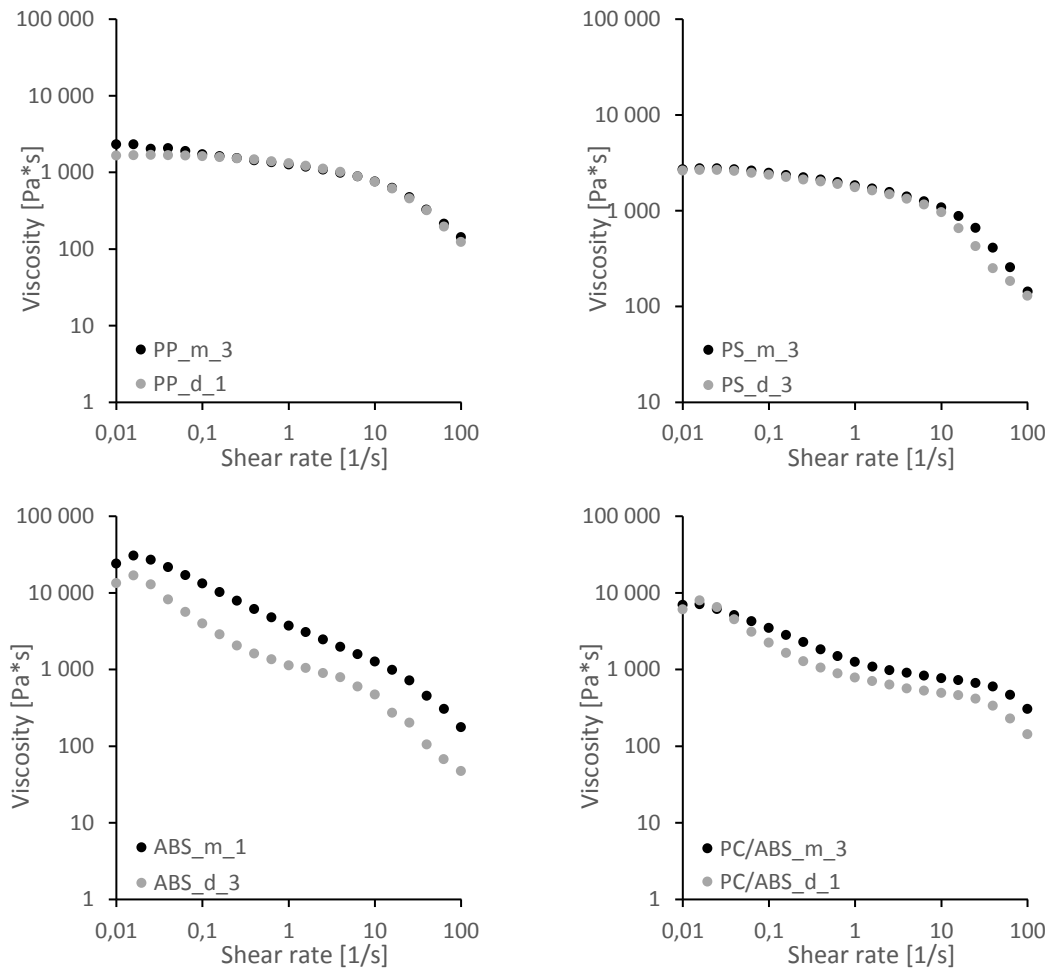


Figure 28. Comparing the viscosity curves measured from the milled plastics (m) and the plastics injection moulded into discs (d).

The processing seems to be having a bigger effect on ABS and PC/ABS than it does on PP and PS. The curves for PP and PS mainly overlap, whereas for ABS and PC/ABS there is a clearer difference. However, the viscosity curves measured from discs are still lower for all plastics, implying that the processing has caused some chain scission, thus lowering the viscosity.

Another significant detail visible from the curves in Figure 28 is the shape of the Newtonian plateau. For each plastic the figure shows the Newtonian plateau, which is typically horizontal, and a small section of the beginning of the shear thinning region at the higher shear rates. For PP and PS, the plateau is clearly visible. However, for ABS and PC/ABS the beginning of the curve is not horizontal. As mentioned in Chapter 3.2, fillers of a very fine size can cause an effect like this in the viscosity curve. For both ABS and PC/ABS the knee where the Newtonian plateau ends, and the shear-thinning region begins is visible, which matches with the “slightly variable” curve in Figure 16, meaning there likely

is some amount of filler in the recycled materials. In order to verify that this effect truly is due to fillers, a TG analysis is done, which is presented in Chapter 7.2.

7.1.2 Zero-shear viscosities

The viscosities of the plastics with additives were measured next. The viscosity curves best describing each plastic-additive combination are shown in Figure 29. Figure 30 shows a closeup of the PS curves, since they are very close together in Figure 29. Here the curves are separated so that one figure has the samples with CEs and GM, and the other has the samples with AOs. The additive-free samples are shown in both figures. Note the different y-axis values compared to Figure 29.

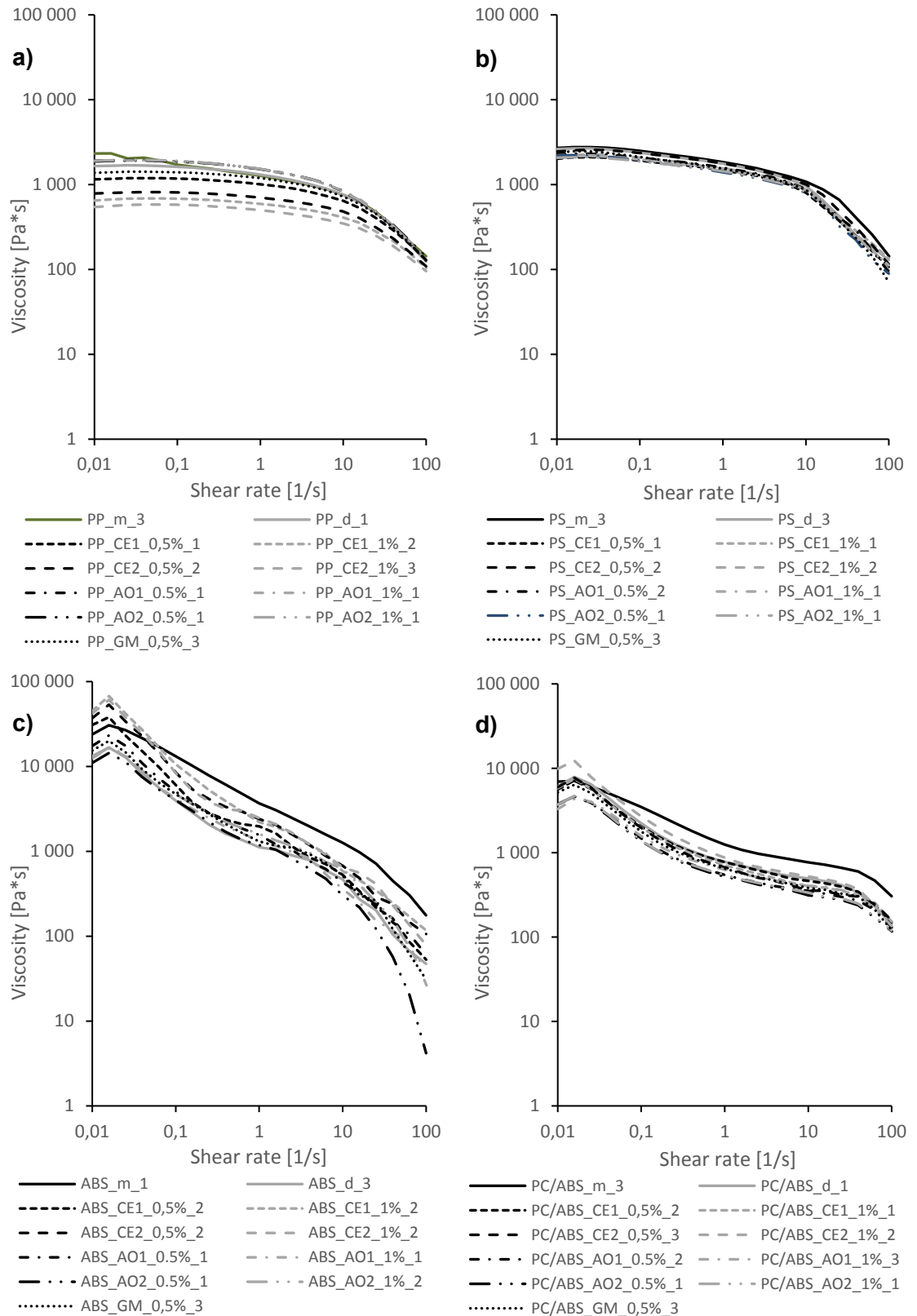


Figure 29. Comparison of the viscosity curves of samples with and without additives. The subindexes “m” and “d” signify the additive-free samples’ viscosities measured from milled plastic and injection moulded discs, respectively. a) PP, b) PS, c) ABS, d) PC/ABS.

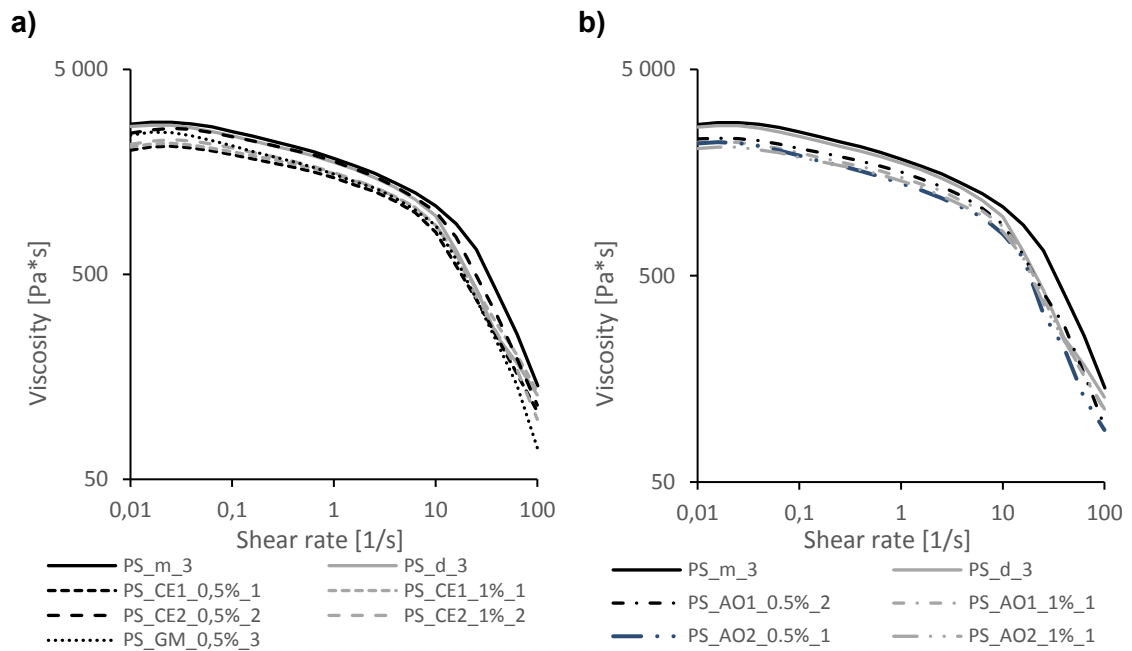


Figure 30. The viscosity curves of the PS samples with and without additives separated so that the curves are more visible. a) Samples with CEs and GM, b) samples with AOs. Both figures have the additive-free curves.

The viscosity curves measured from the milled plastics tend to be among the highest curves for each plastic, since they have endured less processing. The viscosity curves of the plastics with additives as well as the additive-free plastics whose viscosity was measured from the injection moulded discs have been brought to lower levels due to processing. There is quite a bit of variation in the viscosities of the plastics with additives, implying that some of the additives reverse or prevent the effects of thermo-oxidative degradation better than others. PS has the most uniform results, since the curves overlap significantly (Figure 29b), indicating the effect of the additives has little variance. PP and ABS have the largest differences between the different curves.

The shear viscosity curves for both ABS and PC/ABS have some irregularity at low shear rates. The irregularity forms a small bump at the beginning of each curve, where the second data point is higher than the first and third. This can be seen on the viscosity curves of all ABS and PC/ABS samples, but not on the curves for PP and PS. This indicates that the effect is not caused by the measuring equipment, since all measurements were done on the same equipment, nor is it an error during testing, since it happens so consistently for all ABS and PC/ABS samples. Thus, it must be related to the plastics themselves.

To better compare the results, the zero-shear viscosities were calculated as averages from the repeated tests. They are shown in Table 6. The zero-shear viscosities of PP and PS were read directly from the test data at 0,01 1/s since the Newtonian plateaus

for them were so clear. For ABS and PC/ABS the values were calculated by taking an average of the first three data points to minimize the effect of the irregularities causing the bump at the beginning.

Table 6. The absolute zero-shear viscosity values and standard deviations of the plastic-additive combinations, and how they compare to the viscosities of the additive-free plastics.

Additive	PP			PS		
	absolute (Pa*s)	milled (%)	disc (%)	absolute (Pa*s)	milled (%)	disc (%)
milled -	2215 ± 387	100	108	2833 ± 232	100	106
disc -	2050 ± 390	93	100	2680 ± 85	95	100
CE 1 0,5 %	1262 ± 275	57	62	2083 ± 83	74	78
CE 1 1 %	602 ± 48	27	29	2060 ± 30	73	77
CE 2 0,5 %	755 ± 77	34	37	2347 ± 68	83	88
CE 2 1 %	553 ± 33	25	27	2197 ± 81	78	82
AO 1 0,5 %	1910 ± 0	86	93	2327 ± 38	82	87
AO 1 1 %	1890 ± 20	85	92	2200 ± 10	78	82
AO 2 0,5 %	1895 ± 15	86	92	2300 ± 110	81	86
AO 2 1 %	2035 ± 125	92	99	2080 ± 10	73	78
GM 0,5 %	1430 ± 78	65	70	2373 ± 103	84	89
Additive	ABS			PC/ABS		
	absolute (Pa*s)	milled (%)	disc (%)	absolute (Pa*s)	milled (%)	disc (%)
milled -	29550 ± 1630	100	200	7283 ± 698	100	107
disc -	14744 ± 345	50	100	6785 ± 38	93	100
CE 1 0,5 %	34522 ± 14159	117	234	5947 ± 385	82	88
CE 1 1 %	44667 ± 8694	151	303	6460 ± 100	89	95
CE 2 0,5 %	40283 ± 1083	136	273	6329 ± 141	87	93
CE 2 1 %	42544 ± 4722	144	289	9778 ± 956	134	144
AO 1 0,5 %	17689 ± 2929	60	120	4722 ± 760	65	70
AO 1 1 %	13383 ± 650	45	91	3856 ± 21	53	57
AO 2 0,5 %	12050 ± 183	41	82	4193 ± 100	58	62
AO 2 1 %	13583 ± 817	46	92	4084 ± 75	56	60
GM 0,5 %	15300 ± 1310	52	104	6024 ± 546	83	89

Table 6 shows how the viscosities of the different plastic-additive combinations compare to each other, and how they compare to the viscosities of the additive-free plastic sam-

ples. The “absolute” column shows the absolute viscosity values determined as mentioned earlier as well as standard deviations. In general, the standard deviations of the viscosities are quite small compared to the differences between the absolute values. In the “milled” and “disc” columns the viscosities have been normalized with the viscosities measured from the milled plastics or the injection moulded discs, respectively, to see how the viscosities of the plastics with additives compare with the additive-free samples. The grey bars are meant to help visualize the differences between different additives.

Patterns can clearly be seen with how different additives have managed to preserve the viscosity of the less processed sample without additives. For PP the additives that work best are the AOs. They have reduced the effect of the additional processing step significantly compared to most of the CEs, the viscosities having fallen 8 – 15 % of the milled additive-free viscosity, and 1 – 8 % of the disc additive-free viscosity. GM and 0,5 % of CE 1 have also reduced the effects of thermal oxidation somewhat, but not quite as well as the AOs have, the viscosities being 57 – 70 % of the original ones. The viscosities of the other samples with CEs have decreased the most, by about 70 %.

With PS all additives have been equally beneficial, the viscosities averaging around 80 % of the originals. This is in line with the observations earlier from Figure 29b, where it was noted, that the entire viscosity curves, and not just the zero-shear viscosities, were very uniform for all samples.

For ABS the difference in the viscosity curves measured from the milled plastics and the injection moulded discs causes some variation in the results, depending on which additive-free sample the viscosities are compared to. Since the zero-shear viscosity of the milled sample is two times higher than the zero-shear viscosity of the injection moulded disc sample, the effects of the additives seem much higher when compared to the viscosity measured from the disc. However, the relative efficiency of the additives remains, and it can be seen that the CEs were more effective than AOs or GM. When looking at the zero-shear viscosities the CEs have increased the viscosity by 17 – 51 % when compared to the milled sample, and by 134 – 203 % when compared to the disc sample. When comparing the whole viscosity curves of the samples with additives to the viscosity curve of disc sample, the CEs increase the viscosity quite evenly along the whole curve, whereas when comparing them to the viscosity curve of the milled sample, they only increase at the lower shear rates as can be seen in Figure 29c. At higher shear rates the viscosity curves of the chain extended ABS samples fall below the curve of the additive-free milled sample. When comparing the zero-shear viscosities of the samples with AOs and GM to the disc sample, it can be seen, that GM and 0,5 % of AO 1 have increased the viscosity by 4 % and 20 %, respectively. The other AOs decreased it by 8 – 18 %.

The viscosity curves of the additive-free plastics for PC/ABS also had a significant difference between them in Figure 28, but in this case they had very similar zero-shear viscosities, so the effect is not as visible in Table 6 as it was for ABS. For PC/ABS the effective additives were the CEs and the GM, whose zero-shear viscosities have decreased by 7 – 18 % or 5 – 12 % when compared to the milled sample or the disc sample, respectively. The exception to this was the sample with 1 % of CE 2, whose viscosity increased by 34 % or 44 %. The viscosities of the samples with AOs decreased by 35 – 47 % when compared to the milled sample, and 30 – 43 % when compared to the disc sample. PC/ABS had only one zero-shear viscosity above the viscosity of the additive-free milled sample, but as before, this effect was only visible at lower shear rates, and at higher shear rates the viscosity curve of the milled sample was higher. Additionally, in the case of PC/ABS this phenomenon did not seem to be related to CEs universally, since it only occurred with 1 % of CE 2.

7.1.3 Power-law indices

The Power-law indices were calculated according to the procedure presented in Annex C. The Power-law index is the variable in the Power-law equation that describes the steepness of the shear-thinning region. The index varies between 0 and 1, and the lower the index is the steeper the shear-thinning region is. As mentioned in Chapter 3.2, the steeper the slope is, the easier it is for the entanglements to disappear during shearing. The Power-law equation is shown in Equation 1.

$$\eta = K\dot{\gamma}^{n-1} \quad (1)$$

η : viscosity [Pa*s]

K : consistency factor [Pa*sⁿ]

$\dot{\gamma}$: shear rate [1/s]

n : Power-law index [-]

Unfortunately, the Power-law indices calculated in this study are not very reliable for two reasons. The first reason is that the viscosity curves mainly show the Newtonian plateau with just the beginning of the shear-thinning region. This means that only a few data points are available for calculating the Power-law indices. In this case the last three data points at the highest shear rates were used. Since the curves only show the beginning of the shear-thinning region, this region will likely be at least partially still affected by the curve of the knee where the Newtonian plateau changes into the shear-thinning region. This seems to be the case especially for ABS and PC/ABS, whose shear-thinning region seems to begin slightly later (Figures 29c and 29d). The second reason is that when samples are studied on a rotational rheometer, edge fracture begins to occur at shear

rates 1 – 10 1/s, which makes the viscosity results less reliable at higher shear rates. The three data points used to calculate the Power-law indices are at shear rates 40 – 100 1/s, so they will be affected by the edge fracture. For these reasons, the Power-law indices can be used to compare the additives within this study, but do not necessarily accurately describe the plastics' shear-thinning behaviour. The average Power-law indices are shown in Table 7.

Table 7. The absolute Power-law indices and standard deviations of the plastic-additive combinations, and how they compare to the indices of the additive-free plastics.

Additive	PP			PS		
	absolute (-)	milled (%)	disc (%)	absolute (-)	milled (%)	disc (%)
milled -	0,093 ± 0,064	100	400	0,041 ± 0,071	100	30
disc -	0,023 ± 0,033	25	100	0,138 ± 0,108	336	100
CE 1 0,5 %	0,090 ± 0,045	97	387	0,141 ± 0,055	343	102
CE 1 1 %	0,264 ± 0,035	284	1134	0,108 ± 0,078	261	78
CE 2 0,5 %	0,168 ± 0,029	181	724	0,006 ± 0,008	14	4
CE 2 1 %	0,247 ± 0,017	265	1061	0,002 ± 0,003	5	2
AO 1 0,5 %	0,012 ± 0,012	13	50	0,000 ± 0,000	0	0
AO 1 1 %	0,018 ± 0,018	20	79	0,116 ± 0,035	281	84
AO 2 0,5 %	0,026 ± 0,026	28	113	0,041 ± 0,041	100	30
AO 2 1 %	0,002 ± 0,002	2	7	0,084 ± 0,078	203	60
GM 0,5 %	0,045 ± 0,018	48	193	0,045 ± 0,018	109	32
Additive	ABS			PC/ABS		
	absolute (-)	milled (%)	disc (%)	absolute (-)	milled (%)	disc (%)
milled -	0,027 ± 0,031	100	47	0,309 ± 0,070	100	240
disc -	0,058 ± 0,042	214	100	0,129 ± 0,029	42	100
CE 1 0,5 %	0,146 ± 0,207	542	253	0,122 ± 0,058	39	95
CE 1 1 %	0,111 ± 0,082	411	192	0,148 ± 0,148	48	115
CE 2 0,5 %	0,033 ± 0,033	121	57	0,312 ± 0,027	101	243
CE 2 1 %	0,027 ± 0,021	100	46	0,069 ± 0,098	22	54
AO 1 0,5 %	0,040 ± 0,057	149	70	0,151 ± 0,111	49	117
AO 1 1 %	0,000 ± 0,000	0	0	0,163 ± 0,057	53	127
AO 2 0,5 %	0,000 ± 0,000	0	0	0,177 ± 0,049	57	138
AO 2 1 %	0,000 ± 0,000	0	0	0,229 ± 0,032	74	178
GM 0,5 %	0,000 ± 0,000	0	0	0,050 ± 0,038	16	39

As before, the table includes the averages and standard deviations of the absolute Power-law index values. For the indices the standard deviations were quite high when compared to the differences between the absolute values. This decreases the reliability of the results, but they can still be used to make indicative comparisons between the samples. In the “milled” and “disc” columns the absolute values have been compared to the indices determined from the additive-free milled and disc samples, respectively. The grey bars visualize the differences.

The effect of the extra processing step done on the additive-free disc samples is more significant for the Power-law index than it was for the zero-shear viscosity, and the direction in which the index changes is not always the same. For PP and PC/ABS processing causes the index to decrease, for PP to 25 % and for PC/ABS to 42 % of the indices of the milled samples. Conversely, the indices of PS and ABS increase with processing, for PS to 336 % and for ABS to 214 % of the indices of the milled samples.

For PP the sample with 0,5 % of CE 1 kept the index at approximately the same level as the index of the milled sample, and for the other samples with CEs the indices increased to about two to three times the index of the milled sample. Adversely, the indices of the samples with AOs and GM are significantly lower, ranging from 2 % to 48 % when compared to the index of the milled sample. When comparing the indices of the samples with CEs to the index determined from the disc samples, they have all increased, the percentages ranging from 387 % to 1134 %. Additionally, the indices of the samples with GM and 0,5 % of AO 2 have increased above the additive-free disc sample, but not above the milled sample. Generally, the AOs have decreased the index the most.

In the case of PS, the processing caused the Power-law index to increase. However, adding the additives seems to have then lowered the indices back down below the index of the additive-free disc sample. The exception to this is the sample with 0,5 % of CE 1, whose index stayed at about the same level (102 %) when compared to the disc sample. The additives, that returned the indices closest to the index of the less processed milled sample were 0,5 % of AO 2 and GM, whose indices were 100 % and 109 % when compared to the milled sample, respectively. The additives that decreased the index significantly below the one of the additive-free milled samples were CE 2 and 0,5 % of AO 1. Overall, the indices varied in a way that cannot be linked to the additive types.

Processing of ABS also caused the Power-law index to increase. Once again, most of the additives caused the index to decrease significantly below the index of the disc samples, except for the samples with CE 1. 1 % of CE 2 returned the index back to the same level as the index of the less processed milled sample. All samples with GM and AOs,

except the one with 0,5 % of AO 1, decreased the index even below the index of the milled sample.

For PC/ABS processing caused the Power-law index to decrease. Most additives caused the index to then increase again when comparing to the additive-free disc sample. The exceptions to this were 0,5 % of CE 1, 1 % of CE 2, and GM, all of which decreased the index further. Even though most additives slightly reversed the effects of processing, only 0,5 % of CE 1 returned the index to the same level as the less processed milled sample. GM decreased the index the most.

7.2 Thermal properties

7.2.1 Oxidation induction times of samples with antioxidants

The OITs of the samples with and without AOs were measured. The results are shown in Figure 31. The test duration was 60 minutes, but oxidation happened in the first 30 minutes, so only this section is shown.

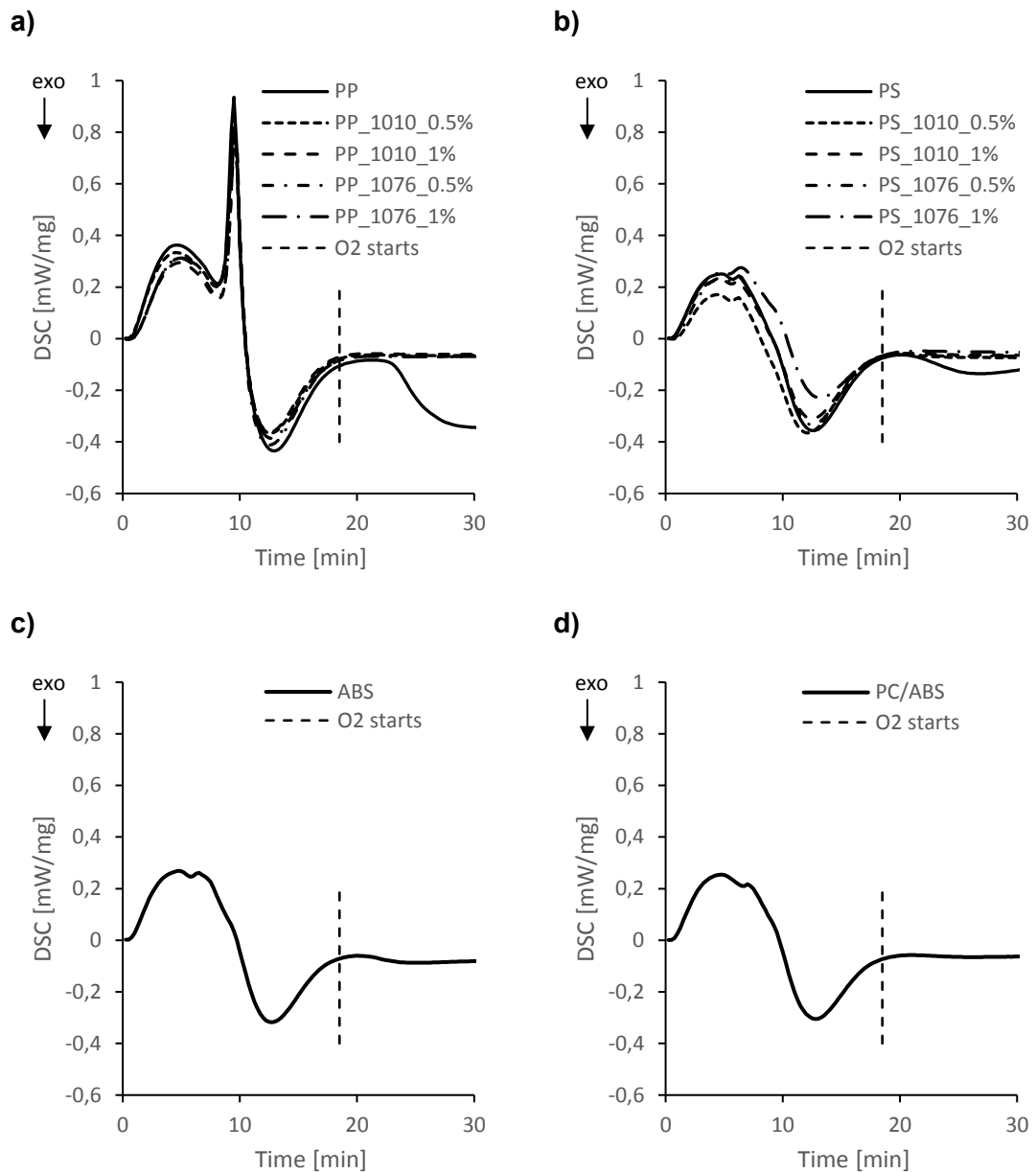


Figure 31. The DSC curves to determine OITs of a) PP, b) PS, c) ABS, and d) PC/ABS

The figure shows the DSC curves of the plastics, as well as where the atmosphere changes from nitrogen to oxygen (vertical dotted line). It can be seen that PP and PS without AOs oxidize quite quickly after contact with oxygen, their OITs being 4,2 min and 2,0 min, respectively. The AOs significantly improved their ability to resist oxidation, since the samples with AOs did not oxidize at all during the 60-minute heating period. ABS and PC/ABS did not oxidize at all even without AOs at the testing temperature. However, ABS and PC/ABS were both processed at temperatures above the testing temperature, so the lack of oxidation here does not necessarily signify a lack of oxidation

during processing. The tests were not done in a higher temperature due to equipment constraints.

7.2.2 Thermogravimetric analysis of additive-free samples

A TG analysis was done to investigate if the sloping of the Newtonian plateaus of ABS and PC/ABS can be explained by fillers. The measured TG curves are shown in Figure 32.

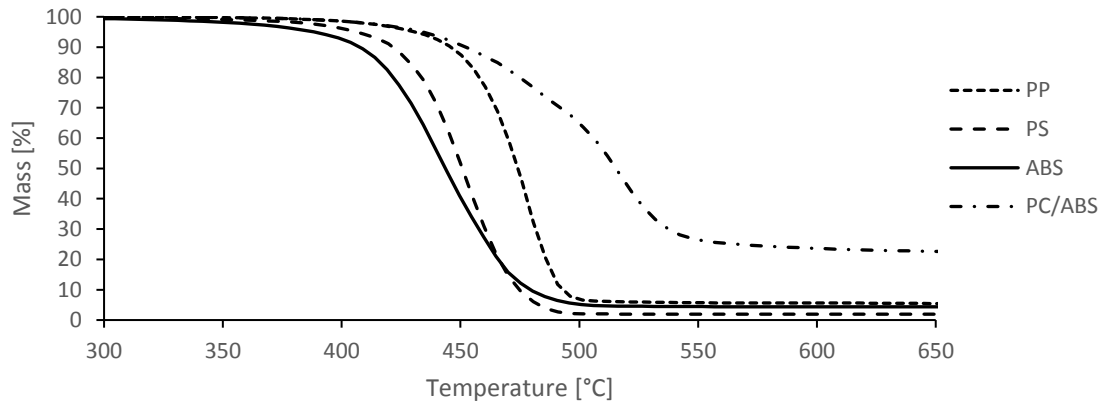


Figure 32. TGA curves of the additive-free plastics

The residual masses for PP, PS, ABS, and PC/ABS were 5,1 %, 1,9 %, 4,3 %, and 22,3 %, respectively. This implies that all of the samples had at least some fillers in them, PC/ABS being the most filled material. This suggests that at least the sloping of the PC/ABS curve's Newtonian region could be caused by fillers. When it comes to ABS, it seems as though the slope of its Newtonian region cannot be caused by the fillers, since the filler content of ABS is at the same level as the filler contents of PP and PS, whose Newtonian plateaus were horizontal. However, as was mentioned in Chapter 3.2, whether fillers cause the Newtonian region to slope depends on the particle size of the filler, small fillers being the ones that cause the sloping, while larger fillers only increase the zero-shear viscosity. Therefore, even if PP, PS, and ABS all have relatively similar filler contents, it could be that the particle size of the fillers in ABS is small enough to cause the sloping, whereas in PP and PS the fillers are too large to induce this effect.

7.3 Mechanical properties

7.3.1 Modulus

Tensile tests were performed, and the mechanical properties were determined according to ISO 527-1 [103]. The extensometer malfunctioned while measuring a few samples, and so the data of these samples was left out when determining yield values using the

extensometer strain. Figure 33 shows the stress-extensometer strain curves best describing each plastic-additive combination, all results can be seen in Annex D, which also indicates the samples which were left out due to extensometer malfunction. The figure shows both the whole stress-extensometer strain curve until the removal of the extensometer, as well as the beginning of the curve where modulus is determined.

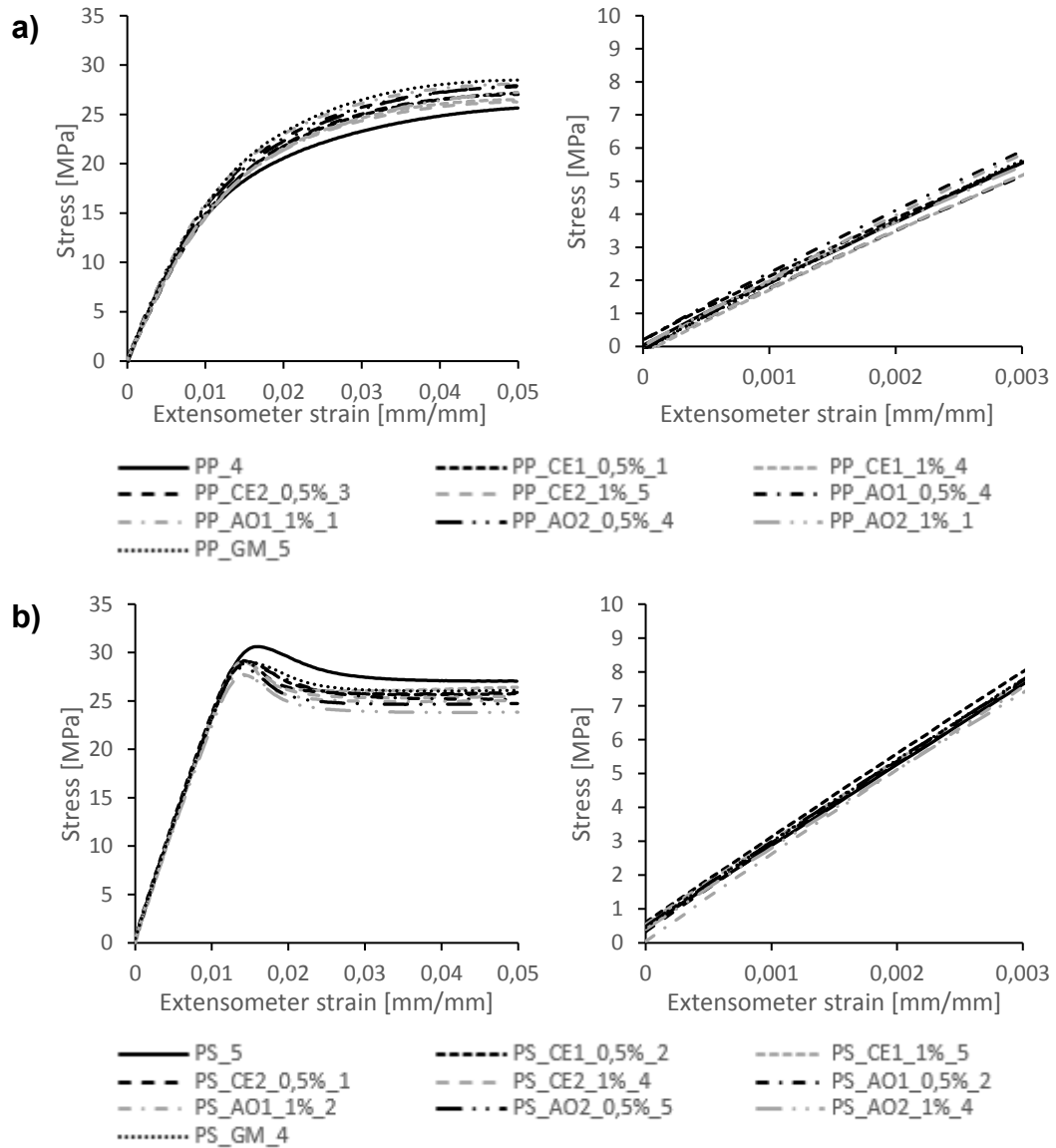


Figure continues →

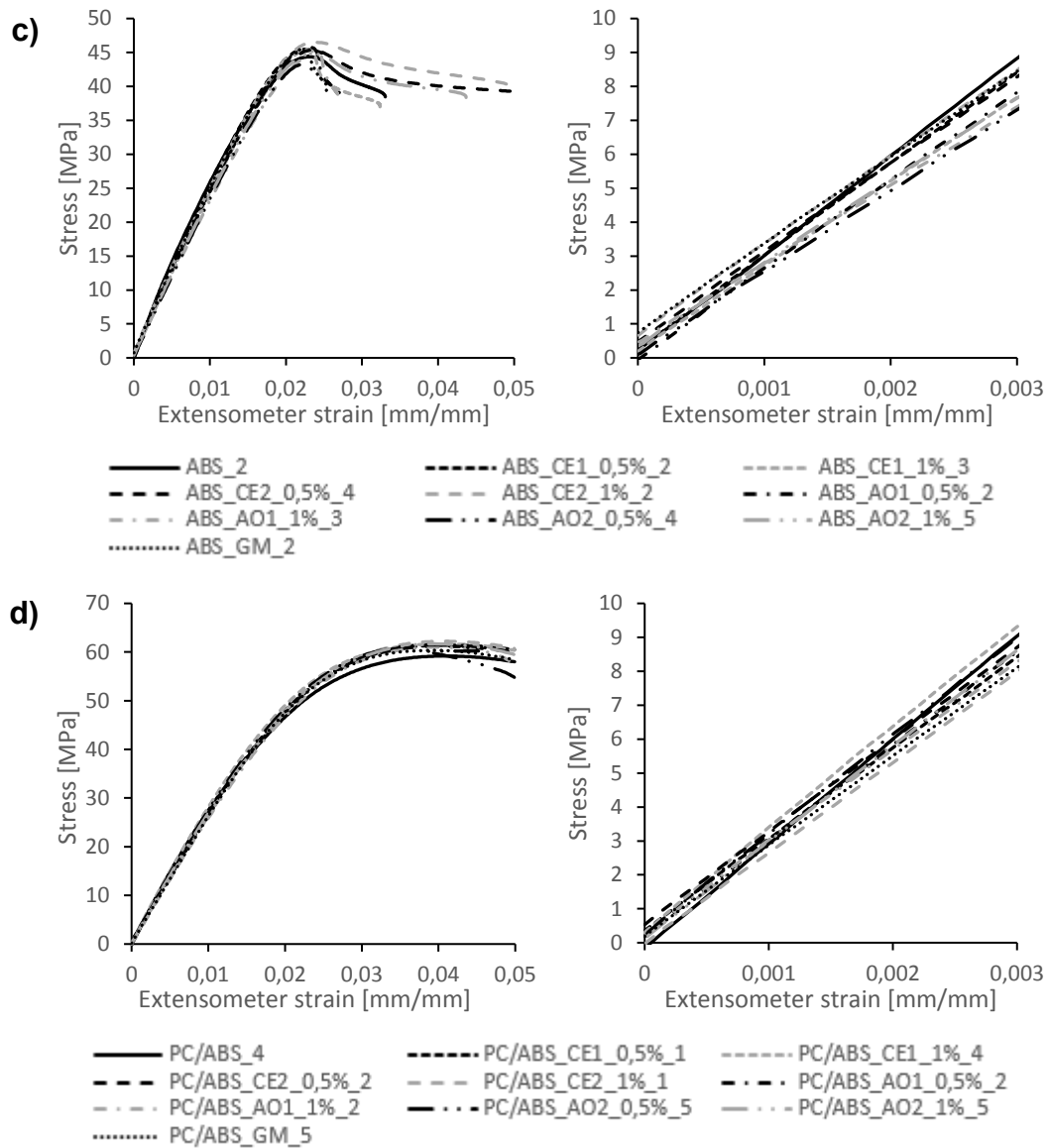


Figure 33. Stress-extensometer strain curves for the studied plastics with and without additives. The curves on the left have the full curve until the removal of the extensometer, and the curves on the right are close-ups of the same curves in the area where the modulus is determined. a) PP, b) PS, c) ABS, d) PC/ABS

Modulus is calculated as the slope of the curve in the strain range 0,0005 – 0,0025 mm/mm [103]. The calculated average modulus values and standard deviations are presented in Table 8.

Table 8. The absolute (abs.) modulus values and standard deviations of the plastic-additive combinations, and the modulus values of the samples with additives normalized (norm.) with the moduli of the additive-free samples.

Additive	PP		PS	
	abs. (Mpa)	norm. (%)	abs. (Mpa)	norm. (%)
- -	1727,6 ± 133,3	100	2429,2 ± 58,7	100
CE 1 0,5 %	1810,7 ± 42,0	105	2344,4 ± 92,9	97
CE 1 1 %	1717,4 ± 45,1	99	2409,0 ± 62,7	99
CE 2 0,5 %	1761,7 ± 52,2	102	2446,8 ± 188,0	101
CE 2 1 %	1702,4 ± 93,9	99	2331,7 ± 40,6	96
AO 1 0,5 %	1861,5 ± 35,8	108	2312,0 ± 89,8	95
AO 1 1 %	1894,2 ± 67,4	110	2380,2 ± 117,4	98
AO 2 0,5 %	1892,9 ± 46,2	110	2405,2 ± 196,5	99
AO 2 1 %	1734,3 ± 121,7	100	2284,4 ± 72,5	94
GM 0,5 %	1969,3 ± 112,5	114	2547,0 ± 170,0	105
Additive	ABS		PC/ABS	
	abs. (Mpa)	norm. (%)	abs. (Mpa)	norm. (%)
- -	2708,7 ± 125,2	100	2831,8 ± 282,3	100
CE 1 0,5 %	2515,6 ± 192,7	93	2755,7 ± 182,7	97
CE 1 1 %	2487,8 ± 112,1	92	2777,8 ± 136,9	98
CE 2 0,5 %	2659,2 ± 130,0	98	2641,5 ± 113,4	93
CE 2 1 %	2597,9 ± 27,8	96	2708,2 ± 131,5	96
AO 1 0,5 %	2487,2 ± 70,8	92	2782,7 ± 84,6	98
AO 1 1 %	2402,1 ± 122,7	89	2720,3 ± 125,4	96
AO 2 0,5 %	2439,6 ± 106,7	90	2755,5 ± 137,3	97
AO 2 1 %	2439,1 ± 84,1	90	2725,7 ± 114,4	96
GM 0,5 %	2462,4 ± 70,5	91	2669,5 ± 86,8	94

The “abs.” column in the table shows the absolute average values and standard deviations calculated for each plastic-additive combination. The standard deviations are very high compared to the differences between the absolute moduli values, but as before, they can still be used to make indicative comparisons to try to find which additive reduces the thermal degradation most efficiently. The “norm.” column shows the moduli of the plastics with additives normalized with the modulus of the additive-free plastic to better see how they compare. The bars are once again meant to help visualize the differences.

For PP it can be seen that the additives generally increase the modulus. The exceptions are 1 % of CE 1, and 1 % of CE 2, which ever so slightly decrease the modulus. The other samples with CEs also have quite low moduli. The AOs have increased the modulus by 0 – 10 %, and the modulus increased the most with GM, by 14 %.

For PS GM increased the modulus by 5 %, whereas CEs and AOs mainly decreased it by 1 – 6 %. The exception to this is 0,5 % of CE 2, which increased the modulus by 1 %.

The moduli of the ABS samples with additives are all lower than the modulus of the additive-free sample. For the samples with AOs or GM the moduli dropped by 8 – 11 %, and for the samples with CEs the moduli only dropped by 2 – 8 %.

The moduli of all plastic-additive combinations for PC/ABS were lower than the modulus of the additive-free plastic. They did not have much variance, ranging between 93 – 98 % of the original modulus.

7.3.2 Yield stress and strain

Yield occurs at the first local maximum, i.e., where the strain increases without the stress increasing [103]. These values were determined from the full stress-extensometer strain curves shown in Figure 33. PP is an exception to this, since it did not reach yield before the extensometer was removed, so its yield values were determined from the stress-nominal strain curves (Figure 34).

For PS and ABS, the yield point is clearly visible in all curves in Figure 33. PS has an extended area, where the material yielded until the extensometer was removed, whereas most ABS samples broke before the removal of the extensometer. The yield points of PC/ABS are not quite as obvious, but nonetheless the stress began to decline before the extensometer was removed. As mentioned, PP did not yield before the removal of the extensometer. The strength of a material is determined as the stress at yield, or the stress at break if the material does not yield before breaking. All of the studied samples did yield, and so their strengths were determined at yield. The effects of the additives on the yield point are more precisely compared in Tables 9 and 10.

Table 9. The absolute (abs.) yield stress values and standard deviations of the plastic-additive combinations, and the yield stress values of the samples with additives normalized (norm.) with the yield stress values of the additive-free samples.

Additive	PP		PS	
	abs. (Mpa)	norm. (%)	abs. (Mpa)	norm. (%)
- -	28,4 ± 0,7	100	29,8 ± 0,9	100
CE 1 0,5 %	29,3 ± 1,4	103	28,6 ± 0,7	96
CE 1 1 %	28,5 ± 0,3	100	29,0 ± 0,7	97
CE 2 0,5 %	28,1 ± 0,9	99	28,8 ± 0,6	97
CE 2 1 %	28,4 ± 0,3	100	28,7 ± 0,4	96
AO 1 0,5 %	30,4 ± 0,1	107	28,3 ± 0,9	95
AO 1 1 %	30,1 ± 0,9	106	28,2 ± 0,9	95
AO 2 0,5 %	29,5 ± 1,4	104	26,6 ± 1,8	89
AO 2 1 %	29,2 ± 1,4	103	26,7 ± 1,3	90
GM 0,5 %	29,8 ± 1,1	105	29,8 ± 0,9	100
Additive	ABS		PC/ABS	
	abs. (Mpa)	norm. (%)	abs. (Mpa)	norm. (%)
- -	43,5 ± 3,0	100	59,1 ± 0,7	100
CE 1 0,5 %	45,6 ± 1,2	105	61,0 ± 0,7	103
CE 1 1 %	45,6 ± 0,8	105	61,6 ± 0,7	104
CE 2 0,5 %	45,6 ± 0,2	105	61,6 ± 0,9	104
CE 2 1 %	46,2 ± 0,7	106	62,0 ± 0,2	105
AO 1 0,5 %	45,4 ± 1,1	104	61,3 ± 0,6	104
AO 1 1 %	44,1 ± 3,0	101	61,4 ± 0,3	104
AO 2 0,5 %	43,4 ± 1,3	100	61,0 ± 0,8	103
AO 2 1 %	44,5 ± 0,3	102	61,7 ± 0,1	104
GM 0,5 %	44,6 ± 0,6	102	59,7 ± 1,8	101

Table 10. The absolute (abs.) yield strain values and standard deviations of the plastic-additive combinations, and the yield strain values of the samples with additives normalized (norm.) with the yield strain values of the additive-free samples.

Additive	PP		PS	
	abs. (mm/mm)	norm. (%)	abs. (mm/mm)	norm. (%)
- -	0,095 ± 0,021	100	0,016 ± 0,001	100
CE 1 0,5 %	0,094 ± 0,010	99	0,014 ± 0,000	91
CE 1 1 %	0,095 ± 0,001	100	0,014 ± 0,001	92
CE 2 0,5 %	0,091 ± 0,010	95	0,014 ± 0,001	88
CE 2 1 %	0,094 ± 0,002	99	0,015 ± 0,001	92
AO 1 0,5 %	0,096 ± 0,002	101	0,015 ± 0,001	93
AO 1 1 %	0,094 ± 0,010	99	0,014 ± 0,001	90
AO 2 0,5 %	0,091 ± 0,010	96	0,016 ± 0,003	103
AO 2 1 %	0,100 ± 0,003	105	0,014 ± 0,001	88
GM 0,5 %	0,088 ± 0,015	92	0,014 ± 0,001	90
Additive	ABS		PC/ABS	
	abs. (mm/mm)	norm. (%)	abs. (mm/mm)	norm. (%)
- -	0,023 ± 0,001	100	0,042 ± 0,001	100
CE 1 0,5 %	0,023 ± 0,000	100	0,041 ± 0,001	98
CE 1 1 %	0,023 ± 0,000	100	0,040 ± 0,003	95
CE 2 0,5 %	0,023 ± 0,001	100	0,040 ± 0,001	97
CE 2 1 %	0,024 ± 0,001	103	0,041 ± 0,001	98
AO 1 0,5 %	0,023 ± 0,000	102	0,040 ± 0,001	96
AO 1 1 %	0,023 ± 0,001	99	0,040 ± 0,000	96
AO 2 0,5 %	0,022 ± 0,001	98	0,039 ± 0,000	94
AO 2 1 %	0,023 ± 0,001	99	0,040 ± 0,001	95
GM 0,5 %	0,022 ± 0,001	98	0,039 ± 0,001	94

As before, the “abs.” columns give the absolute values and standard deviations for stress and strain at yield. The standard deviations were once again quite high in comparison to the differences between the absolute stress and strain values, but the absolute values were still used to make indicative comparisons. The “norm.” columns compare the absolute values of the plastics with additives to the absolute values of plastics without additives.

For PP the stress at yield has largely increased, the exceptions being the yield stresses of the samples with CE 2 and 1 % of CE 1. Overall, the yield stresses have increased less for the samples with CE, as opposed to the samples with AO or GM. For the strain the results are the opposite, the strains have mainly decreased, except for 1 % of CE 1, 0,5 % of AO 1, and 1 % of AO 2. In this case the strain of the sample with GM is quite a bit lower than the strains of the samples with CEs or AOs.

In case of PS the majority of yield stresses of the samples with additives have decreased when comparing to the additive-free sample, except for the sample with GM, for which the yield stress remained the same. The stresses of the samples with AO 2 decreased by about 10 %, whereas the stresses of the other samples decreased by 3 – 5 %. The yield strains decreased by 7 – 12 %, except for the sample with 0,5 % of AO 2. There is no visible correlation between the strains and the additive types.

For ABS the yield stresses have mainly increased by 1 – 6 % due to the additives, except for the stress of the sample with 0,5 % of AO 2, which stayed the same. The changes in the stresses were slightly higher for the CEs (5 – 6 %) than for the AOs or GM (0 – 4 %). The yield strains stayed mainly the same when compared to the additive-free sample. The strains of the samples with CE 1 and 0,5 % of CE 2 remained the same, the samples with 1 % of CE 2 and 0,5 % of AO 1 increased the strain by 2 – 3 %, and the strains of the samples with the rest of the AOs and the GM decreased by 1 – 2 %. Overall, the strains of the samples with CEs were higher.

All the additives caused the yield stresses of the PC/ABS samples to increase by 3 – 5 %, except for the sample with GM, whose stress only increased by 1 %. Conversely, the yield strains of the samples with additives were all lower when compared to the additive-free sample. The strains of the samples with CEs decreased by 2 – 5 %, and the strains of the samples with AOs and GM decreased by 4 – 6 %, so there is only a very slight correlation between the additive types and the changes in the strains.

7.3.3 Break stress and strain

The stress and strain at break are determined at the highest value of stress on the stress-strain curve right before the load drop caused by the crack initiation, which leads to the sample separating [103]. In the case of most samples the samples did not break until after the extensometer was removed, so the break stresses and strains were determined from the stress-nominal strain curves. The stresses in these curves are the exact same as in the stress-extensometer strain curves, but the strains are the nominal strains. The stress-nominal strain curves are shown in Figure 34. The curves chosen for the figure for every plastic type are the ones that best describe the behavior of each plastic-additive

combination. The average break stresses and strains are shown in Tables 11 and 12. All of the results are shown in Annex D.

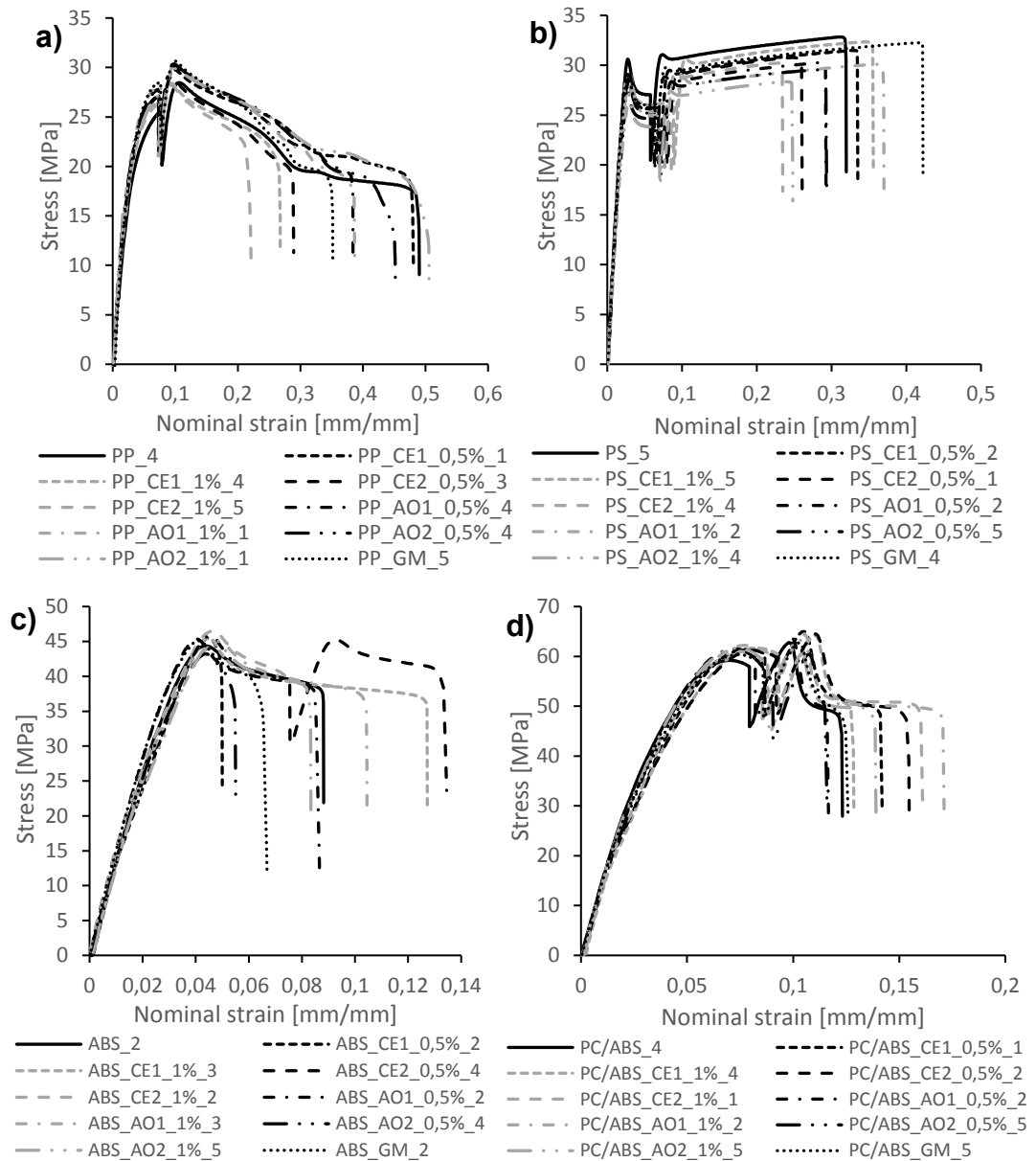


Figure 34. Stress-nominal strain curves for the studied plastics with and without additives. a) PP, b) PS, c) ABS, d) PC/ABS

Table 11. The absolute (abs.) break stress values and standard deviations of the plastic-additive combinations, and the break stress values of the samples with additives normalized (norm.) with the break stress values of the additive-free samples.

Additive	PP		PS	
	abs. (Mpa)	norm. (%)	abs. (Mpa)	norm. (%)
- -	17,8 ± 0,4	100	32,4 ± 1,6	100
CE 1 0,5 %	18,5 ± 2,0	104	31,2 ± 0,8	96
CE 1 1 %	20,7 ± 1,6	116	31,2 ± 1,1	96
CE 2 0,5 %	20,6 ± 0,9	116	30,0 ± 0,9	93
CE 2 1 %	22,5 ± 0,9	126	30,5 ± 1,1	94
AO 1 0,5 %	18,9 ± 1,7	106	30,1 ± 1,4	93
AO 1 1 %	18,6 ± 1,9	104	29,8 ± 1,4	92
AO 2 0,5 %	17,6 ± 0,4	99	28,9 ± 0,8	89
AO 2 1 %	17,1 ± 0,9	96	27,3 ± 2,1	84
GM 0,5 %	18,9 ± 3,4	106	32,1 ± 0,8	99
Additive	ABS		PC/ABS	
	abs. (Mpa)	norm. (%)	abs. (Mpa)	norm. (%)
- -	37,9 ± 2,5	100	48,7 ± 1,0	100
CE 1 0,5 %	40,5 ± 3,3	107	49,7 ± 0,5	102
CE 1 1 %	38,1 ± 1,3	101	52,7 ± 3,8	108
CE 2 0,5 %	39,7 ± 1,7	105	50,3 ± 1,0	103
CE 2 1 %	38,3 ± 1,6	101	50,2 ± 0,7	103
AO 1 0,5 %	39,6 ± 2,9	105	50,7 ± 1,0	104
AO 1 1 %	37,9 ± 2,5	100	50,3 ± 2,8	103
AO 2 0,5 %	38,4 ± 2,0	101	50,1 ± 0,5	103
AO 2 1 %	39,2 ± 2,2	103	50,7 ± 3,9	104
GM 0,5 %	40,0 ± 3,2	105	47,7 ± 2,1	98

Table 12. The absolute (abs.) break strain values and standard deviations of the plastic-additive combinations, and the break strain values of the samples with additives normalized (norm.) with the break strain values of the additive-free samples.

Additive	PP		PS	
	abs. (mm/mm)	norm. (%)	abs. (mm/mm)	norm. (%)
- -	0,408 ± 0,064	100	0,322 ± 0,066	100
CE 1 0,5 %	0,414 ± 0,139	101	0,330 ± 0,096	102
CE 1 1 %	0,289 ± 0,085	71	0,325 ± 0,060	101
CE 2 0,5 %	0,290 ± 0,056	71	0,276 ± 0,068	86
CE 2 1 %	0,228 ± 0,045	56	0,289 ± 0,039	89
AO 1 0,5 %	0,379 ± 0,059	93	0,335 ± 0,064	104
AO 1 1 %	0,377 ± 0,035	92	0,335 ± 0,044	104
AO 2 0,5 %	0,423 ± 0,046	104	0,303 ± 0,058	94
AO 2 1 %	0,478 ± 0,027	117	0,311 ± 0,069	96
GM 0,5 %	0,436 ± 0,128	107	0,360 ± 0,038	112
Additive	ABS		PC/ABS	
	abs. (mm/mm)	norm. (%)	abs. (mm/mm)	norm. (%)
- -	0,085 ± 0,028	100	0,133 ± 0,033	100
CE 1 0,5 %	0,075 ± 0,027	88	0,162 ± 0,015	122
CE 1 1 %	0,092 ± 0,024	108	0,117 ± 0,030	88
CE 2 0,5 %	0,104 ± 0,030	122	0,153 ± 0,023	115
CE 2 1 %	0,091 ± 0,025	108	0,125 ± 0,024	94
AO 1 0,5 %	0,106 ± 0,032	125	0,121 ± 0,019	91
AO 1 1 %	0,080 ± 0,026	95	0,138 ± 0,046	104
AO 2 0,5 %	0,075 ± 0,028	89	0,149 ± 0,040	112
AO 2 1 %	0,074 ± 0,017	87	0,142 ± 0,024	107
GM 0,5 %	0,072 ± 0,038	85	0,131 ± 0,017	99

The “abs.” columns have the absolute values and standard deviations for break stress and strain values for the samples. The standard deviations for the break values were very high compared to the differences between the absolute values, especially for the break strains. However, the values were still used to make indicative comparisons. The “norm.” columns have the relative values normalized with the absolute values of the additive-free values to see how the values of the samples with additives compare.

Most of the additives caused the break stresses of the PP samples to increase, except for the samples with AO 2, which decreased by 1 – 4 %. The samples with the highest stresses compared to the additive-free samples were the ones with CE 2 and 1 % of CE 1, as they increased the stresses by 16 – 26 %. The rest of the samples increased the stresses by 4 – 6 %. The CEs generally increased the stresses more. For the break strains the situation is the opposite for most samples. The samples with CE 2 and 1 % of CE 1 decrease the strain by 29 – 44 %, whereas the sample with 1 % of AO 2, which decreased the stress the most, has the highest strain, 17 % higher than the one of the additive-free sample. Generally, the strains of the samples with AOs or GM are higher.

For PS the additives have caused the break stresses to decrease. The stress of the sample with GM decreased the least, only by 1 %. The stresses of samples with CEs decreased by 4 – 7 %, and the stresses of samples with AOs decreased by 7 – 16 %. For the break strain values the differences between the different additives were visible. The strain was increased by CE 1 (1 – 2 %), AO 1 (4 %), and GM (12 %), and decreased by CE 2 (11 – 14 %), and AO 2 (4 – 6 %). As can be seen, GM increased the strain the most.

The additives have increased the break stress of ABS, except for the sample with 1 % of AO 1, in which case the stress stayed the same. For the other samples with additives the stress increased by 1 – 7 %. There does not seem to be a correlation between the type of additive used and the magnitude of the change in break stress. The effects of the additives on the break strain are significantly less even across all the additives. Only 1 % of CE 1, CE 2, and 0,5 % of AO 1 increased the strains, and the addition ranges from 8 % to 25 %. For the samples with the other additives the strains have decreased by 5 – 15 % in comparison with the additive-free sample. There is a slight correlation between CEs and the strains being higher.

The break stresses of the PC/ABS samples with additives are very consistent. The stresses of most of the samples have increased by 2 – 4 %. The exceptions to this are the sample with 1 % of CE 1, which increased the stress by 8 %, and the sample with GM, which decreased the stress by 2 %. The break strains are significantly less consistent. The strains of the samples with 1 % of CE 1, 1 % of CE 2, 0,5 % of AO 1, and GM decreased by 1 – 12 %. The strains of the remaining samples increased by 4 – 22 %. There is no visible correlation between the strains and the additives used.

8. DISCUSSION

8.1 Analysing results

In this chapter the results from Chapter 7 are compared to what was mentioned about the effects of changing MW and MWD on the properties in Chapter 3 to see which additives are the most effective ones. To review what was said in Chapter 3, thermal degradation causes the MW to decrease and MWD broaden. Increasing MW will increase the zero-shear viscosity. This effect is quite strong. The slope of the shear-thinning region is affected by the MWD, and the broader the MWD is the higher the Power-law index will be. The modulus is not affected much by MW directly, but it does increase with crystallinity and orientation. Crystallinity increases as MW decreases, and orientation increases as MW increases. Stress and strain increase with MW until the effect evens out and they become independent of MW. If the MW of a sample is above this limit, decreasing the MW will have a very small effect on the stress and strain values. Stress and strain are also increased by narrowing the MWD.

To be able to better compare the effects of the additives on the properties, all properties for one plastic type are collected in one table. The information is collected from Tables 6 – 12. Only the normalized values are shown here, as well as the grey bars used to visualize the results in Chapter 7. The diagonal hatching marks indicate which additive type gives the plastic the highest MW or the narrowest MWD based on each property. In the case of the zero-shear viscosity and the Power-law index only the normalized values compared to the disc samples are shown. The comparisons are shown in Tables 13 – 16.

Table 13. Comparing the effects of additives on the properties of PP.

Additive	Zero-shear viscosity (%)	Power-law index (%)	Modulus (%)	Yield stress (%)	Yield strain (%)	Break stress (%)	Break strain (%)
-	100	100	100	100	100	100	100
CE 1 0,5 %	62	387	105	103	99	104	101
CE 1 1 %	29	1134	99	100	100	116	71
CE 2 0,5 %	37	724	102	99	95	116	71
CE 2 1 %	27	1061	99	100	99	126	56
AO 1 0,5 %	93	50	108	107	101	106	93
AO 1 1 %	92	79	110	106	99	104	92
AO 2 0,5 %	92	113	110	104	96	99	104
AO 2 1 %	99	7	100	103	105	96	117
GM 0,5 %	70	193	114	105	92	106	107

The MW of PP affects the zero-shear viscosity and modulus, as well as the stresses and strains. Based on the zero-shear viscosity the samples with AOs have the highest MW, the sample with GM has the second highest MW, and the samples with CEs have the lowest MWs. It was mentioned in Chapter 3.2, that fillers can increase the zero-shear viscosity, but this was only the case for higher filler-contents. The amount of GM used in this study is not high enough to increase the zero-shear viscosity. PP is a semicrystalline polymer, so the modulus will likely increase as the MW decreases since this increases the crystallinity. Judging by the modulus, it seems that the samples with CEs have the highest MW, and the sample with GM has the lowest. As mentioned in Chapter 3.3, fillers, such as GM, can increase the crystallinity and modulus of the polymer, which is likely why the modulus of the GM sample is so high. According to the yield stress the AOs and GM increased the MW more than the CEs did. Based on the yield strain the MW has quite a bit of variance, but the MWs of the samples with CE or AO are still slightly higher than the MW of the sample with GM. The break stresses imply the MWs of the samples with CEs are higher than the MWs of the samples with AOs or GM. The break strains generally suggest the samples with CEs have lower MWs than the samples with AOs and GM do. It was mentioned in Chapter 3.3 that fillers will typically decrease the strength of a polymer. In this case the filler, GM, does not seem to have decreased the yield and break stresses significantly. Based on this comparison it seems the AOs work the best to reduce thermal degradation and maintain the MW of PP.

The MWD affects the Power-law index, as well as the stresses and strains. Based on the Power-law index, the samples with AOs have the narrowest MWDs, and the samples with CEs have the broadest. According to the yield stresses and the break strains the samples with AOs and GM have narrower MWDs than the samples with CEs do. The yield strains suggest the CEs and AOs have narrowed the MWD more than GM has. The break stresses imply the CEs narrowed the MWD more. Based on this the samples with AOs have the narrowest MWDs, meaning they have reduced thermal degradation the most. This is also in line with what was mentioned earlier in Chapter 4.2 about how CEs broaden the MWD.

Table 14. Comparing the effects of additives on the properties of PS.

Additive	Zero-shear viscosity (%)	Power-law index (%)	Modulus (%)	Yield stress (%)	Yield strain (%)	Break stress (%)	Break strain (%)
- -	100	100	100	100	100	100	100
CE 1 0,5 %	78	102	97	96	91	96	102
CE 1 1 %	77	78	99	97	92	96	101
CE 2 0,5 %	88	4	101	97	88	93	86
CE 2 1 %	82	2	96	96	92	94	89
AO 1 0,5 %	87	0	95	95	93	93	104
AO 1 1 %	82	84	98	95	90	92	104
AO 2 0,5 %	86	30	99	89	103	89	94
AO 2 1 %	78	60	94	90	88	84	96
GM 0,5 %	89	32	105	100	90	99	112

The additives seem to have affected the MW equally well based on the zero-shear viscosity and yield strain of PS, and no correlation is visible between the additives and their effects on the viscosity and strain. PS is an amorphous polymer, so the orientation will be the most significant variable affecting the modulus. The moduli imply the MW of the sample with GM is higher than those of the samples with CEs or AOs. However, as mentioned in Chapter 3.3, fillers can increase the modulus. So at least a portion, if not all, of the increasing effect of GM on the modulus might originate from GM acting as a filler, as opposed to its effect on the MW. The yield stresses, break stresses, and break strains all also suggest the sample with GM has the highest MW. Stresses and strains were said to decrease as filler is added, so in this case the increasing effect of GM likely is not due to GM acting as a filler. All in all, GM seems to be the most effective additive for reducing thermal degradation in PS.

The Power-law indices are very varied, and do not seem to imply any sort of correlation between the additives and the development of the MWD, so it must be concluded that all additives work equally well. The same can be said for the yield strains, though they are significantly more even. The stresses and break strain suggest the sample with GM has the narrowest MWD. All in all, the sample with GM has the narrowest MWD, implying GM reduces thermal degradation the most. However, this does not agree with what was said about CEs broadening the MWD in Chapter 4.2, since the anhydride groups cause GM to act as a CE. This suggests the broadening of the MWD caused by thermal degradation is greater than the broadening caused by the CEs.

Table 15. Comparing the effects of additives on the properties of ABS.

Additive	Zero-shear viscosity (%)	Power-law index (%)	Modulus (%)	Yield stress (%)	Yield strain (%)	Break stress (%)	Break strain (%)
- -	100	100	100	100	100	100	100
CE 1 0,5 %	234	253	93	105	100	107	88
CE 1 1 %	303	192	92	105	100	101	108
CE 2 0,5 %	273	57	98	105	100	105	122
CE 2 1 %	289	46	96	106	103	101	108
AO 1 0,5 %	120	70	92	104	102	105	125
AO 1 1 %	91	0	89	101	99	100	95
AO 2 0,5 %	82	0	90	100	98	101	89
AO 2 1 %	92	0	90	102	99	103	87
GM 0,5 %	104	0	91	102	98	105	85

Based on the zero-shear viscosity the CEs have increased the MW significantly more than the AOs and GM have. ABS is also an amorphous polymer, and so the modulus increases as the MW, and thus orientation, increases. Based on the modulus the CEs are the most effective additives, though the effect is considerably more subtle than the effect on the zero-shear viscosity is. The yield stresses and strains also imply the samples with CEs have the highest MWs. The break stresses are varied but seem to have increased evenly for all additives. The break strains are very varied, but the strains of the samples with CEs are generally higher, implying their MWs are the highest. GM acting as a filler does not seem to have had an effect on the modulus or the stresses. Based on these comparisons the CEs reduced thermal degradation and increased the MW the most.

The samples with CEs generally have higher Power-law indices, indicating that their MWDs are broader than those of the samples with AOs and GM. However, based on the yield stresses, yield strains, and break strains the samples with CEs have the narrowest MWDs. The break stresses show no clear correlation. The MWDs of the samples with CEs seem to be generally the narrowest, which indicates they reduced thermal degradation the most. This goes against what was said about CEs broadening the MWD, but this might once again suggest the degradation causes the MWD to broaden more than the CEs do.

Table 16. Comparing the effects of additives on the properties of PC/ABS.

Additive	Zero-shear viscosity (%)	Power-law index (%)	Modulus (%)	Yield stress (%)	Yield strain (%)	Break stress (%)	Break strain (%)
-	100	100	100	100	100	100	100
CE 1 0,5 %	88	95	97	103	98	102	122
CE 1 1 %	95	115	98	104	95	108	88
CE 2 0,5 %	93	243	93	104	97	103	115
CE 2 1 %	144	54	96	105	98	103	94
AO 1 0,5 %	70	117	98	104	96	104	91
AO 1 1 %	57	127	96	104	96	103	104
AO 2 0,5 %	62	138	97	103	94	103	112
AO 2 1 %	60	178	96	104	95	104	107
GM 0,5 %	89	39	94	101	94	98	99

The zero-shear viscosity of PC/ABS implies the samples with CEs and GM have the highest MWs. PC/ABS is an amorphous polymer, so modulus increases with MW. Neither the moduli nor the break strains show any correlation between the additives and the changes in MW, though there is significantly more variation in the break strains. The effect of GM acting as a filler is once again not visible on the modulus. The yield and break stresses both suggest the CEs and AOs have increased the MW more than GM has. It seems as though for PC/ABS GM acting as a filler might have decreased the stresses, since they are lower than the stress values of the samples with AOs or CEs. The yield strain indicates the MWs of the samples with CEs are slightly higher than those of the samples with AOs or GM. It seems that for PC/ABS the CEs are the most effective at reducing thermal degradation.

The Power-law indices imply the MWD of the sample with GM is the narrowest. The yield and break stresses suggest the samples with CEs and AOs have narrower MWDs than

the sample with GM. The MWD of the samples with CEs are the narrowest according to the yield strain. The break strain shows no correlation. Based on this comparison the samples with CEs have the narrowest MWDs and have reduced thermal degradation the most. Once again, this does not agree with how CEs are said to broaden the MWD, and implies thermal degradation broadens the MWD more than CEs do.

The reliability of the properties in accurately estimating the changes in MW varies. Sometimes the additive type that gives the highest MW to the plastic changes based on which property it is deduced from. For example, for PP the additive type giving the highest MW are the AOs based on the zero-shear viscosity, but according to the modulus CEs give the highest MW. Based on the data available, the most correct estimation of which additive type gives the highest MW is the additive, that most properties agreed had given a high MW. In other words, the additive type that had the most diagonal hatching in Tables 13 – 16. The zero-shear viscosities and yield stresses were the most reliable, they estimated the most effective additive correctly for every plastic. The other properties estimated the additive correctly for two or three plastics. Overall, the estimations of the effectiveness of the additives based on the properties agreed quite well.

The properties were significantly less reliable in estimating the MWD. Firstly, since the stresses and strains are thought to be affected by both MW and MWD, it is very difficult to differentiate which one is causing the changes in the properties. However, as the estimations based on the stresses and strains are in good agreement with the estimations based on the zero-shear viscosities, which only depend on the MW, it can be assumed the changes in stresses and strains are mainly governed by the MW. Especially, since, when estimating which additive type gives the narrowest MWD, the estimations based on the stresses and strains mostly do not agree with the estimations made on the basis of the Power-law indices, which only depend on the MWD. Secondly, the properties were overall slightly worse at correctly estimating the additive giving the narrowest MWD. The stresses and strains estimated the narrowness of the MWD similarly to how they estimated the largeness of the MW, since properties that indicated a high MW simultaneously indicated a narrow MWD. This means the yield stress estimated the narrowest MWD correctly for all plastics, and the other stresses and strains estimated them correctly two or three times. The Power-law index only predicted MWD correctly once. If the stresses and strains were ignored when estimating the narrowest MWD, and the assessment was only based on the Power-law index, the additive type that gave the narrowest MWD would be the AOs for PP, AOs and GM for ABS, and GM for PC/ABS. For PS there was no visible correlation between the additives and the changes in the index.

The assumption at the beginning of this work was that the MWs would either remain the same or increase as a consequence of adding the additives. However, in many cases the properties changed after the addition of additives in a way that implies the MW decreased. Since the only thing different between the testing of the samples with and without additives are the additives themselves, they must be the reason for this effect. One of the causes for the effect might be plasticization. Zero-shear viscosity, modulus, and stress would decrease after the addition of a plasticizer, whereas strain would increase [143]. The molecules of AOs and CEs are quite small and could therefore act as plasticizers in the plastics, causing the zero-shear-viscosity, modulus, and the stresses to decrease. This, however, seems to be an unlikely explanation for the phenomenon, since during a literature review, no articles were found discussing the plasticizing effect of AOs or CEs. Additionally, the MWs of plasticizers tend to be very low, usually below 1000 g/mol, whereas the MWs of the AOs and CEs in this study were all higher, except for the MW of AO 2 (Tables 4 and 5) [143]. This suggests the AO and CE molecules might be too large to work well as plasticizers. In addition, the plasticization theory does not explain the decrease in strains since they should increase after the addition of a plasticizer. Another explanation for the seemingly decreasing MWs could be that there is something in the plastics that the additives can interact with, that will result in the properties decreasing, even if the MW has not decreased. As the plastics in this study are recycled materials, and thus quite heterogeneous, it is very likely that there are some previous additives and impurities in them that do not function well with the added additives. This might explain the drop in the properties.

Chapter 4.2 described how the anhydride groups in GM can react with hydroxyl groups, and how the epoxy groups in the CEs chosen for this study can react with hydroxyl and carboxyl groups. As was mentioned, the reactivity of epoxy groups with carboxyl groups is higher than their reactivity with hydroxyl groups. Some information about the active groups in the oxidized polymers of this study can be deduced based on which additive types were the most effective for the plastics. Since the AOs increased the MWs of PP most, this implies the oxidized PP maybe did not have that many hydroxyl or carboxyl groups that GM or the CEs could react with. As mentioned, anhydride groups can only react with hydroxyl groups and epoxy groups are more prone to reacting with carboxyl groups. Since GM was the most effective additive for PS, and CEs were most effective for ABS and PC/ABS, this suggests the hydroxyl groups were the dominant reactive group for oxidized PS, whereas ABS and PC/ABS likely had more carboxyl groups.

8.2 Can recycled plastics be used in new EEE?

To see if the plastics studied in this thesis could replace virgin polymers in EEE, and to see how they compare to other recycled plastics, the tensile properties of the studied plastics were compared to the properties of virgin plastics [144] – [152] and recycled plastics [6] – [20] from previous literature. For the rest of this chapter the plastics studied in this thesis are referred to as studied recycled plastics, the plastics studied in previous literature are called previous recycled plastics, and the virgin plastics are called virgin plastics. The virgin plastic products were chosen so that all products are sold in Europe, the properties were tested according to ISO standards, and the suggested applications mentioned EEE. The full list of products is shown in Annex E. The articles the properties of the previous recycled plastics were taken from were chosen so that the plastics were recycled from EEE. There were not enough articles available to only use articles with European plastics tested according to ISO standards. Significantly more articles about ABS and PC/ABS fitting this criterion were found, than articles about PP and PS recycled from EEE. Only the properties of previous recycled plastics without added additives were included in the comparisons, since very few of the articles studied the effects of additives, and even fewer used additives that were also used in the current study. The information of the previous recycled plastics is shown in Annex F. The properties are compared in Figure 35.

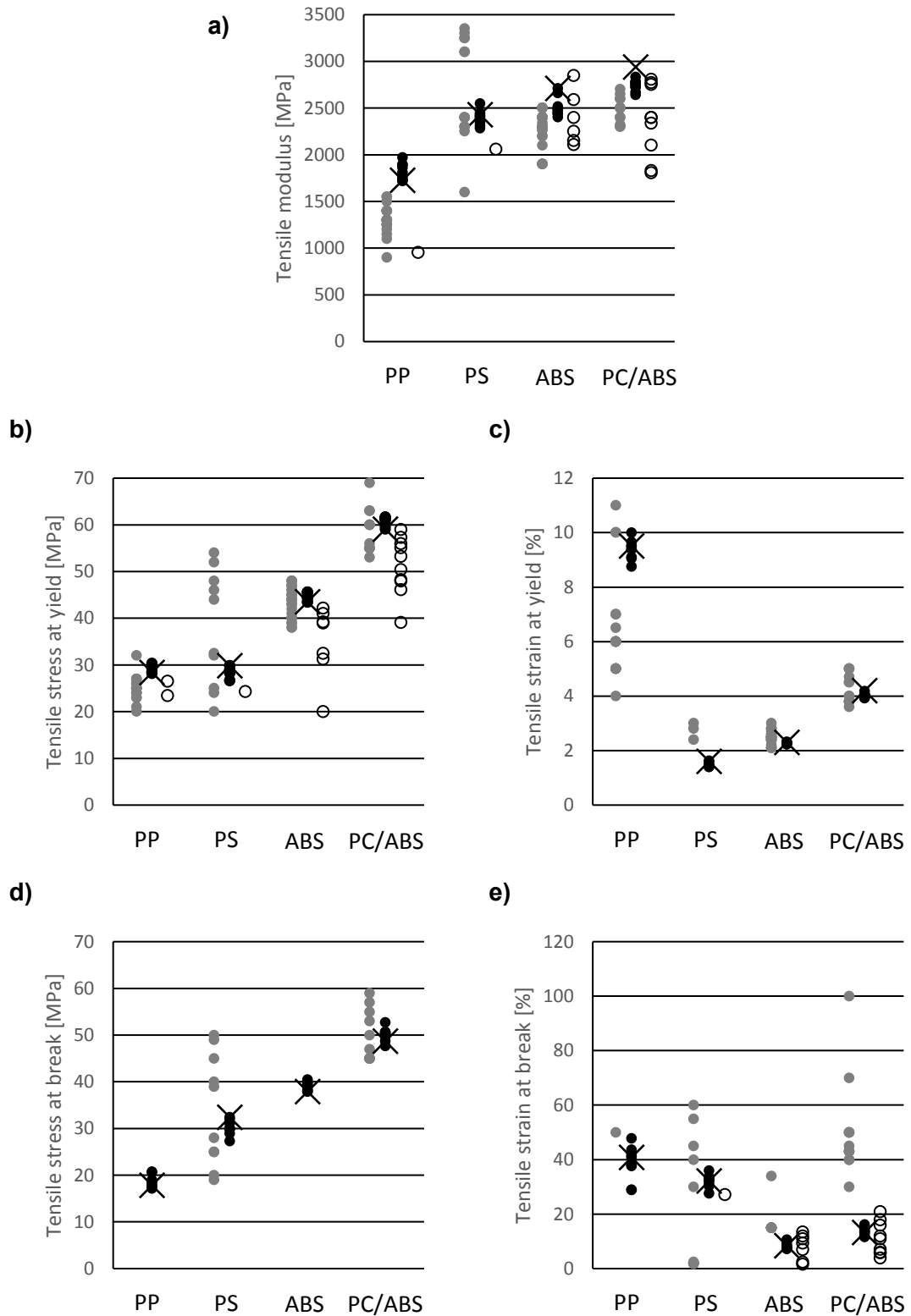


Figure 35. The properties of the studied recycled plastics compared to virgin and previous recycled plastics. X = properties of the additive-free samples, black dots = properties of studied recycled plastics with additives, grey dots = properties of virgin plastics, circles = properties of previous recycled plastics. a) modulus, b) yield stress, c) yield strain, d) break stress, e) break strain.

It can be seen in Figure 35a that the recycled plastics from this study generally had quite high moduli when compared to either the virgin or the previous recycled plastics. For PP the moduli of the studied recycled plastics were higher than those of either the virgin or previous recycled plastics. PS was an exception, since when compared to the virgin plastics, the moduli of the studied recycled plastics was average. However, the modulus of the previous recycled PS was still lower. For ABS the moduli of the previous recycled plastics were on average slightly higher than those of the virgin plastics. The moduli of the studied recycled ABS samples were approximately at the same level with the upper values of both virgin and previous recycled plastics. The moduli of PC/ABS were similarly at the same level with the upper values of virgin and previous recycled plastics, but this time the virgin plastics had a higher average modulus than the previous recycled plastics did.

Figure 35b shows the yield stresses of the plastics. Most articles on previous recycled plastics did not explicitly give a yield stress, and instead a tensile strength was given. However, as the tensile strength was determined as the yield stress for all plastics in this study, the previous recycled plastics were assumed to behave similarly, and thus the tensile strengths of the previous recycled plastics were compared with the yield stresses of the virgin and studied recycled plastics. The average yield stresses of the studied recycled plastics were approximately at the same level as the average yield stresses of the virgin plastics, especially for ABS and PC/ABS. For PP the average yield stress of studied recycled samples was slightly above average, and for PS it was below average. The yield stresses of the previous recycled plastics were mostly below those of the studied recycled plastics and were also on average worse than the yield stresses of the virgin plastics. PP was an exception to this, as the average yield stresses of virgin and previous recycled PP were quite close to each other.

The articles on the previous recycled plastics had only one yield strain value, so previous recycled plastics were omitted from Figure 35c. The relationship of the yield strains of the studied recycled plastics, when compared to the virgin plastics, varied. The yield strains of the studied recycled ABS and PC/ABS samples were slightly below the average strains of the virgin plastics. The strains of the studied recycled PS samples were quite significantly below the average strain of the virgin PS. However, the strains of the studied recycled PP samples were considerably higher than the average strain of the virgin PP.

Very few break stress values were available for previous recycled plastics, and so they were left out again from Figure 35d. Similarly, no break stresses were available for virgin PP and ABS, so only the break stresses of the studied recycled PS and PC/ABS samples

can be compared. Both of their stresses were slightly below the average stress of the virgin plastics.

There were no break strain values available for previous recycled PP, so in Figure 35e the studied recycled PP samples can only be compared to the virgin PP. The average break strains of the studied and previous recycled plastics were at about the same level for PS, ABS, and PC/ABS. The break strains of the studied and previous recycled plastics were quite significantly below the strains of the virgin plastics, except for PS, whose average strains for studied recycled, previous recycled, and virgin plastics were all relatively close to each other.

As can be seen, the properties of the studied recycled plastics resembled the properties of the virgin plastics in some cases, but in other cases they were reminiscent of the properties of the previous recycled plastics. Based on yield stress the studied recycled plastics were closer to the virgin plastics, but the break strains were closer to the previous recycled plastics. The higher yield stress of the studied recycled plastics might be explained, if the fillers found in Chapter 7.2 are the kind, that has a reinforcing effect on the polymer, which was mentioned to be possible in some cases in Chapter 3.3. They might also explain why the break strains of the studied recycled plastics are so low compared to the break strains of the virgin plastics, as in Chapter 3.3 fillers were said to typically decrease strains. It might also be that the recycling process described in Chapter 2.2.3 was exceptionally good compared to the previous recycled plastics, meaning there were less impurities in the studied recycled materials to weaken them. However, the degradation during use and processing seems to have weakened the studied recycled plastics enough to decrease the break strain.

Engineering plastics generally have good properties even after recycling and can therefore be effectively reused [153]. The comparisons in Figure 35 are mainly consistent with this observation, except for the break strains, which had decreased quite significantly in some cases. The amount of recycled plastic used in EEE today is still very low [49] [50]. However, the companies in the industry are constantly working to improve their products on this front. This can be seen in the publications written by Nordic Council of Ministers [49] and DIGITALEUROPE [154], which describe how several EEE manufacturers plan to increase the amount of recycled plastic in their products in the future. As the properties of the recycled plastics studied in this thesis were quite good, they would likely be suitable to be used as material in new EEE, as long as the inferior break strains will not be an issue or can be improved. This would be the ideal situation, as the ultimate goal of a circular economy would be to set up a closed-loop system, where the material will circulate within the EEE industry [49]. However, if the decreased break strains are an issue

and the plastics need to be downcycled, they can be used as blends or in composites [153]. The composites can be used in such applications as construction, the transportation industry, and the aerospace industry [153].

8.3 Is recycling WEEE plastics rational?

In many cases the reason why more recycled plastics are not used in products is due to the higher price of the recycled plastic. However, as a large portion of plastics used in EEE are engineering plastics, which are expensive, using recycled plastics can in this case be cheaper [49] [153]. Additionally, the prices of recycled plastics are less affected by crude oil prices [50]. In addition to being economically beneficial, using more recycled plastic is of course also ecologically advantageous. Using recycled plastics when making a product could reduce the environmental impact of the product considerably, even by over 20 % [49].

So, if the price of recycled plastic is not the reason why they are not used more in EEE, then what is? One problem is the number of different types of plastics used in EEE. The high number of plastics makes sorting them a complicated process. If sorting is done, the resulting batches of different plastics will be too small to be economically worthwhile. This can be solved by harmonising the plastic types used in EEE. This would reduce the number of plastics used and increase the individual material streams after recycling. Another problem are the large number of different chemicals and additives used in EEE plastics, which can form an obstacle against recycling. The solution to this problem is to design the products so that the amount of chemicals and additives used can be reduced. A problem related to the identification of plastics has to do with the identification codes used to mark the plastic types of the parts in EEE, and how they are often not correct. This means they cannot be used in recycling the plastic parts of EEE, and instead another method must be used, such as NIR. The incorrect markings are caused by using a mould, that was originally only meant to be used with one type of plastic, with another one, which means the identification code marking on the mould is now incorrect. This could be corrected by being stricter about mould usage. Additionally, if the number of plastic types were to be reduced, there would be less of a need to use the same mould to make parts out of different plastics. Finally, a list of guidelines for the designing of EEE ought to be compiled as a collaboration between the producers and the manufacturers that would encourage the producers to design more circular and easier to recycle products. [49]

9. CONCLUSIONS

This study aimed to find out which additive types would be best at preventing thermal oxidation and preserving the MW and MWD, whether rheological and mechanical properties can be used to assess how well the additives have maintained the MW and MWD, and if the recycled plastics had good enough properties to be used in EEE. It was found that there are differences in how additive types affect the properties of different plastics. The MW was found to increase the most with AOs for PP, with GM for PS, and with CEs for ABS and PC/ABS. The results indicated that the zero-shear viscosity and modulus, as well as the yield and break stresses and strains agreed rather well on which additive type gave the highest MW for each plastic and are thus quite reliable in assessing changes in MW. However, the Power-law index, as well as the yield and break stresses and strains were significantly less reliable in estimating the MWD. The properties of the recycled plastics were quite good in comparison to the virgin plastics, except for the break strains, and could likely be used to replace at least a portion of virgin plastics in new EEE.

A micro compounder was used to produce the samples for the study, for which tensile and rheological properties were determined. The micro compounder was chosen as a method of producing the samples even though it causes more degradation in the polymer. An idea for a further study could be to do the same experiments on samples produced on a full-sized injection moulding machine and extruder to see how the higher shear stresses of the micro compounder affected the properties of the polymers. In addition, the additives chosen for the study were quite limited, only epoxy-type CEs and primary AOs were used, so additional studies could be done using different types of AOs and CEs. The tensile and rheological properties were chosen as the way to assess the changes in the MW and MWD. However, as the properties can also be altered due to the interactions between the new additives and the previous additives in the recycled plastics, a subject for a further study could be finding a more direct way to estimate the changes in MW and MWD that is less dependent on other factors. Additionally, a study could be carried out to see what previous additives are present in the recycled plastics, and what interactions they have with the new additives that could cause the changes in the properties. Finally, it was stated, based on the most effective additive types for each plastic, that PP had few hydroxyl and carboxyl groups, PS had more hydroxyl groups, and ABS and PC/ABS had more carboxyl groups. This could be studied further to see if

this conclusion is true, and if it is what explains why certain additive types were more effective for different plastics than others.

This study has provided plenty of valuable information. Most importantly, it has proven that preventing or reducing the degradation during processing requires different types of additives for different polymers. Additionally, it has shown, that the recycling process used to obtain the recycled plastics studied in this study produced plastic fractions with higher tensile strengths than the recycled plastics found in literature. This study has also produced more data on the properties of PP and PS recycled from WEEE, which were lacking, since the majority of the previous literature on the recycled WEEE plastics was concerned with ABS and PC/ABS. Additionally, no data was found in previous literature on Joncryl ADR 4400 and Joncryl ADR 4468 being used with PP, PS, ABS, or PC/ABS, and it has now been produced.

As the properties of the recycled WEEE plastics are generally very close to the virgin plastics, it is recommended that the amount of recycled plastic in new EEE be increased. In order to make recycling easier, the products should be designed accordingly. As mentioned, the number of plastic types used should be reduced to a few essential ones, and the overall amount of additives and chemicals should be decreased.

REFERENCES

- [1] A new Circular Economy Action Plan For a cleaner and more competitive Europe. Brussels 11.3.2020, European Commission. Communication, 20 p. Available: <https://eur-lex.europa.eu/legal-content/EN/TXT/?qid=1583933814386&uri=COM:2020:98:FIN>
- [2] On the implementation of the Circular Economy Action Plan. Brussels 4.3.2019, European Commission. Report, 12 p. Available: <https://eur-lex.europa.eu/legal-content/EN/TXT/?uri=CELEX:52019DC0190>
- [3] A European Strategy for Plastics in a Circular Economy. Brussels 16.1.2018, European Commission. Communication, 17 p. Available: <https://eur-lex.europa.eu/legal-content/EN/TXT/?qid=1516265440535&uri=COM:2018:28:FIN>
- [4] Plastics Roadmap for Finland. 2018, Ministry of the Environment. Communication, 34 p. Available: <https://ym.fi/suomen-muovitekartta>
- [5] PLASTin. Website. [Referenced: 28.11.2021]. Available: <https://clcinnovation.fi/project/plastin/>
- [6] Mural, P. K. S., Mohanty, S., Nayak, S. K., Anbudayanidhi, S. Polypropylene/high impact polystyrene blend nanocomposites obtained from E-waste: evaluation of mechanical, thermal and morphological properties. *International journal of plastics technology* 15(2011)supplement 1, pp. 46 – 60.
- [7] Wang, J., Li, Y., Song, J., He, M., Song, J., Xia, K. Recycling of acrylonitrile–butadiene–styrene (ABS) copolymers from waste electrical and electronic equipment (WEEE), through using an epoxy-based chain extender. *Polymer degradation and stability* 112(2015), pp. 167 – 174.
- [8] Farzadfar, A., Khorasani, S. N., Khalili, S. Blends of recycled polycarbonate and acrylonitrile-butadiene-styrene: comparing the effect of reactive compatibilizers on mechanical and morphological properties. *Polymer international* 63(2014)1, pp. 145 – 150.
- [9] Liu, X., Bertilsson, H. Recycling of ABS and ABS/PC blends. *Journal of applied polymer science* 74(1999)3, pp. 510 – 515.
- [10] Ye, Q., Li, Z., Liu, J., Wang, D., Wang, P., Wang, X., Hu, X. Waste ABS plastics used in electrical packaging appliances: regeneration and properties. *Iranian polymer journal* 30(2021)5, pp. 445 – 452.
- [11] Wang, Y., Li, Y., Wang, W., Lv, L., Li, C., Zhang, J. Recycled polycarbonate/acrylonitrile–butadiene–styrene reinforced and toughened through chemical compatibilization. *Journal of applied polymer science* 136(2019)21, pp. 47537.
- [12] Biswal, M., Mohanty, S., Nayak, S. K., Babu, S. A. Effect of reactive compatibilizers and impact modifier on the performance characteristics of polycarbonate/poly(acrylonitrile-butadiene-styrene) blends obtained from E-waste. *International journal of plastics technology* 17(2014)2, pp. 209 – 225.

- [13] Ramesh, V., Biswal, M., Mohanty, S., Nayak, S. K. Compatibilization effect of EVA-g-MAH on mechanical, Morphological and rheological properties of recycled PC/ABS blend. *Materials express* 4(2014)6, pp. 499 – 507.
- [14] Pogorelčnik, B., Pulko, I., Wilhelm, T., Žigon, M. Influence of phosphorous-based flame retardants on the mechanical and thermal properties of recycled PC/ABS copolymer blends. *Journal of applied polymer science* 137(2020)7, pp. 48377.
- [15] Beigbeder, J., Perrin, D., Mascaro, J.-F., Lopez-Cuesta, J.-M. Study of the physico-chemical properties of recycled polymers from waste electrical and electronic equipment (WEEE) sorted by high resolution near infrared devices. *Resources, conservation and recycling* 78(2013), pp. 105 – 114.
- [16] K, J., Biswal, M., Mohanty, S., Nayak, S. K. Compatibility effect of r-ABS/r-HIPS/r-PS blend recovered from waste keyboard plastics: evaluation of mechanical, thermal and morphological performance. *Journal of polymer research* 28(2021)4, pp. 129.
- [17] de Souza, A. M. C., Cucchiara, M. G., Ereio, A. V. ABS/HIPS blends obtained from WEEE: Influence of processing conditions and composition. *Journal of applied polymer science* 133(2016)34, pp. 43831.
- [18] Ha, K. H., Kim, M. S. Application to refrigerator plastics by mechanical recycling from polypropylene in waste-appliances. *Materials in engineering* 34(2012), pp. 252 – 257.
- [19] Schlummer, M., Mäurer, A., Leitner, T., Spruzina, W. Report: Recycling of flame-retarded plastics from waste electric and electronic equipment (WEEE). *Waste management & research* 24(2006)6, pp. 573 – 583.
- [20] Wagner, F., Peeters, J. R., De Keyzer, J., Janssens, K., Duflo, J. R., Dewulf, W. Towards a more circular economy for WEEE plastics – Part B: Assessment of the technical feasibility of recycling strategies. *Waste management (Elmsford)* 96(2019), pp. 206 – 214.
- [21] Francis, R. *Recycling of Polymers: Methods, Characterization and Applications*. 1st edition. 2016, John Wiley & Sons. 285 p.
- [22] Singh, N., Hui, D., Singh, R., Ahuja, I. P. S., Feo, L., Fraternali, F. Recycling of plastic solid waste: A state of art review and future applications. *Composites Part B* 115(2017), pp. 409 – 422.
- [23] Ragaert, K., Delva, L., Van Geem, K. Mechanical and chemical recycling of solid plastic waste. *Waste Management* 69(2017), pp. 24 – 58.
- [24] *Plastics – the Facts 2020*. 2020, PlasticsEurope. Analysis. 64 p. Available: file:///C:/Users/lida/AppData/Local/Temp/Plastics_the_facts-WEB-2020_versionJun21_final.pdf
- [25] Roschier, S., Mikkola, J., Värre, U., Saario, M., Gaia Consulting AB. *Chemical recovery solutions and the market for plastic waste in the circular economy*. 2020, Ministry of Economic Affairs and Employment, Publications of the Ministry of Economic Affairs and Employment 2019:64. 111p.

- [26] Kaikki kiertää. 2018, Suomen Palautuspakkaus Oy. Brochure. 12 p. Available: https://www.e-julkaisu.fi/palpa/kaikki_kiertaa/2019/mobile.html#pid=1
- [27] Rakentamisen muovit. 2020, Ramboll Finland Oy. Report. 66 p. Available: https://muovitiekartta.fi/userassets/uploads/2019/03/rakentamisen_muovit_A4_v3.pdf
- [28] Autoliikenne – Muovi liikuttaa maailmaa. 2017, Muoviteollisuus ry. Report. 24 p. Available: file:///C:/Users/lida/AppData/Local/Temp/autoliikenne-muovi-liikuttaa-maailmaa-2017_net.pdf
- [29] Romuajoneuvotilastot [Statistics]. Centre for Economic Development, Transport and the Environment of Pirkanmaa. Published 6.9.2013, updated 24.6.2021 [Referenced 25.11.2021]. Available: https://www.ymparisto.fi/fi-FI/Kartat_ja_tilastot/Jatetilastot/Tuottajavastuun_tilastot/Romuajoneuvotilastot
- [30] Apila Group Oy Ab. Edistyksellistä renkaan kierrätystä. 2019, Suomen Rengaskierrätys Oy. Report. 34 p. Available: https://www.rengaskierratys.com/files/599/Suomen_Rengaskierratys_Edistyksellista_Renkaan_Kierratysta_2019.pdf
- [31] Electrical and electronic equipment and producer responsibility [Website]. Finland's environmental administration. Published 24.1.2017, updated 24.1.2017 [Referenced 25.11.2021]. Available: https://www.ymparisto.fi/en-US/Consumption_and_production/Waste_and_waste_management/Producer_responsibility/Waste_electrical_and_electronic_equipment
- [32] Ignatius, S.-M., Myllymaa, T., Dahlbo, H. Sähkö- ja elektroniikkaromun käsittely Suomessa. Helsinki 2009, Finnish Environment Institute, Suomen ympäristökeskuksen raportteja 20. 57 p.
- [33] Erälinna, L., Järvenpää, A.-M. Maatalousmuovijätteen keräys ja kierrätys, haasteet ja mahdollisuudet. Turku 2019, University of Turku. Report. 30 p. Available: https://maatalousmuovijate.fi/wp-content/uploads/2019/03/MaatalousmuovijateC3%A4tteen-kerC3%A4ys-ja-kierrC3%A4tys_-LiMuKe-eng.pdf
- [34] Martinho, G., Pires, A., Saraiva, S., Ribeiro, R. Composition of plastics from waste electrical and electronic equipment (WEEE) by direct sampling. Waste Management 32(2012), pp. 1213 – 1217.
- [35] Malpass, D. B., Band, E. Introduction to Industrial Polypropylene: Properties, Catalysts Processes. 1st edition. Somerset 2012, John Wiley & Sons. 356 p.
- [36] Niessner, N., Wagner, D. Practical guide to structures, properties and applications of styrenic polymers. Shrewsbury 2013, iSmithers Rapra Publishing. 168 p.
- [37] Peacock, A. J., Calhoun, A. R. Polymer chemistry: properties and applications. Munich 2006, Hanser Publishers. 385 p.
- [38] Rutkowski, J. V., Levin, B. C. Acrylonitrile-Butadiene-Styrene Copolymers (ABS): Pyrolysis and Combustion Products and their Toxicity-A Review of the Literature. Fire and Materials 10(1986), pp. 93 – 105.

- [39] Margolis, J. M. Engineering plastics handbook. 1st edition. New York 2006, McGraw-Hill. 436 p.
- [40] Directive 2012/19/EU on waste electrical and electronic equipment (WEEE). 4.7.2012, The European Parliament and the Council.
- [41] Directive 2011/65/EU on the restriction of the use of certain hazardous substances in electrical and electronic equipment. 8.6.2011, The European Parliament and the Council.
- [42] Regulation No 1907/2006 concerning the Registration, Evaluation, Authorisation and Restriction of Chemicals (REACH). 18.12.2006, The European Parliament and the Council.
- [43] Malin, Tiina. Master of Science (M.Sc.), R&D Manager, Kuusakoski Oy. Phone meeting 17.8.2021.
- [44] Sähkö- ja elektroniikkalaitetilastot [Statistics]. Centre for Economic Development, Transport and the Environment of Pirkanmaa. Published 6.9.2013, updated 8.7.2021 [Referenced 25.11.2021]. Available: https://www.ymparisto.fi/fi-FI/Kartat_ja_tilastot/Jatetilastot/Tuottajavastuun_tilastot/Sahko_ja_elektroniikkalaitetilastot
- [45] Kalmykova, Y., Patrício, J., Rosado, L., EO, B. P. Out with the old, out with the new – The effect of transitions in TVs and monitors technology on consumption and WEEE generation in Sweden 1996–2014. *Waste Management* 46(2015), pp. 511 – 522.
- [46] Tähkämö, L., Puolakka, M., Halonen, L., Zissis, G. Comparison of life cycle assessments of LED light sources. *Journal of light & visual environment* 36(2012)2, pp. 44 – 53.
- [47] Buekens, A., Yang, J. Recycling of WEEE plastics: a review. *Journal of material cycles and waste management* 16(2014)3, pp. 415 – 434.
- [48] Duflo, J. R., Peeters, J. R., Altamirano, D., Bracquene, E., Dewulf, W. Demanufacturing photovoltaic panels: Comparison of end-of-life treatment strategies for improved resource recovery. *CIRP Annals – Manufacturing Technology* 67(2018), pp. 29 – 32.
- [49] Raudaskoski, A., Lenau, T., Jokinen, T., Gisslén, A. V. Designing plastics circulation: electrical and electronic products. Copenhagen 2019, Nordic Council of Ministers, TemaNord 2019:534. 41 p.
- [50] Maisel, F., Emmerich, J., Dimitrova, G., Berwald, A., Nissen, N. F., Schneider, Ramelow, M. Using Post-Consumer Recycled Plastics in new EEE: A promising Circular Business Model for the Electronics Sector. *Electronics Goes Green 2020+*, Berlin 1.9.2020. 2020, Fraunhofer IZM. pp. 288 – 295.
- [51] Gijsman, P. Review on the thermo-oxidative degradation of polymers during processing and in service. *e-Polymers* 8(2008)1, pp. 727 – 760.
- [52] Gryn'ova, G., Hodgson, J. L., Coote, M. L. Revising the mechanism of polymer autooxidation. *Organic & biomolecular chemistry* 9(2011)2, pp. 480 – 490.

- [53] Smith, L. M., Aitken, H. M., Coote, M. L. The Fate of the Peroxyl Radical in Autoxidation: How Does Polymer Degradation Really Occur? *Accounts of chemical research* 51(2018)9, pp. 2006 – 2013.
- [54] Bolland, J. L. Kinetic studies in the chemistry of rubber and related materials. I. The thermal oxidation of ethyl linoleate. *Proceedings of the Royal Society of London. Series A, Mathematical and physical sciences* 186(1946)1005, pp. 218 – 236.
- [55] Bolland J. L., Gee, G. Kinetic studies in the chemistry of rubber and related materials. II. The kinetics of oxidation of unconjugated olefins. *Transactions of the Faraday Society* 42(1946), pp. 236 – 243.
- [56] Bolland, J. L., Gee, G. Kinetic studies in the chemistry of rubber and related materials. III. Thermochemistry and mechanisms of olefin oxidation. *Rubber chemistry and technology* 20(1947)3, pp. 617 – 626.
- [57] Bolland, J. L., Tenhave, P. Kinetic studies in the chemistry of rubber and related materials. IV. The inhibitory effect of hydroquinone on the thermal oxidation of ethyl linoleate. *Transactions of the Faraday Society* 43(1947), pp. 201 – 210.
- [58] Bolland, J. L. Kinetic studies in the chemistry of rubber and related materials. VI. The benzoyl peroxide-catalysed oxidation of ethyl linoleate. *Transactions of the Faraday Society* 44(1948), pp. 669 – 677.
- [59] Bateman, L., Gee, G. A kinetic investigation of the photochemical oxidation of certain nonconjugated olefins. *Proceedings of the Royal Society of London. Series A, Mathematical and physical sciences* 195(1948)1042, pp. 376 – 391.
- [60] Adams, J. H. Analysis of the nonvolatile oxidation products of polypropylene I. Thermal oxidation. *Journal of polymer science. Part A-1, Polymer chemistry* 8(1970)5, pp. 1077 – 1090.
- [61] Crompton, T. R. *Thermo-oxidative degradation of polymers*. Shrewsbury 2010, iSmithers. 146 p.
- [62] Chien, J. C. W., Boss, C. R. Polymer reactions. V. Kinetics of autoxidation of polypropylene. *Journal of Polymer Science Part A-1: Polymer Chemistry* 5(1967)12, pp. 3091 – 3101.
- [63] Scott, G. Initiation processes in polymer degradation. *Polymer degradation and stability* 48(1995)3, pp. 315 – 324.
- [64] Opeida, I. A., Zalevskaya, N. M., Zamashchikov, V. V., Rybachenko, V. I., Chotii, K. Y. The oxidation of polystyrene in solution. *Polymer science USSR* 23(1981)11, pp. 2731 – 2737.
- [65] Achhammer, B. G., Reiney, M. J., Reinhart, F. W. Study of degradation of polystyrene, using infrared spectrophotometry. *Journal of Research of the National Bureau of Standards* 47(1951)2, pp. 116 – 125.
- [66] McNeill, I. C., Razumovskii, L. P., Gol'dberg, V. M., Zaikov, G. E. The thermo-oxidative degradation of polystyrene. *Polymer degradation and stability* 45(1994)1, pp. 47 – 55.

- [67] Jellinek, H. H. G. Thermal Degradation of Polystyrene. Part II. *Journal of Polymer Science* 4(1949), pp. 1 – 12.
- [68] Adeniyi, J. B. Clarification and discussion of chemical transformations involved in thermal and photo-oxidative degradation of ABS. *European polymer journal* 20(1984)3, pp. 291 – 299.
- [69] Kovarskaya, B. M., Akutin, M. S., Sidney, A. I., Yazvikova, M. P., Neiman, M. B. Thermal-oxidative degradation of a polycarbonate. *Polymer science USSR* 4(1963)6, pp. 1346 – 1353.
- [70] Qian, S., Igarashi, T., Nitta, K.-H. Thermal degradation behavior of polypropylene in the melt state: molecular weight distribution changes and chain scission mechanism. *Polymer bulletin (Berlin, Germany)* 67(2011)8, pp. 1661 – 1670.
- [71] Jellinek, H. H. G. Thermal degradation of polystyrene Part 1. *Journal of Polymer Science* 3(1948)6, pp. 850 – 865.
- [72] Dong, D., Tasaka, S., Aikawa, S., Kamiya, S., Inagaki, N., Inoue, Y. Thermal degradation of acrylonitrile-butadiene-styrene terpolymer in bean oil. *Polymer degradation and stability* 73(2001)2, pp. 319 – 326.
- [73] Robertson, J. E. Thermal Degradation Studies of Polycarbonate. Doctoral thesis. Blacksburg, VA 2001. Virginia Polytechnic Institute and State University, Chemical Engineering. 213 p.
- [74] Wilkes, G. L. An overview of the basic rheological behavior of polymer fluids with an emphasis on polymer melts. *Journal of chemical education* 58(1981)11, pp. 880 – 892.
- [75] Bird, R. B., Armstrong, R. C., Hassager, O. Dynamics of polymeric liquids Volume 1 Fluid mechanics. 2nd edition. York 1987, John Wiley & Sons. 670 p.
- [76] Graessley, W. W., Segal, L. Effect of molecular weight distribution on the shear dependence of viscosity in polymer systems. *AIChE journal* 16(1970)2, pp. 261 – 267.
- [77] Nichetti, D., Manas-Zloczower, I. Viscosity model for polydisperse polymer melts. *Journal of rheology* 42(1998)4, pp. 951 – 969.
- [78] Nanda, M., Tripathy, D. K. Rheological behavior of chlorosulfonated polyethylene composites: Effect of filler and plasticizer. *Journal of applied polymer science* 126(2012)1, pp. 46 – 55.
- [79] Shenoy, A. V. Rheology of filled polymer systems. 1st edition. 1999, Springer Netherlands. 484 p.
- [80] Kutz, M. Applied Plastics Engineering Handbook – Processing and Materials. 1st edition. Waltham 2011, Elsevier. 661 p.
- [81] Clark, E. J. Molecular and microstructural factors affecting mechanical properties of polymeric cover plate materials. U.S Department of Commerce, National Bureau of Standards, Center for Building Technology, 1985. 72 p.

- [82] Martin, J. R., Johnson, J. F., Cooper, A. R. Mechanical Properties of Polymers: The Influence of Molecular Weight and Molecular Weight Distribution. *Journal of Macromolecular Science, Part C* 8(1972)1, pp. 57 – 199.
- [83] Rothon, R. *Fillers for Polymer Applications*. 1st edition. Switzerland 2017, Springer International Publishing. 313 p.
- [84] Nunes, R. W., Martin, J. R., Johnson, J. F. Influence of molecular weight and molecular weight distribution on mechanical properties of polymers. *Polymer engineering and science* 22(1982)4, pp. 205 – 228.
- [85] SFS-EN ISO 11357-6:2018. *Plastics. Differential scanning calorimetry (DSC). Part 6: Determination of oxidation induction time (isothermal OIT) and oxidation induction temperature (dynamic OIT)*. 2018, Finnish Standards Association. 19 p.
- [86] SFS-EN ISO 11358-1:2014. *Plastics - Thermogravimetry (TG) of polymers - Part 1: General principles* 2014, Finnish Standards Association. 19 p.
- [87] Allen, N. S., Edge, M. *Perspectives on additives for polymers. 1. Aspects of stabilization*. *Journal of vinyl & additive technology* 27(2021)1, pp. 5 – 27.
- [88] Vulic, I., Vitarelli, G., Zenner, J. M. Structure–property relationships: phenolic antioxidants with high efficiency and low colour contribution. *Polymer degradation and stability* 78(2002)1, pp. 27 – 34.
- [89] Tolinski, M. *Additives for polyolefins: getting the most out of polypropylene, polyethylene and TPO*. 2nd edition. Amsterdam, Netherlands 2015, William Andrew. 234 p.
- [90] Standau, T., Nofar, M., Dörr, D., Ruckdäschel, H., Altstädt, V. A Review on Multifunctional Epoxy-Based Joncryl® ADR Chain Extended Thermoplastics. *Polymer reviews* (2021), pp. 1 – 55.
- [91] Villalobos, M., Awojulu, A., Greeley, T., Turco, G., Deeter, G. Oligomeric chain extenders for economic reprocessing and recycling of condensation plastics. *Energy (Oxford)* 31(2006)15, pp. 3227 – 3234.
- [92] Bennett, S. G. *Isocyanates*. Hauppauge 2017, Nova Science Publishers. 181 p.
- [93] Yang, Z., Xin, C., Mughal, W., Li, X., He, Y. High-melt-elasticity poly(ethylene terephthalate) produced by reactive extrusion with a multi-functional epoxide for foaming. *Journal of applied polymer science* 135(2018)8, pp. 45805 – 45805.
- [94] Inata, H., Matsumura, S. Chain extenders for polyesters. IV. Properties of the polyesters chain-extended by 2,2'-bis(2-oxazoline). *Journal of applied polymer science* 33(1987)8, pp. 3069 – 3079.
- [95] Stloukal, P., Jandikova, G., Koutny, M., Sedlařík, V. Carbodiimide additive to control hydrolytic stability and biodegradability of PLA. *Polymer testing* 54(2016), pp. 19 – 28.
- [96] Stloukal, P., Kalendova, A., Mattausch, H., Laske, S., Holzer, C., Koutny, M. The influence of a hydrolysis-inhibiting additive on the degradation and biodegradation of PLA and its nanocomposites. *Polymer testing* 41(2015), pp. 124 – 132.

- [97] Meng, X., Shi, G., Chen, W., Wu, C., Xin, Z., Han, T., Shi, Y. Structure effect of phosphite on the chain extension in PLA. *Polymer degradation and stability* 120(2015), pp. 283 – 289.
- [98] Cicero, J. A., Dorgan, J. R., Dec, S. F., Knauss, D. M. Phosphite stabilization effects on two-step melt-spun fibers of polylactide. *Polymer degradation and stability* 78(2002)1, pp. 95 – 105.
- [99] Seo, J.-M., Baek, J.-B. A solvent-free Diels–Alder reaction of graphite into functionalized graphene nanosheets. *Chemical communications* 50(2014)93, pp. 14651 – 14653.
- [100] Seo, J.-M., Jeon, I.-Y., Baek, J.-B. Mechanochemically driven solid-state Diels–Alder reaction of graphite into graphene nanoplatelets. *Chemical science* 4(2013)11, pp. 4273 – 4277.
- [101] Carey, F. A. *Advanced Organic Chemistry Part B: Reaction and Synthesis*. 5th edition. New York 2007, Springer US. 1346 p.
- [102] Sarkar, S., Bekyarova, E., Niyogi, S., Haddon, R. C. Diels–Alder Chemistry of Graphite and Graphene: Graphene as Diene and Dienophile. *Journal of the American Chemical Society* 133(2011)10, pp. 3324 – 3327.
- [103] SFS-EN ISO 527-1:2019. *Plastics. Determination of tensile properties. Part 1: General principles*. 2019, Finnish Standards Association. 31 p.
- [104] Dewi, I. R., Indrajati, I. N., Nurhajati, D. W. Effect of compatibilizers on the mechanical and morphological properties of polycarbonate/poly (acrylonitrile-butadiene-styrene) blends. *IOP conference series. Materials Science and Engineering* 432(2018)1, pp. 1 – 8.
- [105] Luzuriaga, S., Kovářová, J., Fortelný, I. Degradation of pre-aged polymers exposed to simulated recycling: Properties and thermal stability. *Polymer degradation and stability* 91(2006)6, pp. 1226 – 1232.
- [106] Prasad, A. V., Singh, R. P. Recent Developments in the Degradation and Stabilization of High-Impact Polystyrene. *Journal of Macromolecular Science, Part C* 37(1997)4, pp. 581 – 598.
- [107] Marek, A., Kaprálková, L., Schmidt, P., Pflieger, J., Humlíček, J., Pospíšil, J., Pilař, J. Spatial resolution of degradation in stabilized polystyrene and polypropylene plaques exposed to accelerated photodegradation or heat aging. *Polymer degradation and stability* 91(2006)3, pp. 444 – 458.
- [108] Niroumand, J. S., Peighambardoust, S. J., Shenavar, A. Polystyrene-based composites and nanocomposites with reduced brominated-flame retardant. *Iranian polymer journal* 25(2016)7, pp. 607 – 614.
- [109] Nasir, A., Yasin, T., Islam, A. Thermo-oxidative degradation behavior of recycled polypropylene. *Journal of applied polymer science* 119(2011)6, pp. 3315 – 3320.
- [110] Zhang, G., Nam, C., Petersson, L., Jämbeck, J., Hillborg, H., Chung, T. C. M. Increasing Polypropylene High Temperature Stability by Blending Polypropylene-Bonded Hindered Phenol Antioxidant. *Macromolecules* 51(2018)5, pp. 1927 – 1936.

- [111] Alin, J., Hakkarainen, M. Microwave Heating Causes Rapid Degradation of Antioxidants in Polypropylene Packaging, Leading to Greatly Increased Specific Migration to Food Simulants As Shown by ESI-MS and GC-MS. *Journal of agricultural and food chemistry* 59(2011)10, pp. 5418 – 5427.
- [112] Hamskog, M., Klügel, M., Forsström, D., Terselius, B., Gijsman, P. The effect of adding virgin material or extra stabilizer on the recyclability of polypropylene as studied by multi-cell imaging chemiluminescence and microcalorimetry. *Polymer degradation and stability* 91(2006)3, pp. 429 – 436.
- [113] Hamskog, M., Klügel, M., Forsström, D., Terselius, B., Gijsman, P. The effect of base stabilization on the recyclability of polypropylene as studied by multi-cell imaging chemiluminescence and microcalorimetry. *Polymer degradation and stability* 86(2004)3, pp. 557 – 566.
- [114] Liu, X., Bertilsson, H. Recycling of ABS and ABS/PC blends. *Journal of applied polymer science* 74(1999)3, pp. 510 – 515.
- [115] Li, G., Guo, X., Na, W., Hao, D., Zhang, M., Zhang, H., Xu, J. Performance and synergistic effect of phenolic and thio antioxidants in ABS graft copolymers. *Frontiers of chemical engineering in China* 5(2010)1, pp. 26 – 34.
- [116] Fiorio, R., D'hooge, D. R., Ragaert, K., Cardon, L. A statistical analysis on the effect of antioxidants on the thermal-oxidative stability of commercial mass and emulsion-polymerized ABS. *Polymers* 11(2018)1, p. 25.
- [117] Wang, Y., Chen, M., Lan, M., Li, Z., Lu, S., Wu, G. GM-improved antiaging effect of acrylonitrile butadiene styrene in different thermal environments. *Polymers* 12(2020)1, p. 46.
- [118] Fiorio, R., Díez, S. V., Sánchez, A., D'hooge, D. R., Cardon, L. Influence of different stabilization systems and multiple ultraviolet a (UVA) aging/recycling steps on physicochemical, mechanical, colorimetric, and thermal-oxidative properties of ABS. *Materials* 13(2020)1, p. 212.
- [119] Zeinalov, E., Koßmehl, G. Fullerene C60 as an antioxidant for polymers. *Polymer degradation and stability* 71(2001)2, pp. 197 – 202.
- [120] Haghtalab, A., Kateh, M. S. Rheology of PC/ABS/SiO₂ nanocomposites; effect of size and loading of particles. The 8th International Chemical Engineering Congress & Exhibition (IChEC 2014), Kish, Iran 2014.
- [121] Wang, J., Li, Y., Song, J., He, M., Song, J., Xia, K. Recycling of acrylonitrile–butadiene–styrene (ABS) copolymers from waste electrical and electronic equipment (WEEE), through using an epoxy-based chain extender. *Polymer degradation and stability* 112(2015), pp. 167 – 174.
- [122] CN111286182 (A). Low-cost halogen-free flame-retardant PCABS alloy and preparation method thereof. Applicant: Nanjing Yongju New Material Tech Co LTD. Inventors: Ming, Z., Xiaojian, G., Changyong, Z. Application number: CN202010116736 20200225. 2020. 4 p.
- [123] CN104893101 (A). Chain-extension-branching-modified polypropylene foamed sheet and manufacturing method thereof. Applicant: Shantou Jinpin Plastic Ind

Co LTD. Inventor: Ruocheng, Z. Application number: CN201510286442 20150530. 2015. 13 p.

- [124] Chiu, H.-T., Huang, J.-K., Kuo, M.-T., Huang, J.-H. Characterisation of PC/ABS blend during 20 reprocessing cycles and subsequent functionality recovery by virgin additives. *Journal of polymer research* 25(2018)5, pp. 1 – 8.
- [125] CN105778459 (A). PC/ABS functional regenerated alloy for casing materials and production technology of PC/ABS functional regenerated alloy. Applicant: Changzhou Plasking Polymer Tech Co LTD. Inventors: Jinping, Z., Xiaomin, M., Lei, Y., Yonggang, W., Jianghao, Q., Fei, F. Application number: CN201610148170 20160315. 2016. 9 p.
- [126] Irganox 1010 Technical Data Sheet. 2015, BASF Corporation. Technical data sheet. 3 p.
- [127] Irganox 1076 Technical Data Sheet. 2019, BASF Corporation. Technical data sheet. 3 p.
- [128] Joncryl ADR 4400 Technical Data Sheet. 2014, BASF Corporation Technical data sheet. 6 p.
- [129] Joncryl ADR 4468 Technical Data Sheet. 2014, BASF Corporation. Technical data sheet. 6 p.
- [130] Upgrade your recycled plastic! Plastic additives – the JONCRYL selection guide. BASF Corporation. Guide. 16 p.
- [131] Ramos, M., Dominici, F., Luzi, F., Jiménez, A., Garrigós, M. C., Torre, L., Puglia, D. Effect of almond shell waste on physicochemical properties of polyester-based biocomposites. *Polymers* 12(2020)4, pp. 835.
- [132] Grigora, M.-E., Terzopoulou, Z., Tsongas, K., Klonos, P., Kalafatakis, N., Bikiaris, D. N., Kyritsis, A., Tzetzis, D. Influence of Reactive Chain Extension on the Properties of 3D Printed Poly(Lactic Acid) Constructs. *Polymers* 13(2021)9, pp. 1381.
- [133] Garcia-Campo, M. J., Quiles-Carrillo, L., Masia, J., Reig-Pérez, M. J., Montanes, N., Balart, R. Environmentally friendly compatibilizers from soybean oil for ternary blends of poly(lactic acid)-PLA, poly(ϵ -caprolactone)-PCL and poly(3-hydroxybutyrate)-PHB. *Materials* 10(2017)11, pp. 1339.
- [134] Kahraman, Y., Özdemir, B., Kılıç, V., Goksu, Y. A., Nofar, M. Super toughened and highly ductile PLA/TPU blend systems by in situ reactive interfacial compatibilization using multifunctional epoxy-based chain extender. *Journal of applied polymer science* 138(2021)20, pp. 50457.
- [135] Nofar, M., Oğuz, H. Development of PBT/Recycled-PET Blends and the Influence of Using Chain Extender. *Journal of polymers and the environment* 27(2019)7, pp. 1404 – 1417.
- [136] Chen, D., Luo, D., Zhen, W., Zhao, L. Effect of functionalized organic saponite on performance, crystallization and rheology of poly (lactic acid). *Applied clay science* 207(2021), pp. 106091.

- [137] Karkhanis, S. S., Matuana, L. M. Extrusion blown films of poly(lactic acid) chain-extended with food grade multifunctional epoxies. *Polymer engineering and science* 59(2019)11, pp. 2211 – 2219.
- [138] Zhao, Y., Li, Y., Xie, D., Chen, J. Effect of chain extender on the compatibility, mechanical and gas barrier properties of poly(butylene adipate-co-terephthalate)/poly(propylene carbonate) bio-composites. *Journal of applied polymer science* 138(2021)21, pp. 50487.
- [139] Li, X., Xia, M., Qiu, D., Long, R., Huang, Z., Li, J., Long, S., Li, X. Fabrication and Properties of Modified Poly(butylene terephthalate) with Two-Step Chain Extension. *Macromolecular materials and engineering* 306(2021)3, pp. 2000638.
- [140] Nuchanong, P., Seadan, M., Khankrua, R., Suttiruengwong, S. Thermal stability enhancement of poly(hydroxybutyrate-co-hydroxyvalerate) through in situ reaction. *Designed monomers and polymers* 24(2021)1, pp. 113 – 124.
- [141] Aliotta, L., Vannozzi, A., Canesi, I., Cinelli, P., Coltelli, M.-B., Lazzeri, A. Poly(Lactic acid) (PLA)/poly(butylene succinate-co-adipate) (PBSA) compatibilized binary biobased blends: Melt fluidity, morphological, thermo-mechanical and micromechanical analysis. *Polymers* 13(2021)2, pp. 218.
- [142] Vostrejs, P., Adamcová, D., Vaverková, Magdalena D., Enev, V., Kalina, M., Machovsky, M., Šourková, M., Marova, I., Kovalcik, A. Active biodegradable packaging films modified with grape seeds lignin. *RSC advances* 10(2020)49, pp. 29202 – 29213.
- [143] Wypych, G. *Handbook of plasticizers*. 2nd edition. Burlington 2013, Elsevier Science. 700 p.
- [144] Braskem. Website. [Referenced: 28.11.2021]. Available: <https://www.braskem.com/product-search>
- [145] SABIC. Website. [Referenced: 28.11.2021]. Available: <https://www.sabic.com/en/products/polymers>
- [146] TotalEnergies. Website. [Referenced: 28.11.2021]. Available: https://polymers.totalenergies.com/catalog?f%5B%5D=im_field_polymer_origins%3A1398&nid=832&parent=0&term=
- [147] Covestro. Website. [Referenced: 28.11.2021]. Available: https://solutions.covestro.com/en/products/?query=:relevance:countries:US&_gl=1*14ucy6*_ga*MjEyNTU0ODY2MS4xNjE5NjE2NjI2*_ga_TFHFN82HNF*MTYxOTcwNzk5NS40LjEuMTYxOTcwNzk5OS4w
- [148] Trinseo. Website. [Referenced: 28.11.2021]. Available: <https://www.trinseo.com/>
- [149] ELIX Polymers. Website. [Referenced: 28.11.2021]. Available: <https://www.elix-polymers.com/products-and-markets>
- [150] Ineos Styrolution. Website. [Referenced: 28.11.2021]. Available: <https://www.ineos-styrolution.com/index.html>

- [151] Versalis. Website. [Referenced: 28.11.2021]. Available: <https://www.versalis.eni.com/irj/portal/anonymous?standAlone=true&sapDocumentRendering-Mode=EmulateIE8&>windowId=WID1620112504313&NavMode=0>
- [152] Synthos. Website. [Referenced: 28.11.2021]. Available: <https://www.synthosps.com/en/products/catalogues>
- [153] Chauhan, V., Varis, J., Kärki, T. The Potential of Reusing Technical Plastics. *Procedia manufacturing* 39(2019), pp. 502 – 508.
- [154] Best Practices in Recycled Plastics. 2016, DIGITALEUROPE. Paper. 16 p. Available: <https://www.digitaleurope.org/wp/wp-content/uploads/2019/01/Best%20practices%20-%20Recycled%20plastics%20paper.pdf>

ANNEX A: MATERIAL FLOW OF PLASTIC FROM WEEE IN 2019

Table A.1. How much WEEE plastic was generated and recycled in Finland in 2019. The amounts were calculated by multiplying the data in [44] with the plastic content percentages. * Not including filament bulbs. ** An average value calculated from the values given in the article/articles

	Plastic content (%)	Reference	Collected from households (t)	Collected from other sources (t)	Prepared for re-use (t)	Recycled as material (t)	Burned for energy (t)	Final disposal (e.g., landfill) (t)	Unassigned (t)
Temperature exchange equipment	10,4	[34]	1666	73	4	1462	253	19	0
Screens/monitors over 100 cm ²	3,4	[45]**	254	13	4	239	11	10	2
Lamps *	23,9	[46]**	1	224	0	203	14	9	0
Large equipment over 50 cm	9	[47]	2397	235	16	2253	204	158	1
Photovoltaic panels	2,85	[48]	0	0	0	0	0	0	0
Small equipment below 50 cm	48,6	[47, 34]**	4851	2519	1371	5349	255	383	14
Small IT and telecommunication equipment	52	[47]**	1502	238	77	1575	26	25	36
TOTAL	-	-	10672	3302	1473	11081	762	604	54

ANNEX B: VISCOSITY RESULTS

Viscosity curves of PP samples

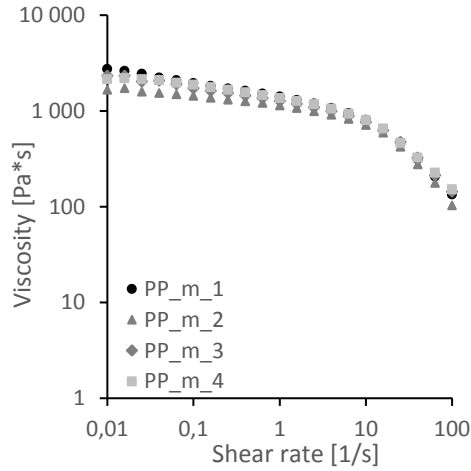


Figure B.1. Viscosity curves of additive-free PP milled samples.

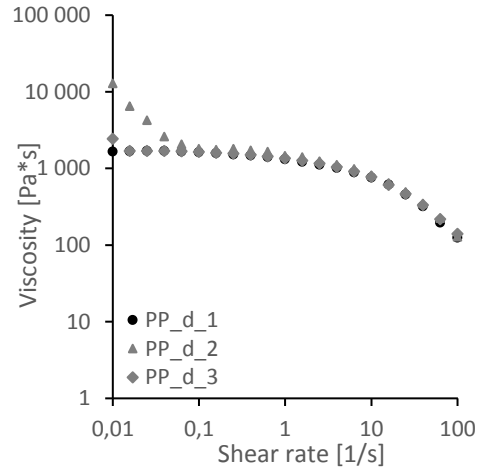


Figure B.2. Viscosity curves of additive-free PP disc samples.

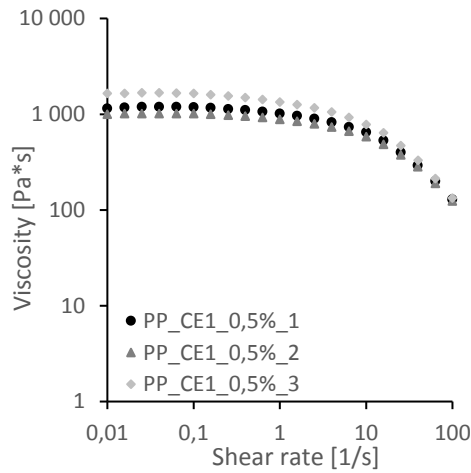


Figure B.3. Viscosity curves of PP with 0,5 % of CE 1 (Joncryl ADR 4400).

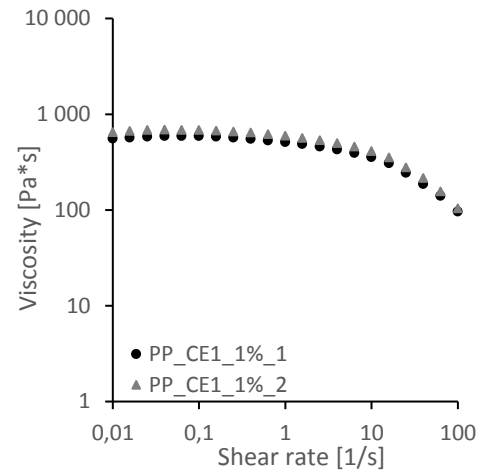


Figure B.4. Viscosity curves of PP with 1 % of CE 1 (Joncryl ADR 4400).

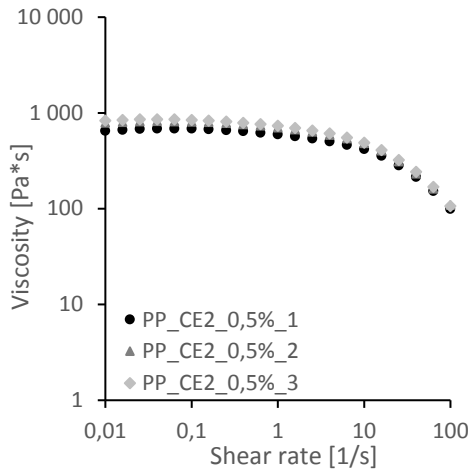


Figure B.5. Viscosity curves of PP with 0,5 % of CE 2 (Joncryl ADR 4468).

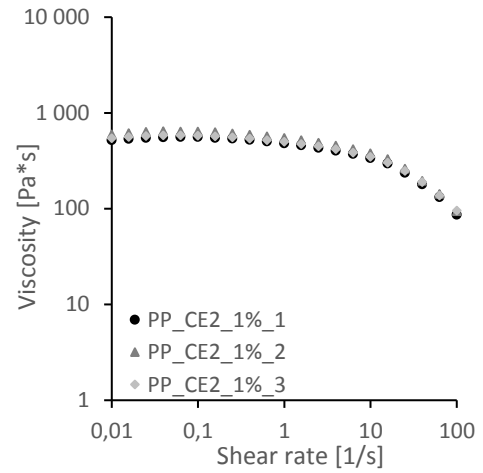


Figure B.6. Viscosity curves of PP with 1 % of CE 2 (Joncryl ADR 4468).

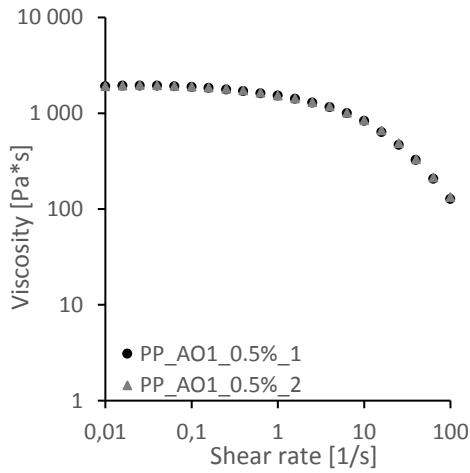


Figure B.7. Viscosity curves of PP with 0,5 % of AO 1 (Irganox 1010).

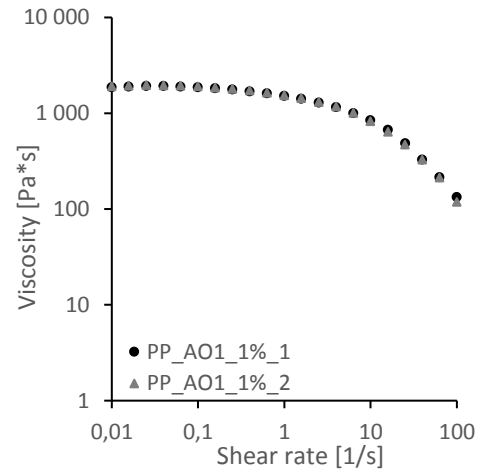


Figure B.8. Viscosity curves of PP with 1 % of AO 1 (Irganox 1010).

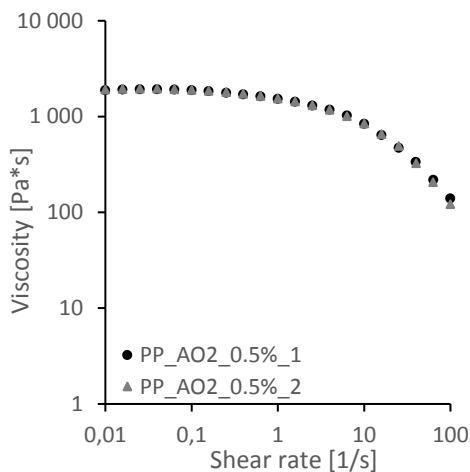


Figure B.9. Viscosity curves of PP with 0,5 % of AO 2 (Irganox 1076).

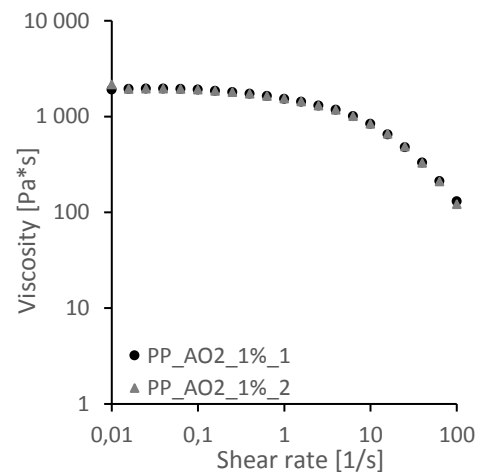


Figure B.10. Viscosity curves of PP with 1 % of AO 2 (Irganox 1076).

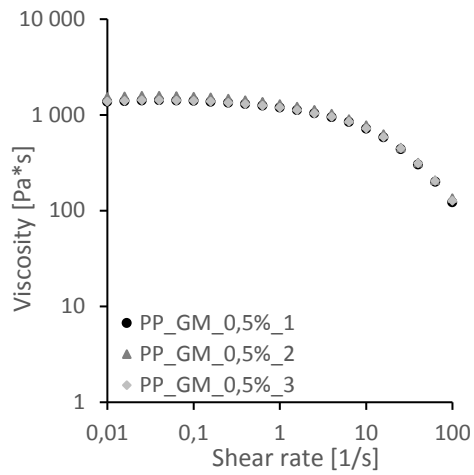


Figure B.11. Viscosity curves of PP with 0,5 % of GM.

Viscosity curves of PS samples

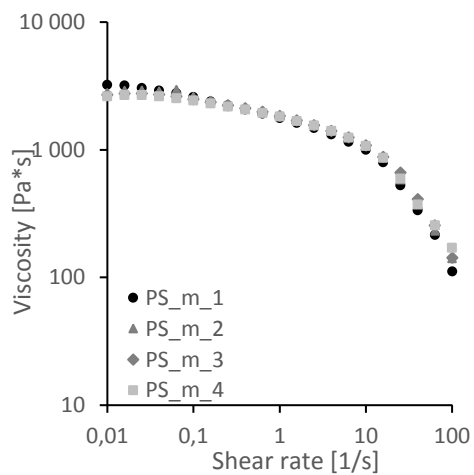


Figure B.12. Viscosity curves of additive-free PS milled samples.

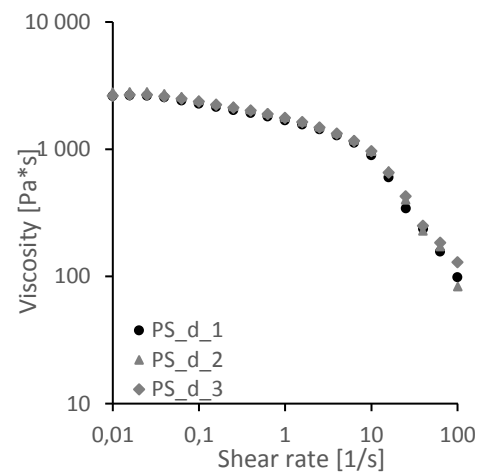


Figure B.13. Viscosity curves of additive-free PS disc samples.

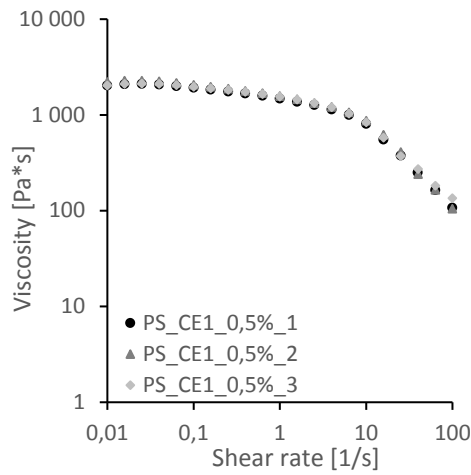


Figure B.14. Viscosity curves of PS with 0,5 % of CE 1 (Joncryn ADR 4400).

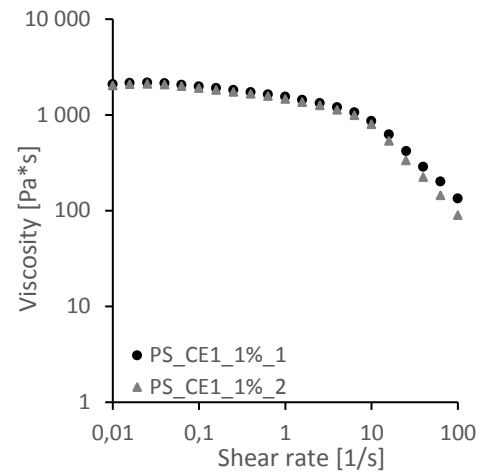


Figure B.15. Viscosity curves of PS with 1 % of CE 1 (Joncryn ADR 4400).

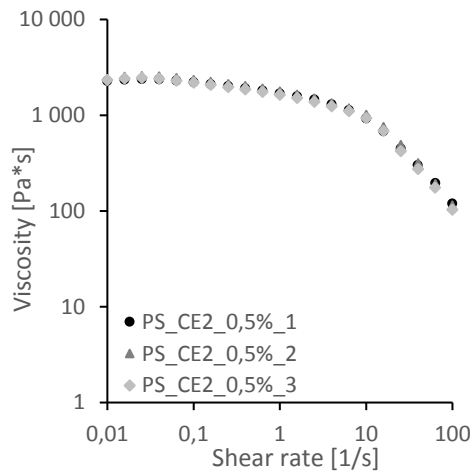


Figure B.16. Viscosity curves of PS with 0,5 % of CE 2 (Joncryn ADR 4468).

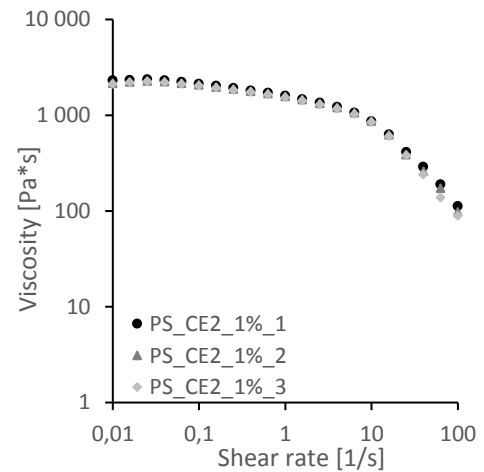


Figure B.17. Viscosity curves of PS with 1 % of CE 2 (Joncryn ADR 4468).

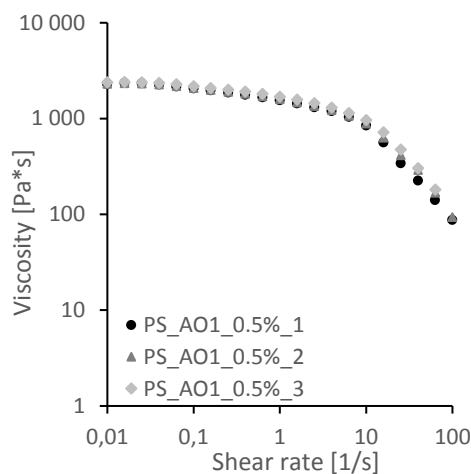


Figure B.18. Viscosity curves of PS with 0,5 % of AO 1 (Irganox 1010).

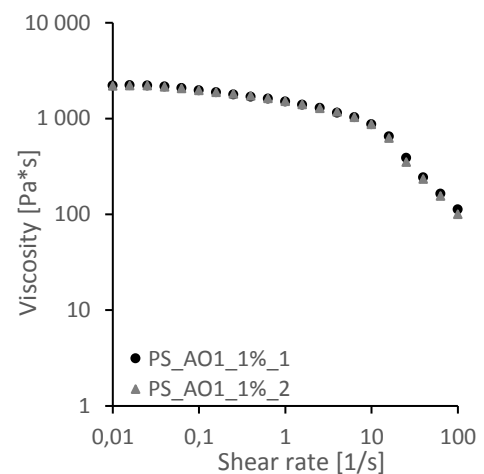


Figure B.19. Viscosity curves of PS with 1 % of AO 1 (Irganox 1010).

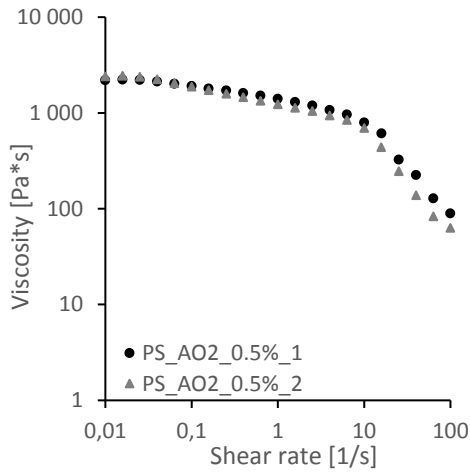


Figure B.20. Viscosity curves of PS with 0,5 % of AO 2 (Irganox 1076).

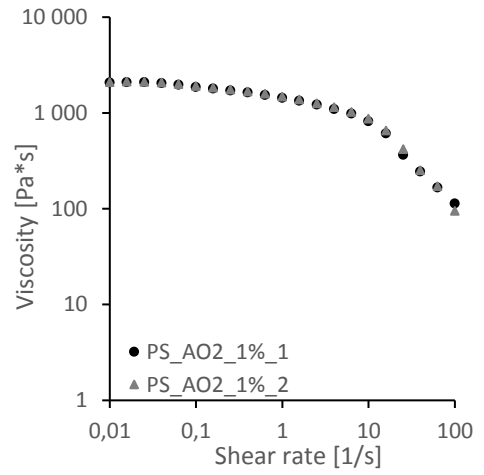


Figure B.21. Viscosity curves of PS with 1 % of AO 2 (Irganox 1076).

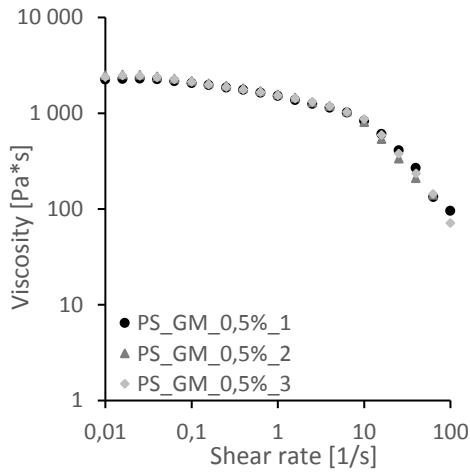


Figure B.22. Viscosity curves of PS with 0,5 % of GM.

Viscosity curves of ABS samples

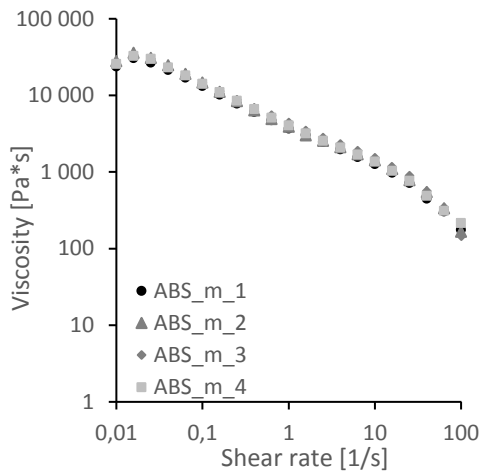


Figure B.23. Viscosity curves of additive-free ABS milled samples.

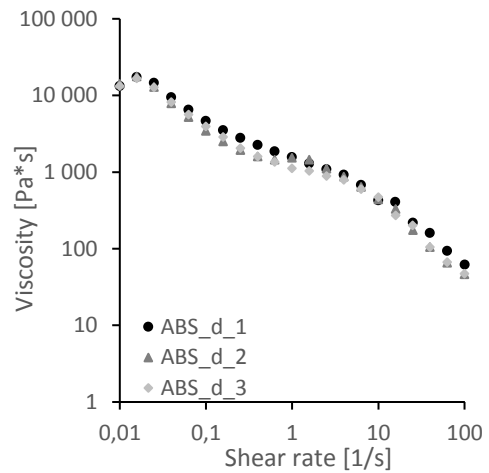


Figure B.24. Viscosity curves of additive-free ABS disc samples.

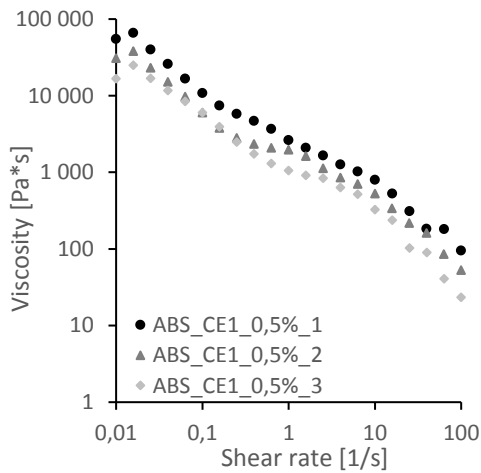


Figure B.25. Viscosity curves of ABS with 0,5 % of CE 1 (Joncryl ADR 4400).

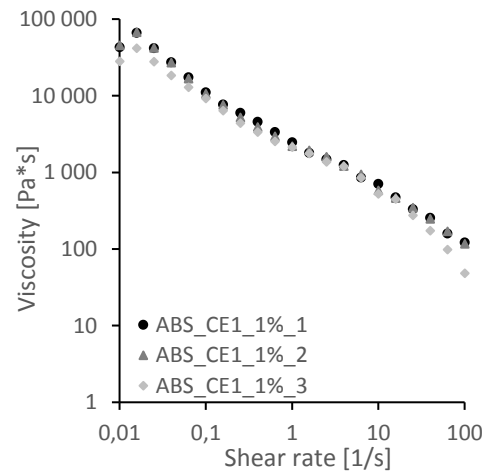


Figure B.26. Viscosity curves of ABS with 1 % of CE 1 (Joncryl ADR 4400).

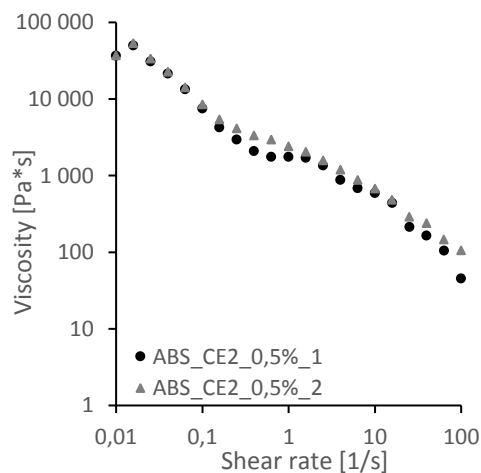


Figure B.27. Viscosity curves of ABS with 0,5 % of CE 2 (Joncryl ADR 4468).

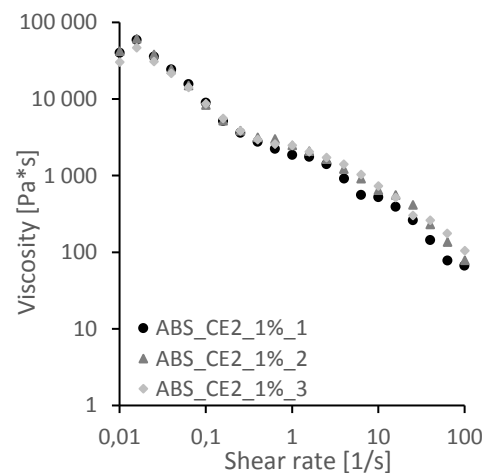


Figure B.28. Viscosity curves of ABS with 1 % of CE 2 (Joncryl ADR 4468).

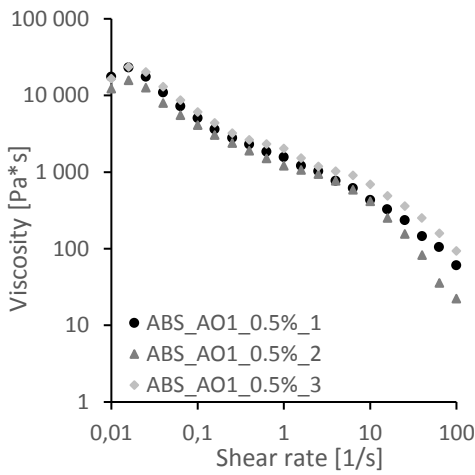


Figure B.29. Viscosity curves of ABS with 0,5 % of AO 1 (Irganox 1010).

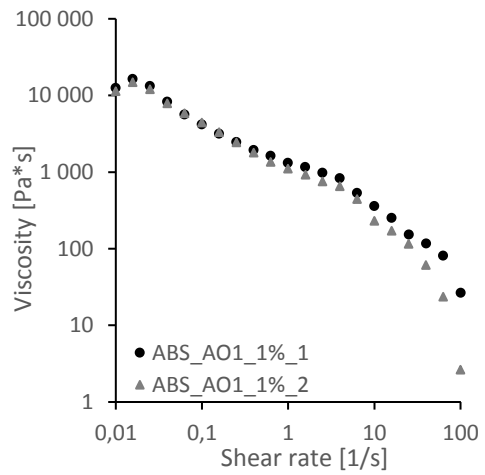


Figure B.30. Viscosity curves of ABS with 1 % of AO 1 (Irganox 1010).

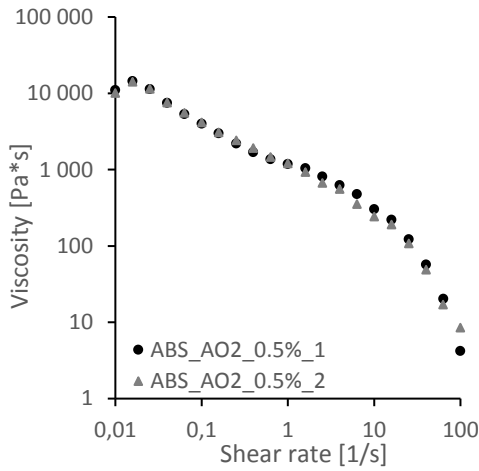


Figure B.31. Viscosity curves of ABS with 0,5 % of AO 2 (Irganox 1076).

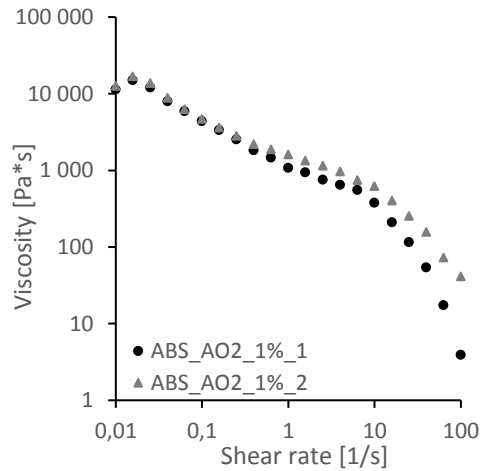


Figure B.32. Viscosity curves of ABS with 1 % of AO 2 (Irganox 1076).

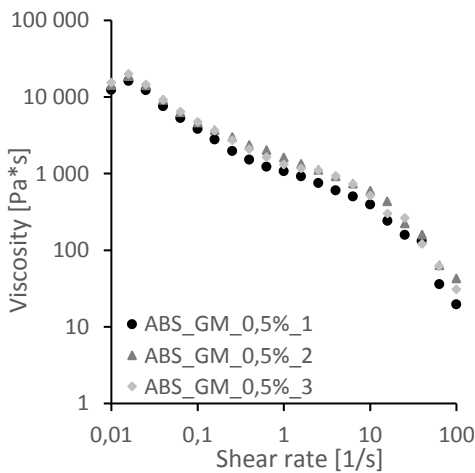


Figure B.33. Viscosity curves of ABS with 0,5 % of GM.

Viscosity curves of PC/ABS samples

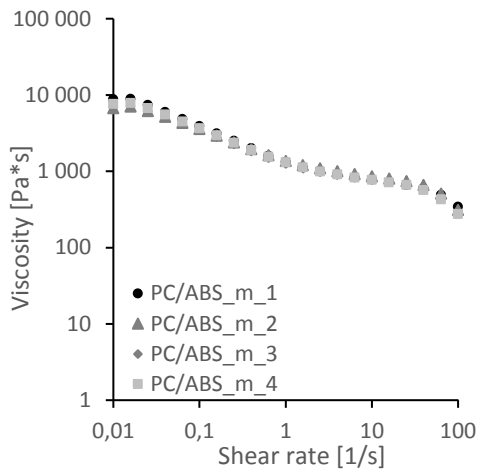


Figure B.34. Viscosity curves of additive-free PC/ABS milled samples.

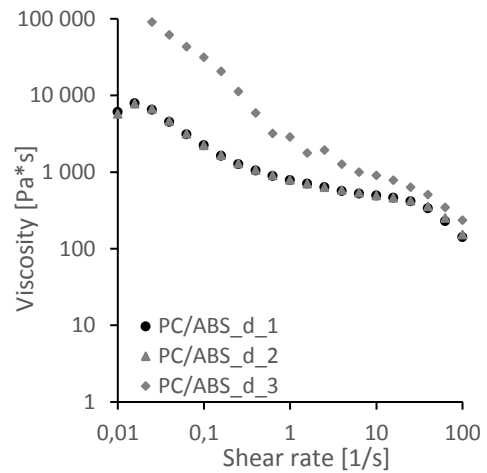


Figure B.35. Viscosity curves of additive-free PC/ABS disc samples.

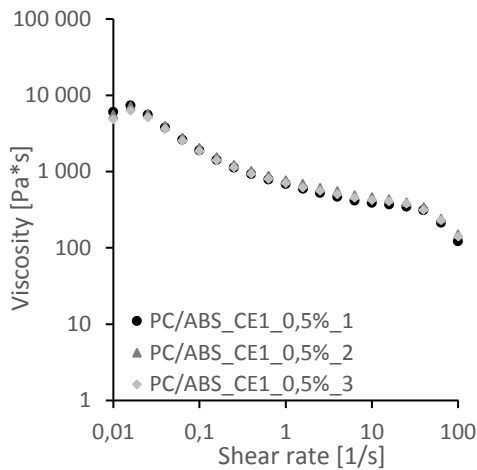


Figure B.36. Viscosity curves of PC/ABS with 0,5 % of CE 1 (Joncryl ADR 4400).

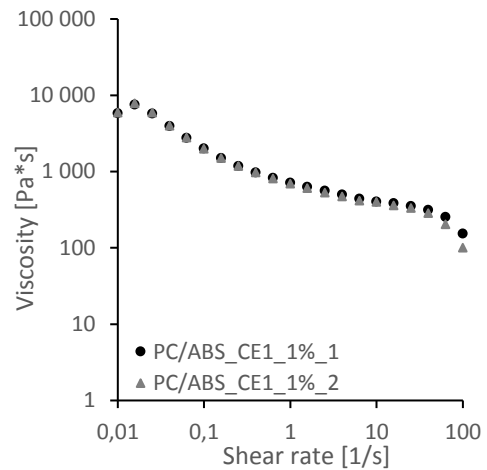


Figure B.37. Viscosity curves of PC/ABS with 1 % of CE 1 (Joncryl ADR 4400).

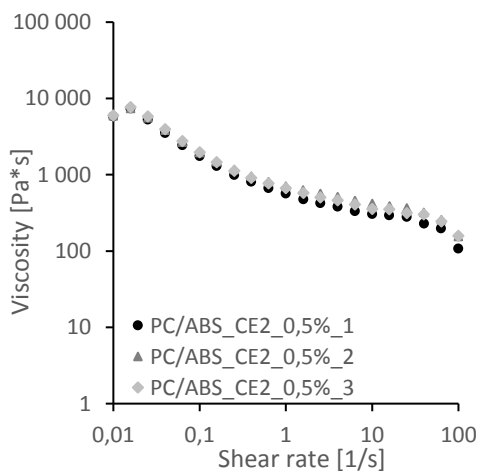


Figure B.38. Viscosity curves of PC/ABS with 0,5 % of CE 2 (Joncryl ADR 4468).

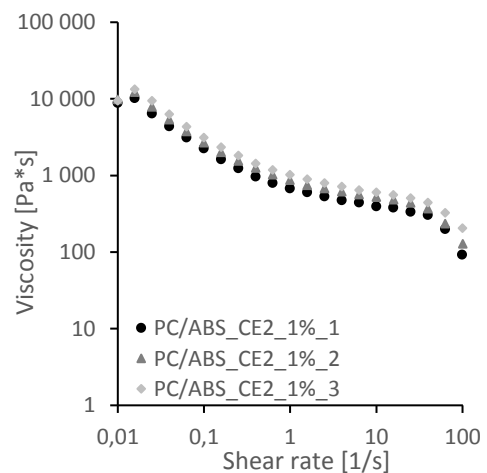


Figure B.39. Viscosity curves of PC/ABS with 1 % of CE 2 (Joncryl ADR 4468).

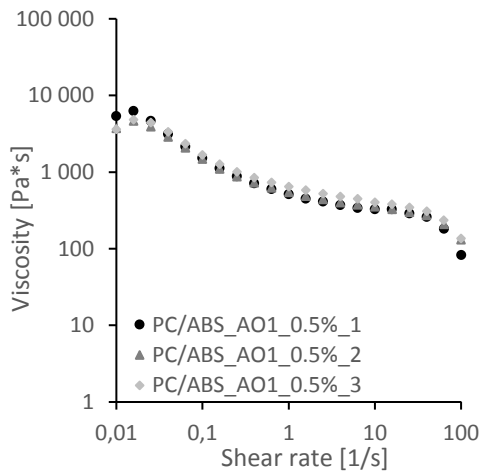


Figure B.40. Viscosity curves of PC/ABS with 0,5 % of AO 1 (Irganox 1010).

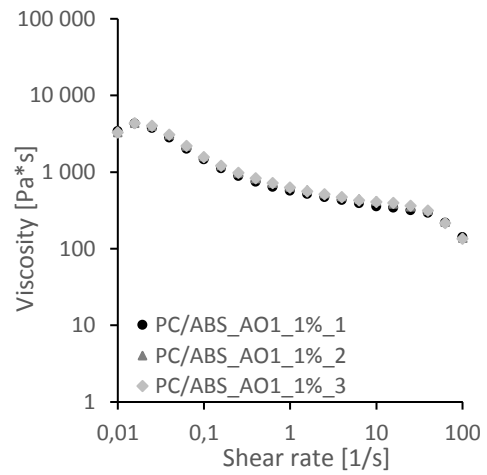


Figure B.41. Viscosity curves of PC/ABS with 1 % of AO 1 (Irganox 1010).

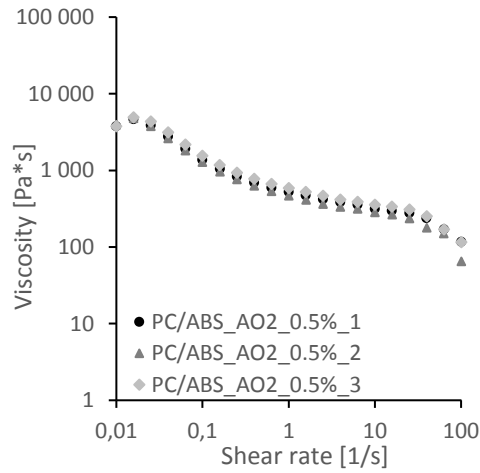


Figure B.42. Viscosity curves of PC/ABS with 0,5 % of AO 2 (Irganox 1076).

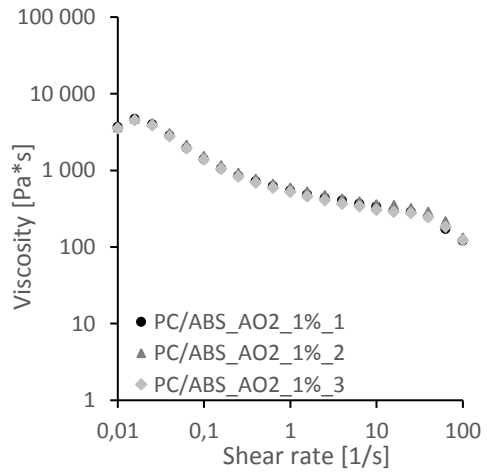


Figure B.43. Viscosity curves of PC/ABS with 1 % of AO 2 (Irganox 1076).

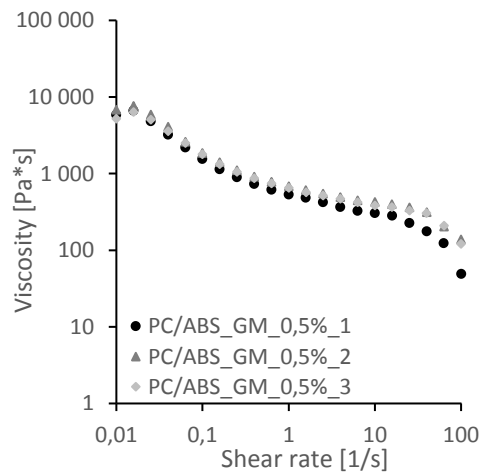


Figure B.44. Viscosity curves of PC/ABS with 0,5 % of GM.

ANNEX C: PROCEDURE FOR CALCULATING THE POWER-LAW INDICES

The Power-law indices were calculated by using the Excel add-in Solver. The indices were determined by fitting a Power-law model onto the last three data points of each viscosity curve. The index of the first additive-free milled PP sample is calculated as an example of the procedure (Figure C.1).

	A	B	C	D
1	PP_m			
2	1			
3	shear rate	viscosity (measured)	viscosity (calculated)	error
4	1/s	Pa*s	Pa*s	Pa*s
5	39,9	311	311,4366164	0,190633872
6	63,3	206	204,6650739	1,782027791
7	100	134	135,0164276	1,033125096
8				
9	Sum	3,005786759	(Pa*s)^2	
10	n	0,090	-	
11	K	8906,908303	Pa*s^n	

Figure C.1. Values for calculating the Power-law index for a viscosity curve.

Cells A5 – A7 show the shear rates of the last three data points of the viscosity curve. Cells B5 – B7 show the viscosities measured at these shear rates. Cells C5 – C7 show the viscosities calculated with the Power-law model shown in Equation C.1.

$$\eta_c = K\dot{\gamma}^{n-1} \quad (\text{C.1})$$

η_c : calculated viscosity [Pa*s], in cells C5 – C7

K : consistency factor [Pa*sⁿ], in cell B11

$\dot{\gamma}$: shear rate [1/s], in cells A5 – A7

n : Power-law index [-], in cell B10

Cells D5 – D7 show the difference between the calculated and measured viscosities raised to the power of 2 (Equation C.2). Cell B9 shows the sum of all the errors in cells D5 – D7.

$$error = (\eta_c - \eta_m)^2 \quad (\text{C.2})$$

η_c : calculated viscosity [Pa*s], in cells C5 – C7

η_m : measured viscosity [Pa*s], in cells B5 – B7

Figure C.2 shows the setting of the Solver.

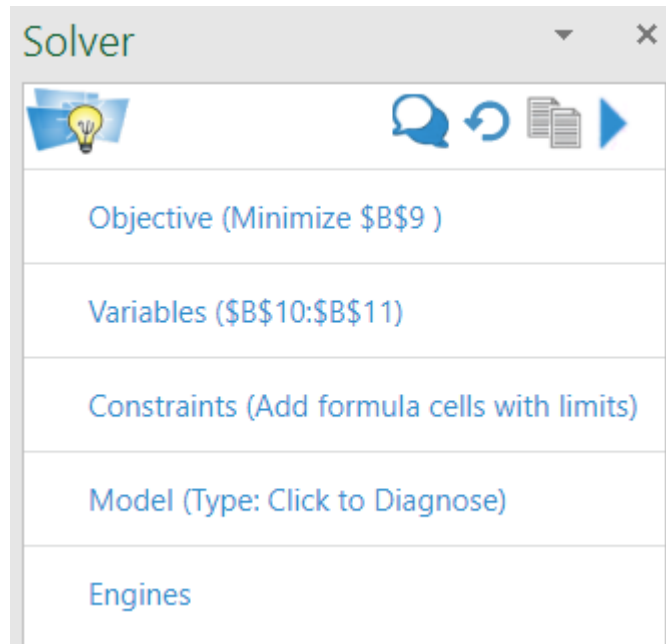


Figure C.2. Excel Solver settings.

The sum of the errors in cell B9 is set as the Objective, and the Solver is asked to minimize the value. The Variables are the Power-law index in B10 and the consistency factor in B11. With these settings the Solver will find values for the Power-law index and consistency factor that make the sum of the errors as small as possible. This means the calculated viscosities of the Power-law model's curve will be as close to the measured viscosities as possible. The Power-law index in B10 then tells the Power-law index of the measured viscosity curve.

ANNEX D: TENSILE PROPERTIES

Tensile test curves of PP samples

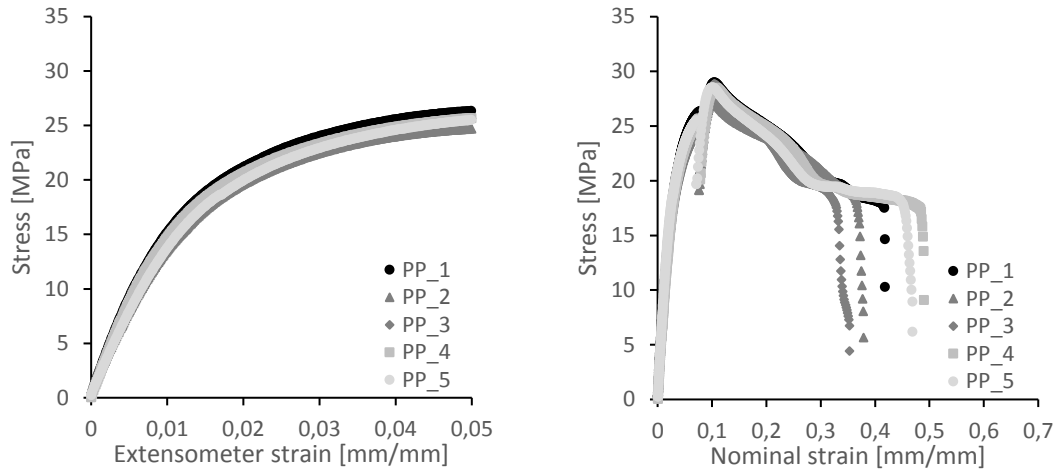


Figure D.1. Stress as a function of extensometer strain (left) and nominal strain (right) for additive-free PP.

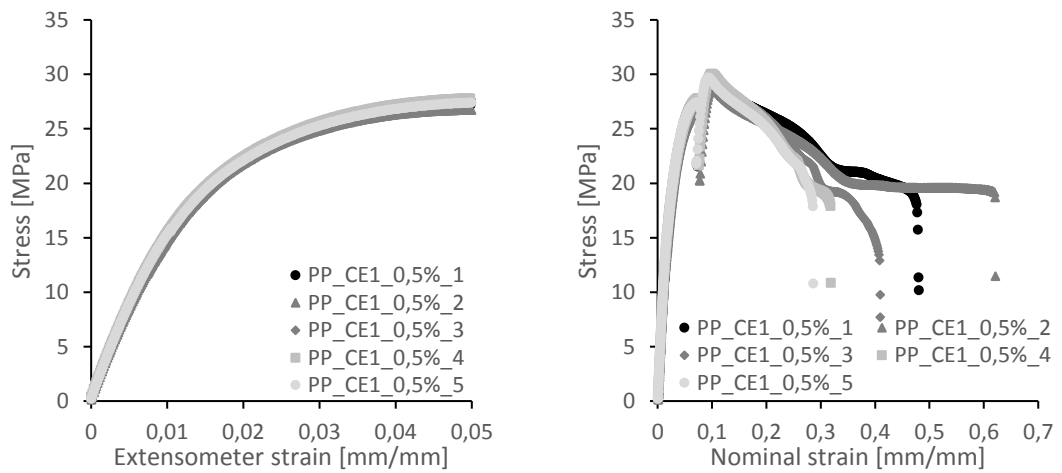


Figure D.2. Stress as a function of extensometer strain (left) and nominal strain (right) for PP with 0,5 % of CE 1 (Joncryl ADR 4400).

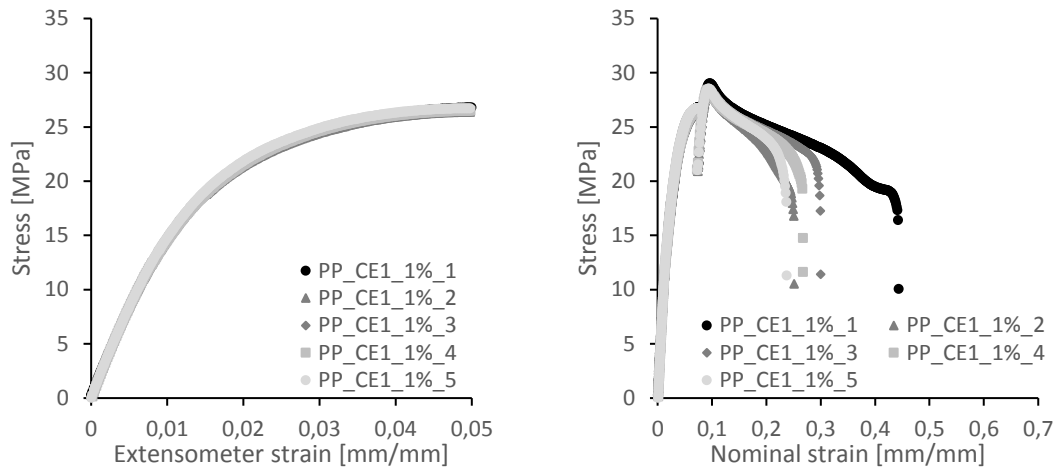


Figure D.3. Stress as a function of extensometer strain (left) and nominal strain (right) for PP with 1 % of CE 1 (Joncryl ADR 4400).

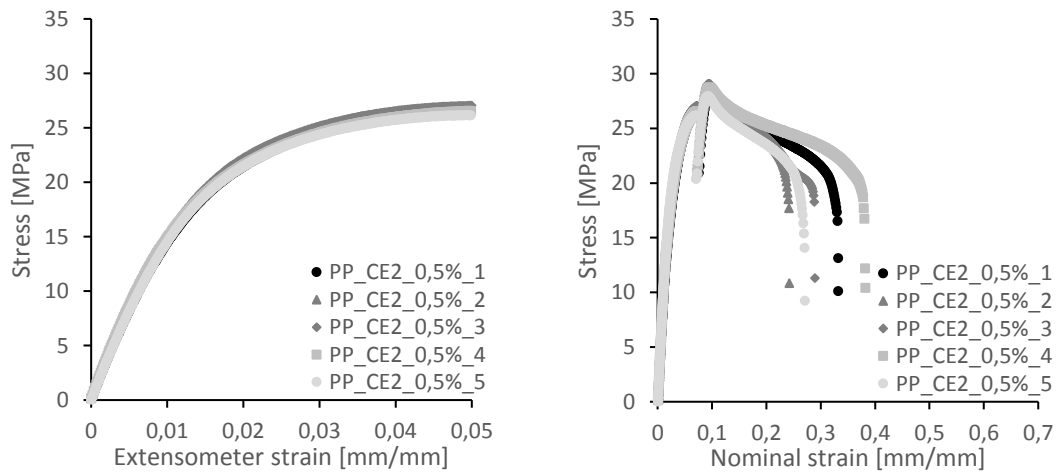


Figure D.4. Stress as a function of extensometer strain (left) and nominal strain (right) for PP with 0,5 % of CE 2 (Joncryl ADR 4468).

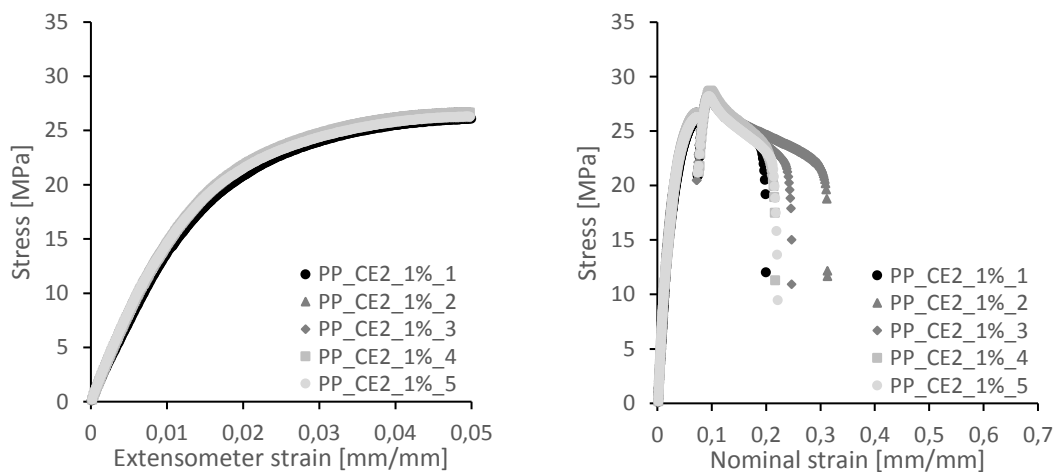


Figure D.5. Stress as a function of extensometer strain (left) and nominal strain (right) for PP with 1 % of CE 2 (Joncryl ADR 4468).

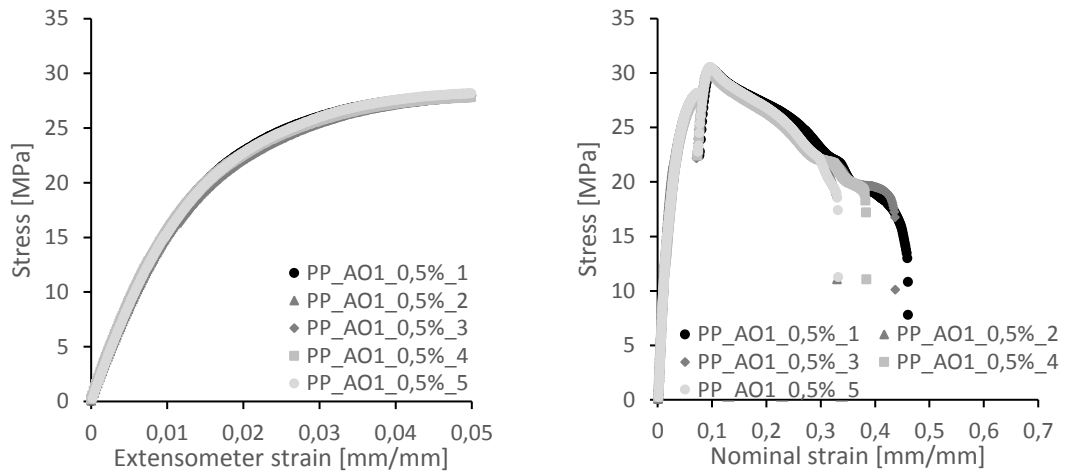


Figure D.6. Stress as a function of extensometer strain (left) and nominal strain (right) for PP with 0,5 % of AO 1 (Irganox 1010).

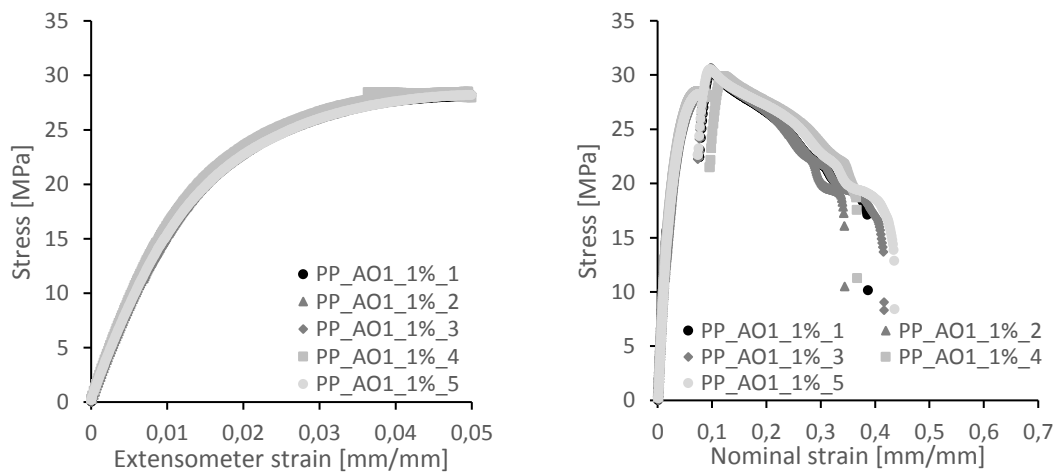


Figure D.7. Stress as a function of extensometer strain (left) and nominal strain (right) for PP with 1 % of AO 1 (Irganox 1010).

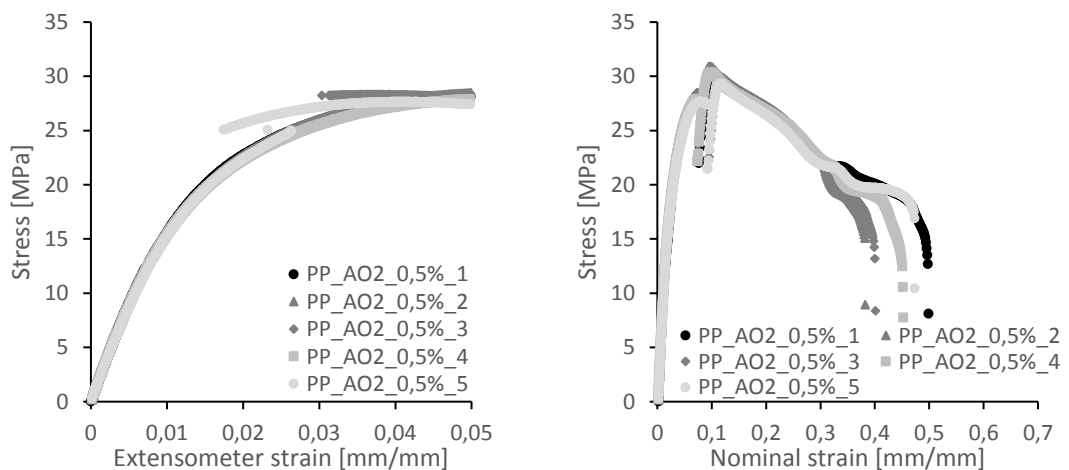


Figure D.8. Stress as a function of extensometer strain (left) and nominal strain (right) for PP with 0,5 % of AO 2 (Irganox 1076).

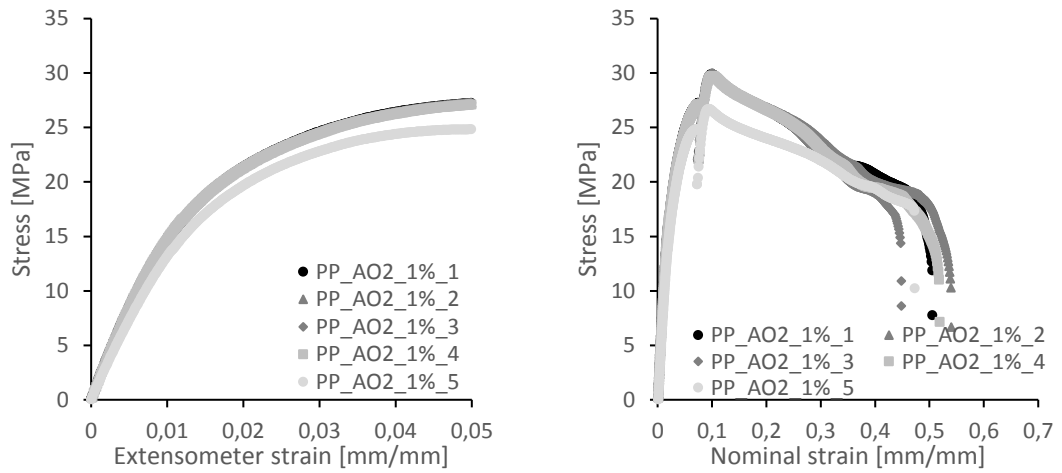


Figure D.9. Stress as a function of extensometer strain (left) and nominal strain (right) for PP with 1 % of AO 2 (Irganox 1076).

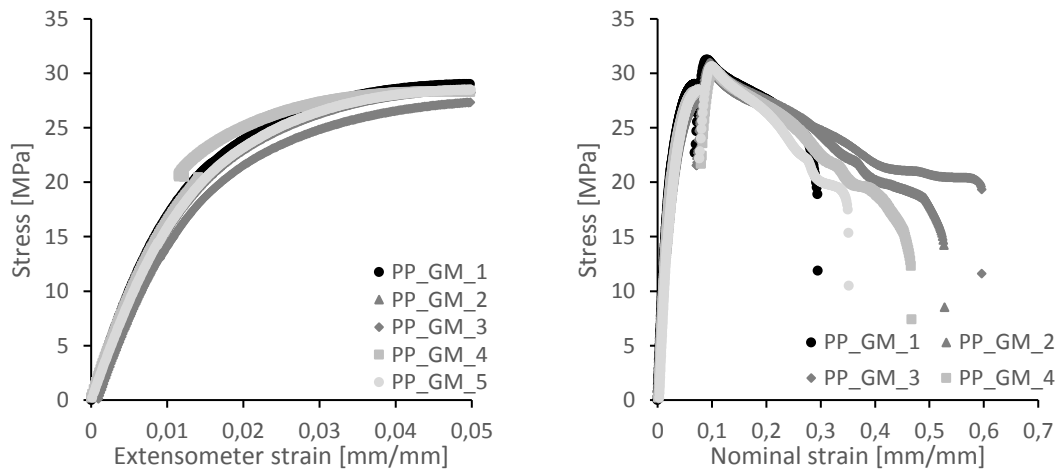


Figure D.10. Stress as a function of extensometer strain (left) and nominal strain (right) for PP with 0,5 % of GM.

The extensometer malfunctioned while measuring samples PP_AO1_1%_4, PP_AO2_0,5%_3, PP_AO2_0,5%_5, and PP_GM_4. As the yield stresses and strains were not determined with the extensometer strains for PP this did not affect the results. The malfunctioning happened at high enough strains so that it did not affect the moduli.

Tensile test curves of PS samples

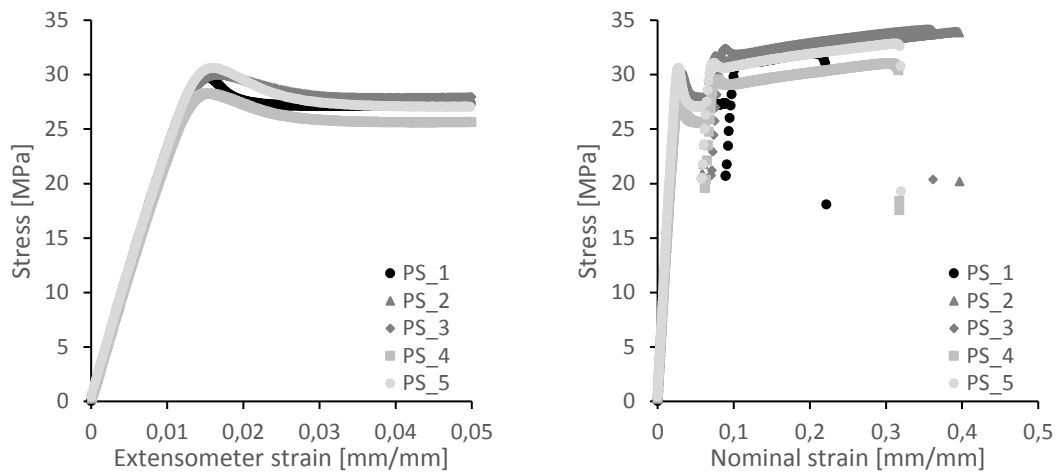


Figure D.11. Stress as a function of extensometer strain (left) and nominal strain (right) for additive-free PS.

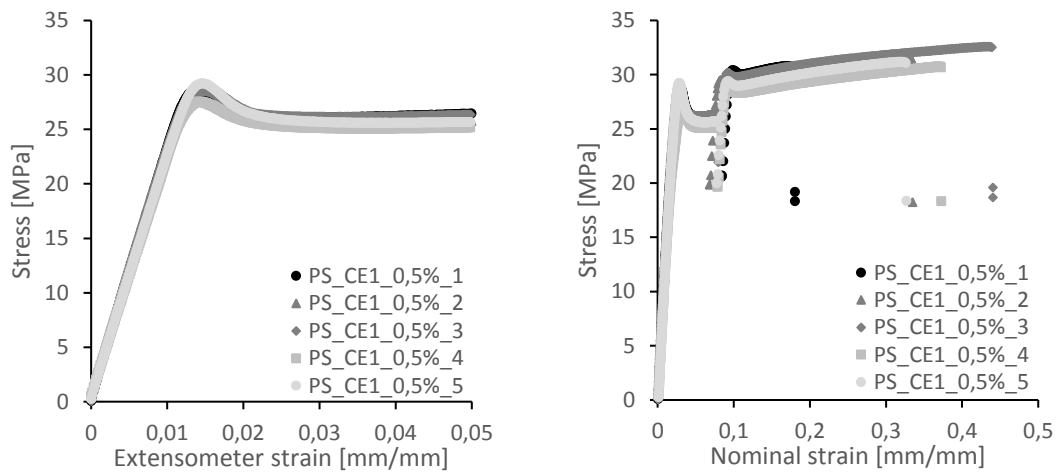


Figure D.12. Stress as a function of extensometer strain (left) and nominal strain (right) for PS with 0,5 % of CE 1 (Joncryl ADR 4400).

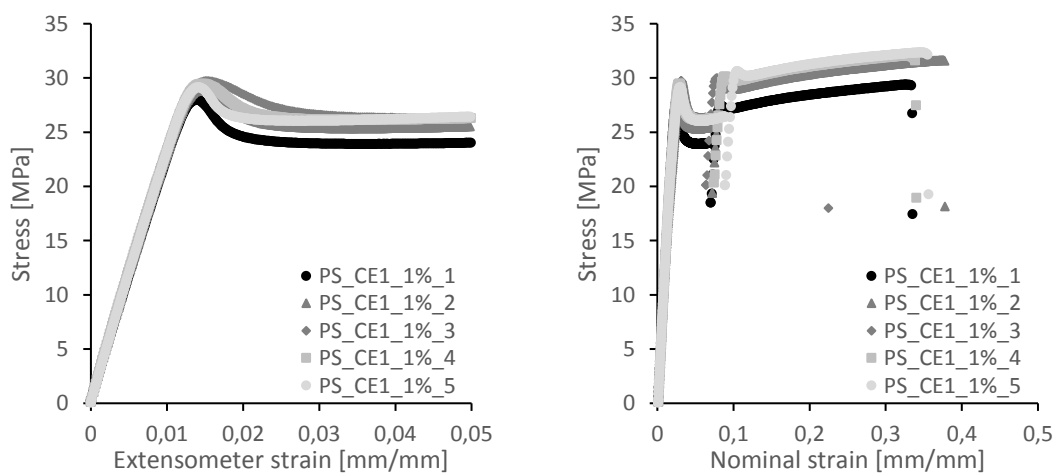


Figure D.13. Stress as a function of extensometer strain (left) and nominal strain (right) for PS with 1 % of CE 1 (Joncryl ADR 4400).

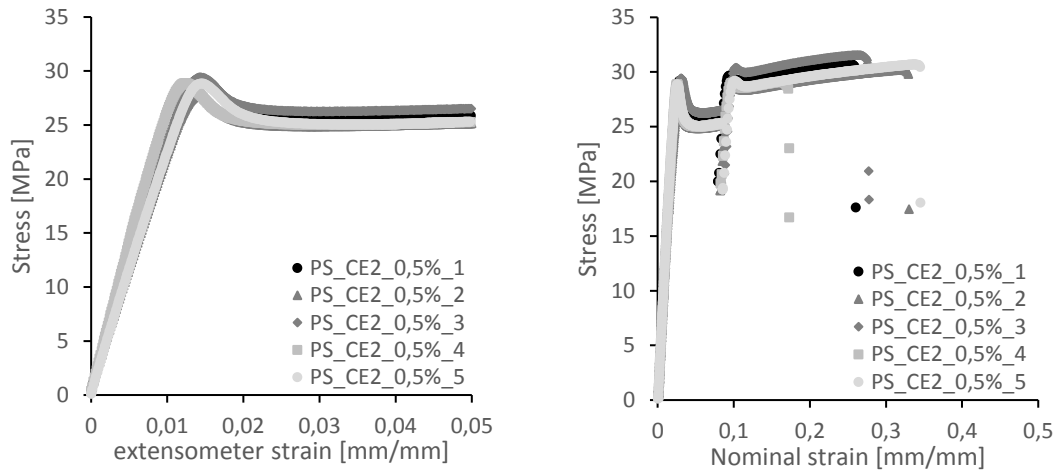


Figure D.14. Stress as a function of extensometer strain (left) and nominal strain (right) for PS with 0,5 % of CE 2 (Joncryl ADR 4468).

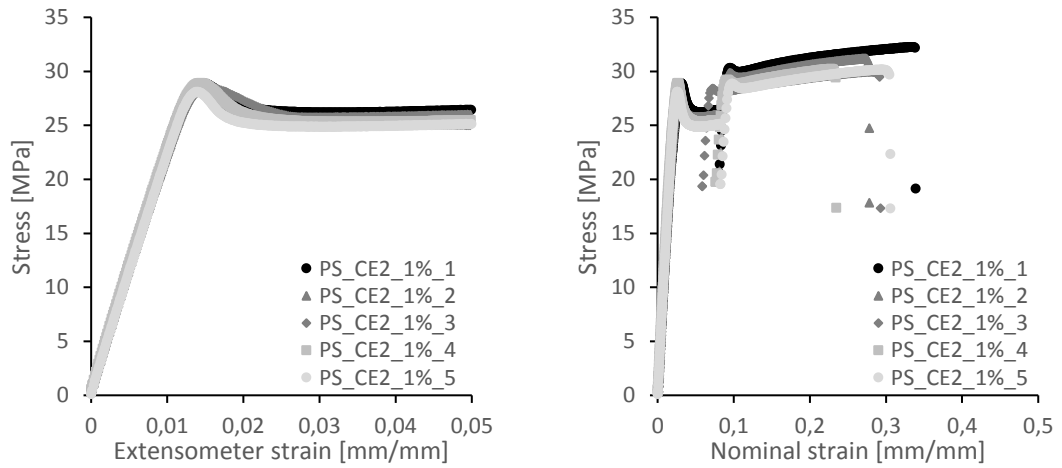


Figure D.15. Stress as a function of extensometer strain (left) and nominal strain (right) for PS with 1 % of CE 2 (Joncryl ADR 4468).

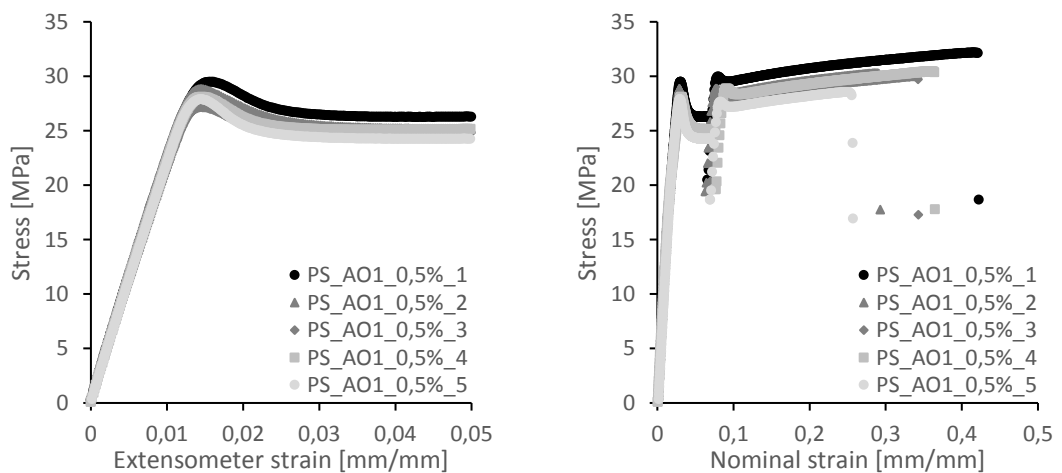


Figure D.16. Stress as a function of extensometer strain (left) and nominal strain (right) for PS with 0,5 % of AO 1 (Irganox 1010).

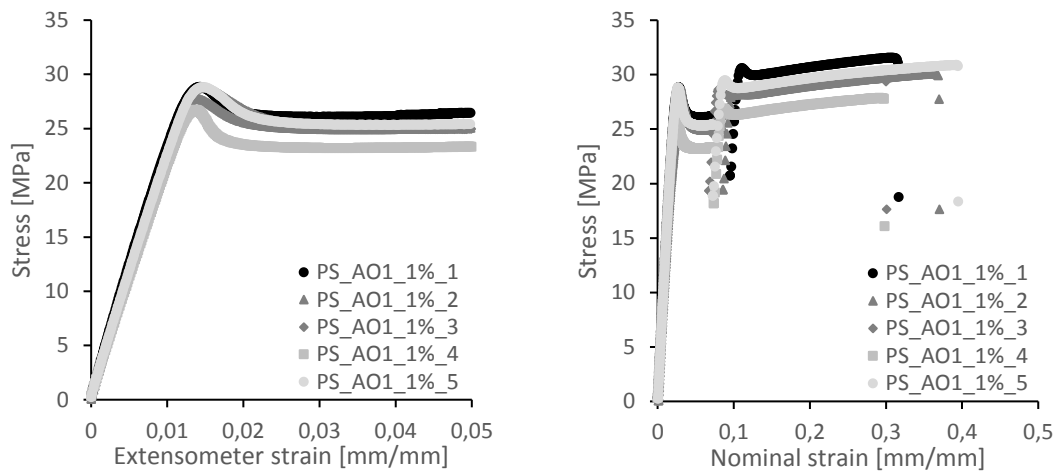


Figure D.17. Stress as a function of extensometer strain (left) and nominal strain (right) for PS with 1 % of AO 1 (Irganox 1010).

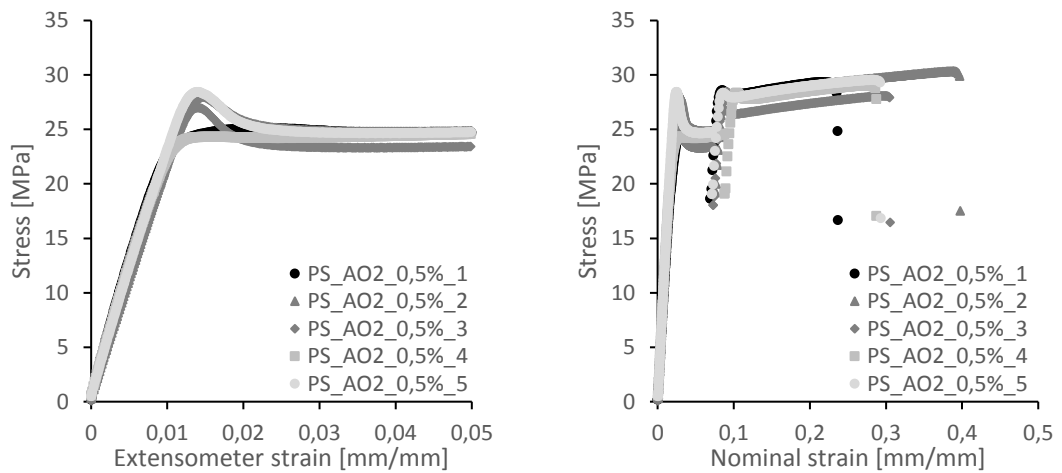


Figure D.18. Stress as a function of extensometer strain (left) and nominal strain (right) for PS with 0,5 % of AO 2 (Irganox 1076).

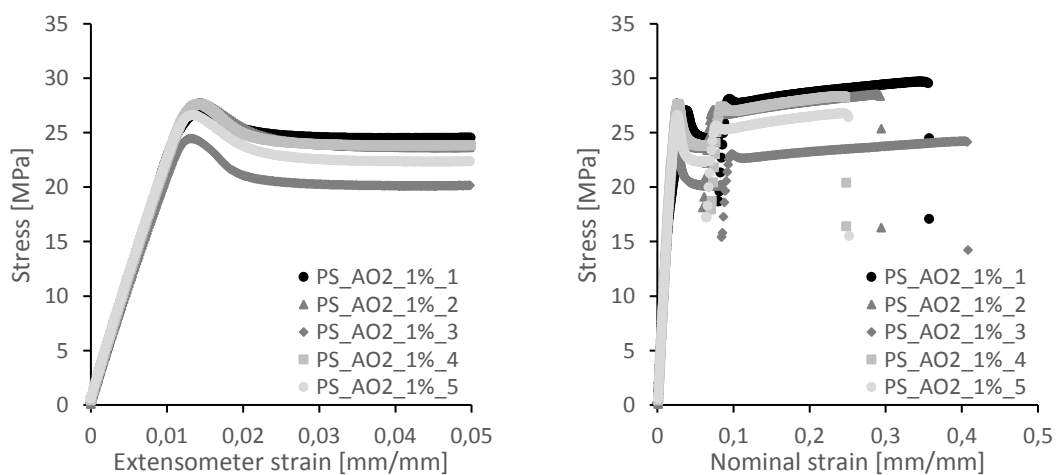


Figure D.19. Stress as a function of extensometer strain (left) and nominal strain (right) for PS with 1 % of AO 2 (Irganox 1076).

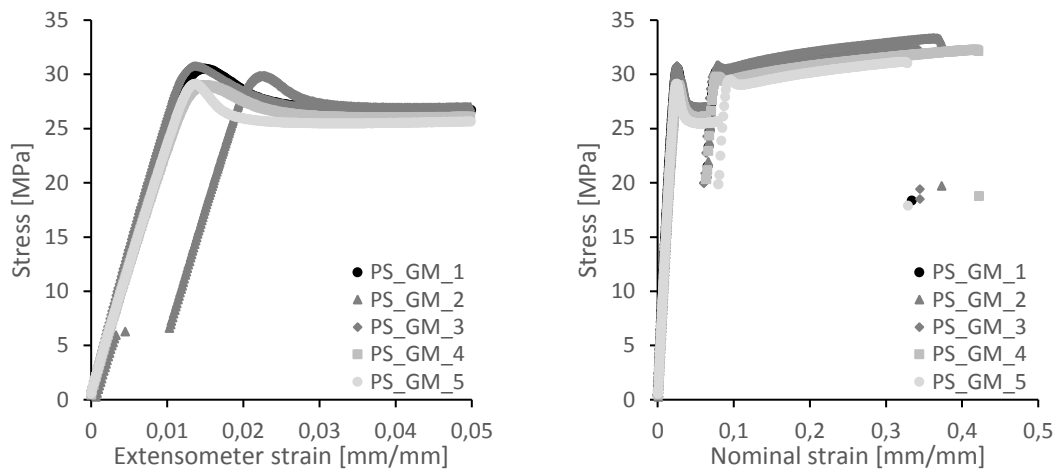


Figure D.20. Stress as a function of extensometer strain (left) and nominal strain (right) for PS with 0,5 % of GM.

The extensometer malfunctioned while measuring sample PS_GM_2. This curve was excluded when calculating the average modulus, yield stress, and yield strain for PS with GM.

Tensile test curves of ABS samples

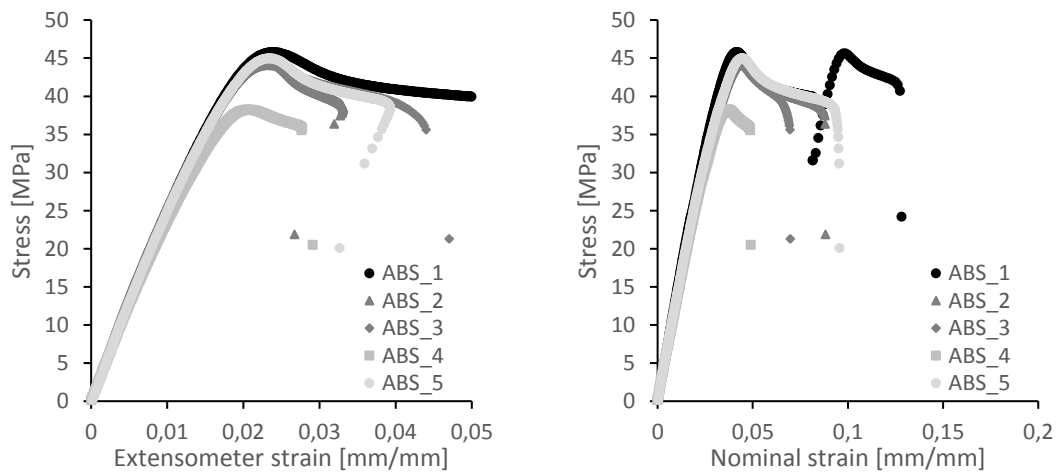


Figure D.21. Stress as a function of extensometer strain (left) and nominal strain (right) for additive-free ABS.

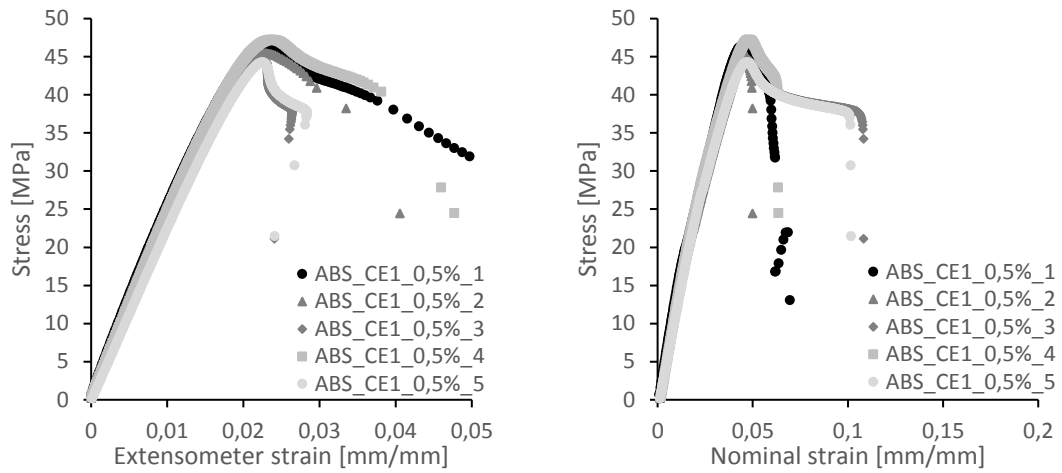


Figure D.22. Stress as a function of extensometer strain (left) and nominal strain (right) for ABS with 0,5 % of CE 1 (Joncryn ADR 4400).

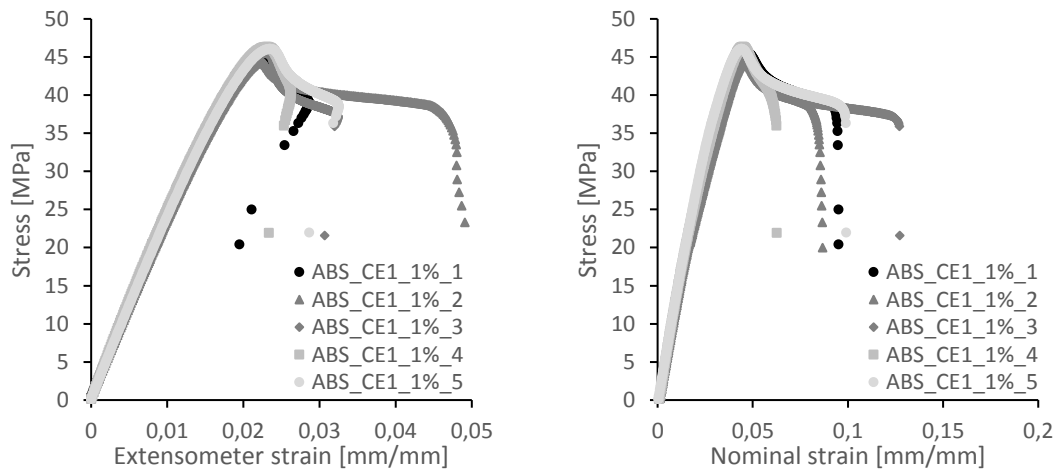


Figure D.23. Stress as a function of extensometer strain (left) and nominal strain (right) for ABS with 1 % of CE 1 (Joncryn ADR 4400).

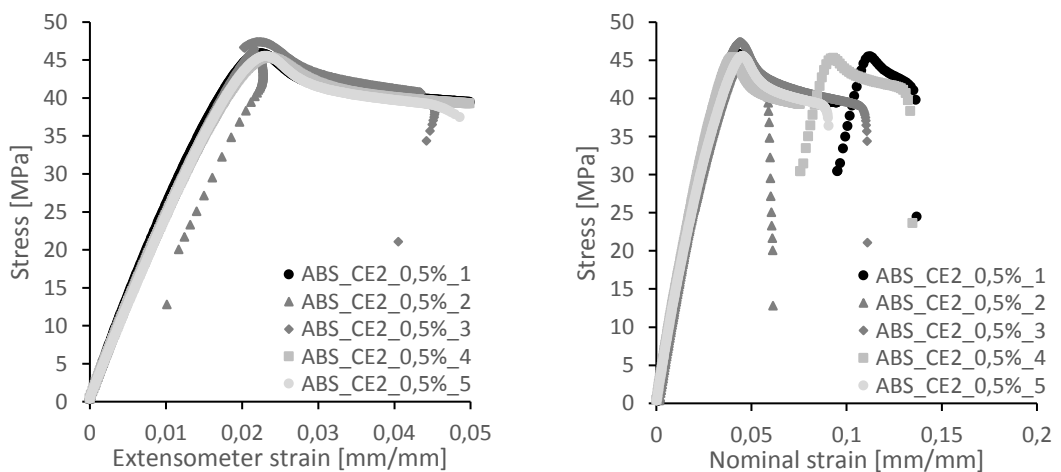


Figure D.24. Stress as a function of extensometer strain (left) and nominal strain (right) for ABS with 0,5 % of CE 2 (Joncryn ADR 4468).

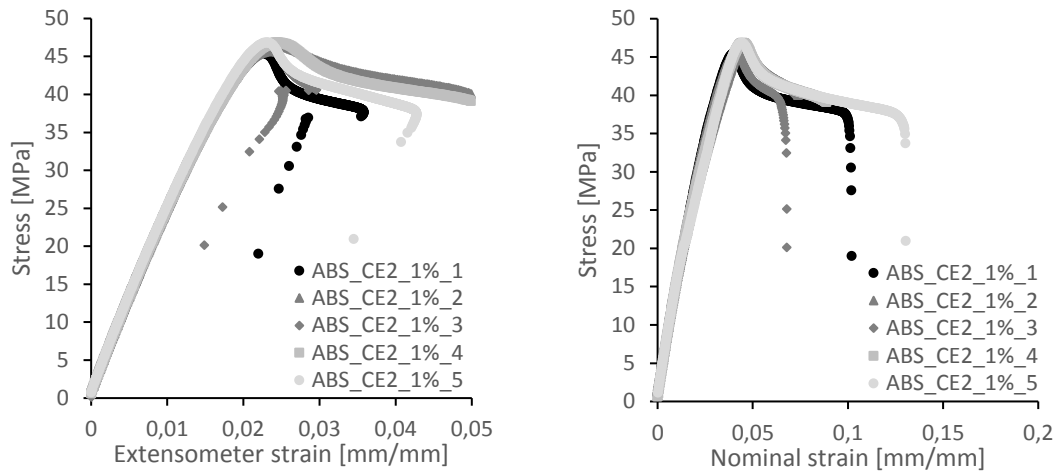


Figure D.25. Stress as a function of extensometer strain (left) and nominal strain (right) for ABS with 1 % of CE 2 (Joncryl ADR 4468).

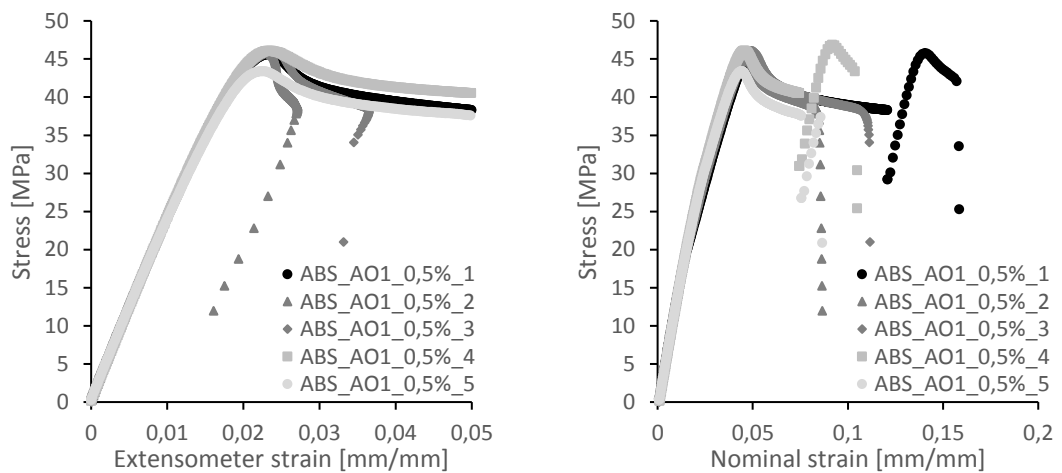


Figure D.26. Stress as a function of extensometer strain (left) and nominal strain (right) for ABS with 0,5 % of AO 1 (Irganox 1010).

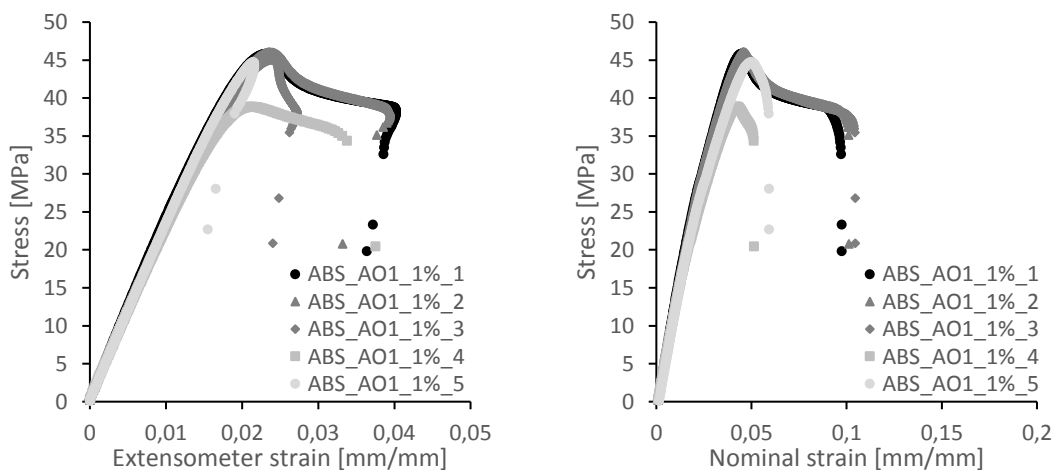


Figure D.27. Stress as a function of extensometer strain (left) and nominal strain (right) for ABS with 1 % of AO 1 (Irganox 1010).

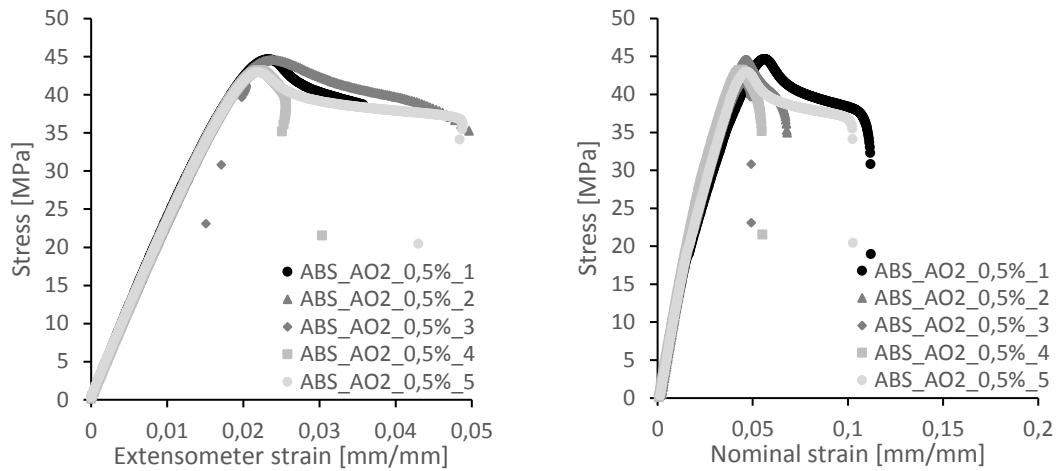


Figure D.28. Stress as a function of extensometer strain (left) and nominal strain (right) for ABS with 0,5 % of AO 2 (Irganox 1076).

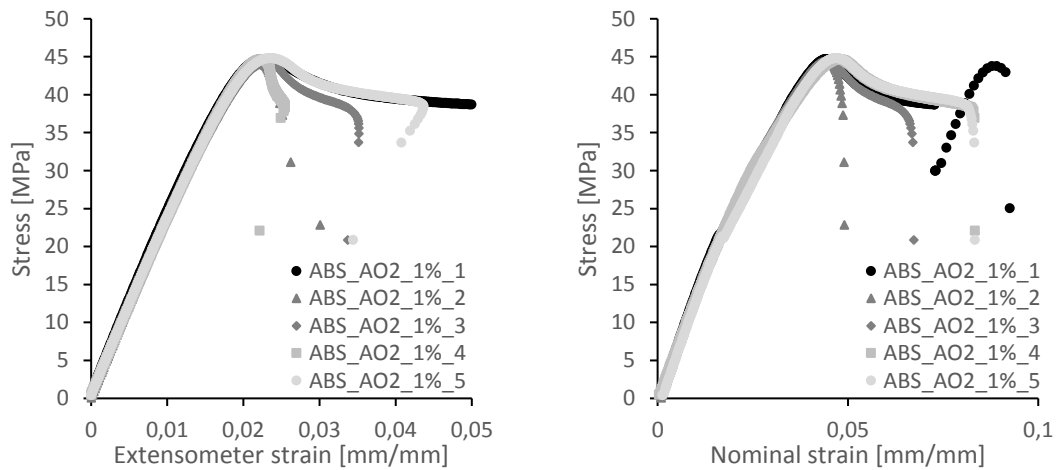


Figure D.29. Stress as a function of extensometer strain (left) and nominal strain (right) for ABS with 1 % of AO 2 (Irganox 1076).

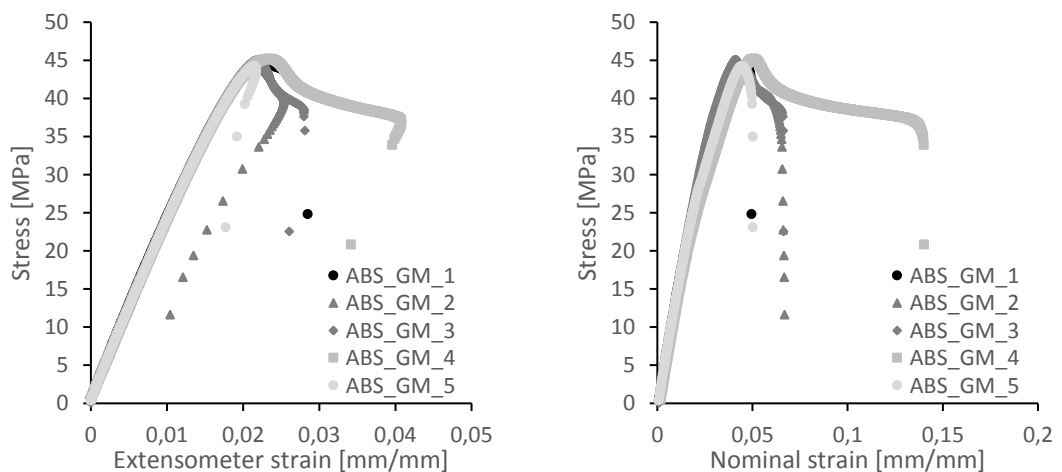


Figure D.30. Stress as a function of extensometer strain (left) and nominal strain (right) for ABS with 0,5 % of GM.

The extensometer malfunctioned while measuring sample ABS_CE2_0,5%_3. This curve was excluded when calculating the average modulus, yield stress, and yield strain for ABS with 0,5 % of CE 2.

Tensile test curves of PC/ABS samples

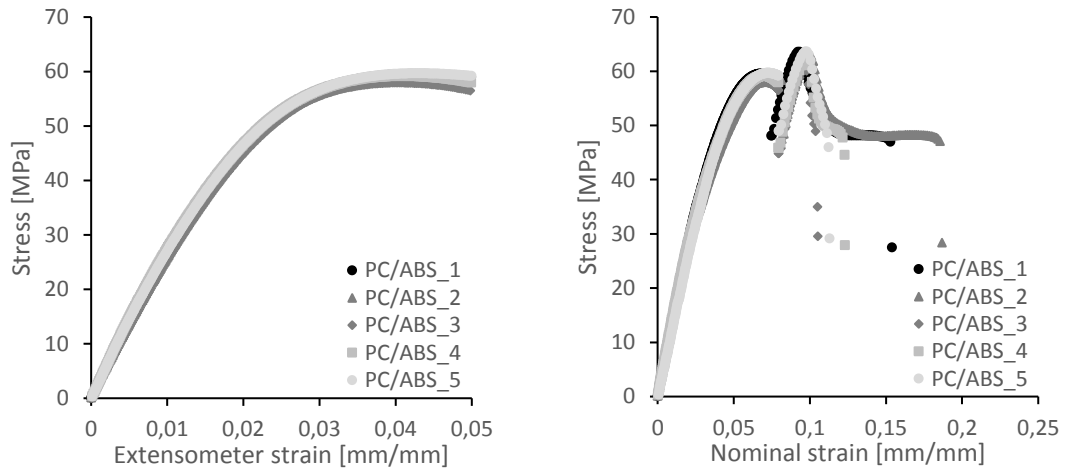


Figure D.31. Stress as a function of extensometer strain (left) and nominal strain (right) for additive-free PC/ABS.

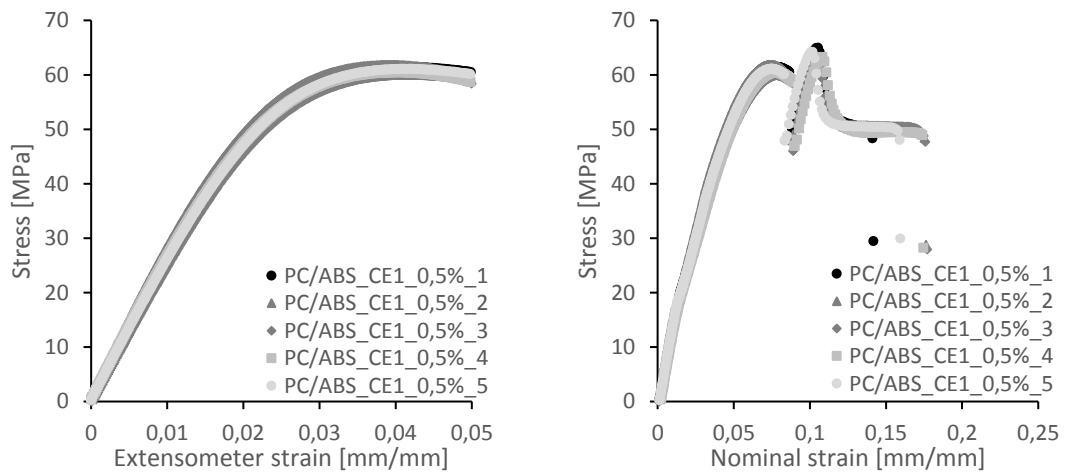


Figure D.32. Stress as a function of extensometer strain (left) and nominal strain (right) for PC/ABS with 0,5 % of CE 1 (Joncryl ADR 4400).

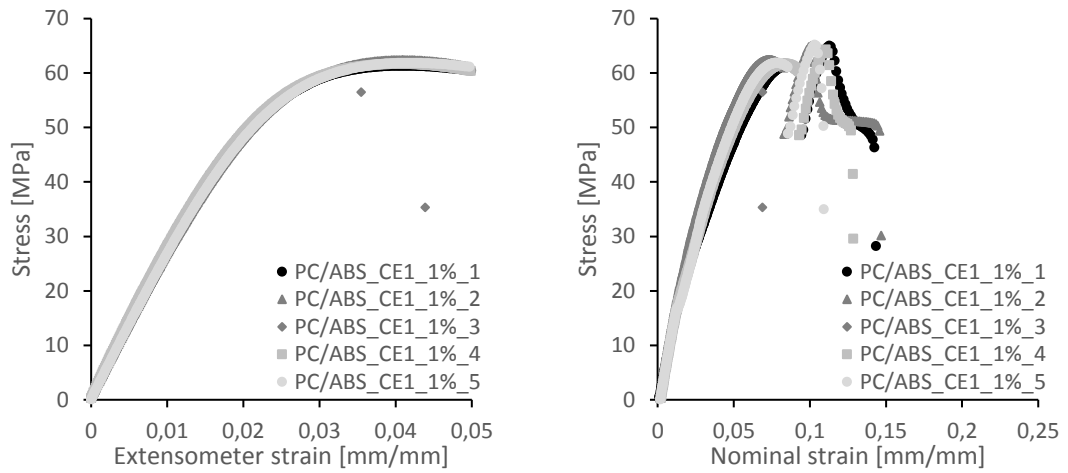


Figure D.33. Stress as a function of extensometer strain (left) and nominal strain (right) for PC/ABS with 1 % of CE 1 (Joncryl ADR 4400).

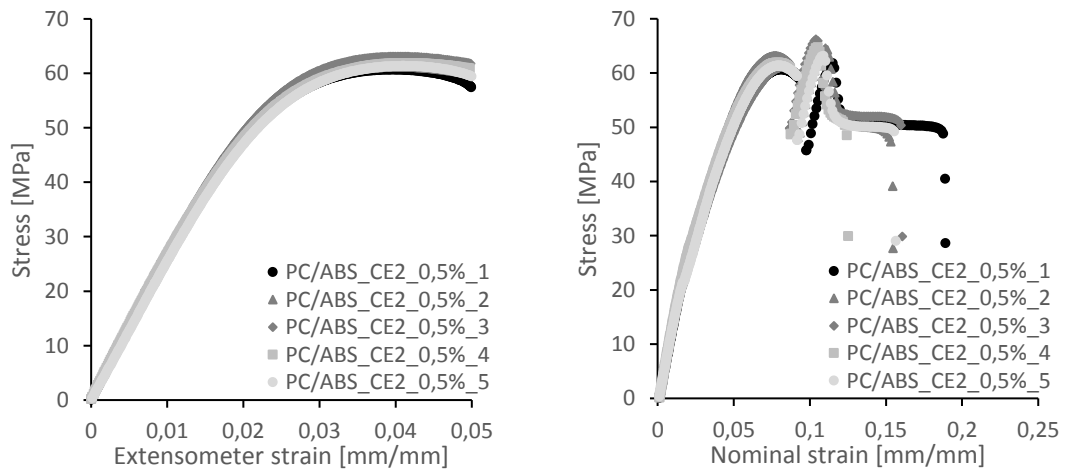


Figure D.34. Stress as a function of extensometer strain (left) and nominal strain (right) for PC/ABS with 0,5 % of CE 2 (Joncryl ADR 4468).

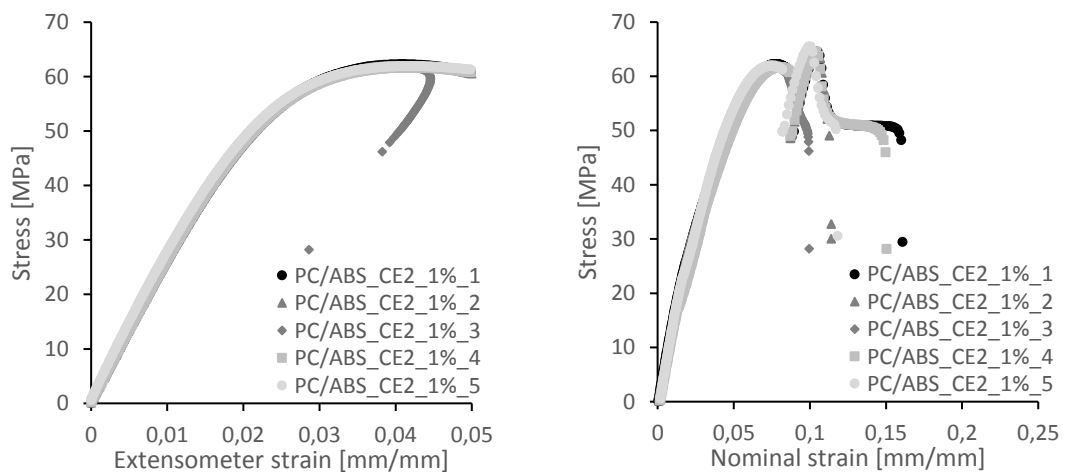


Figure D.35. Stress as a function of extensometer strain (left) and nominal strain (right) for PC/ABS with 1 % of CE 2 (Joncryl ADR 4468).

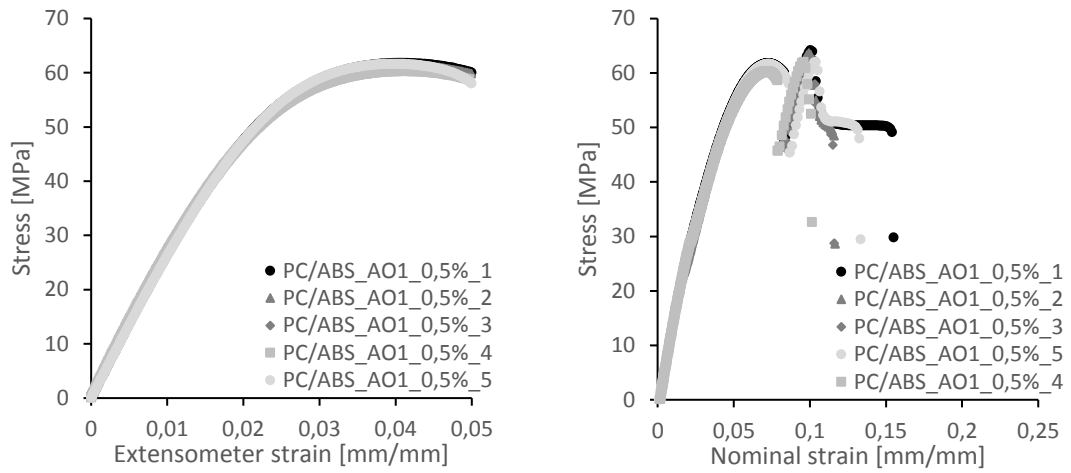


Figure D.36. Stress as a function of extensometer strain (left) and nominal strain (right) for PC/ABS with 0,5 % of AO 1 (Irganox 1010).

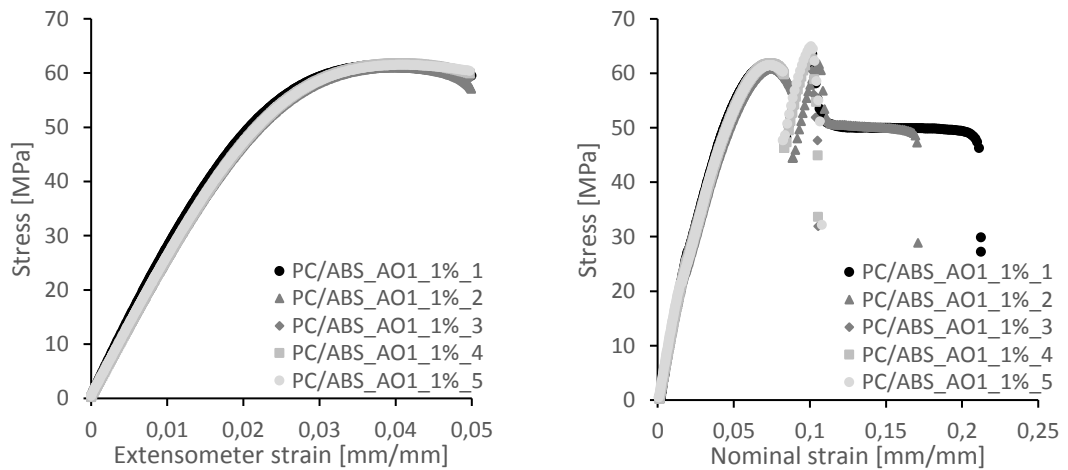


Figure D.37. Stress as a function of extensometer strain (left) and nominal strain (right) for PC/ABS with 1 % of AO 1 (Irganox 1010).

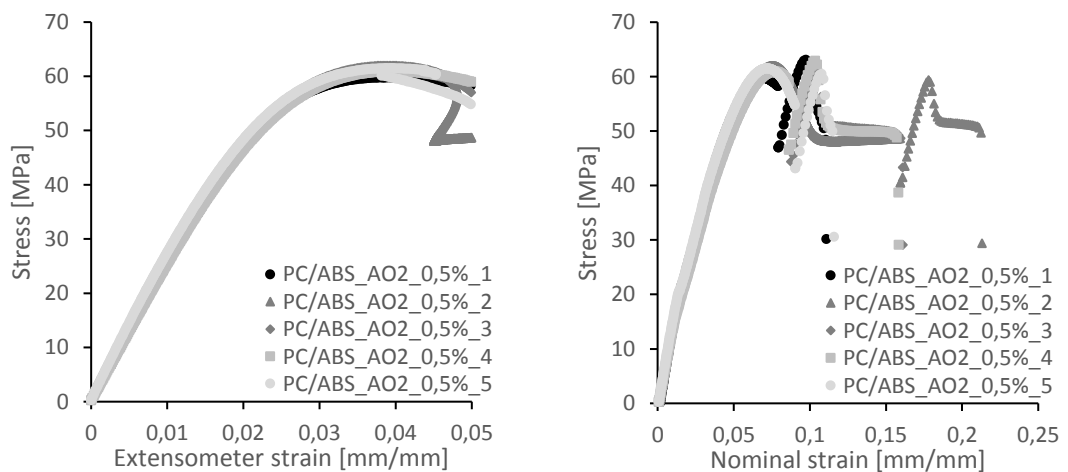


Figure D.38. Stress as a function of extensometer strain (left) and nominal strain (right) for PC/ABS with 0,5 % of AO 2 (Irganox 1076).

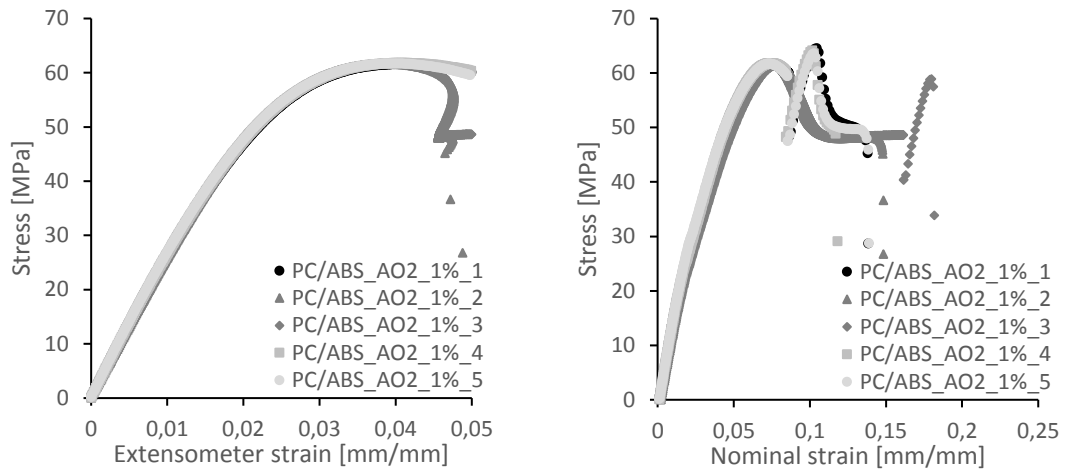


Figure D.39. Stress as a function of extensometer strain (left) and nominal strain (right) for PC/ABS with 1 % of AO 2 (Irganox 1076).

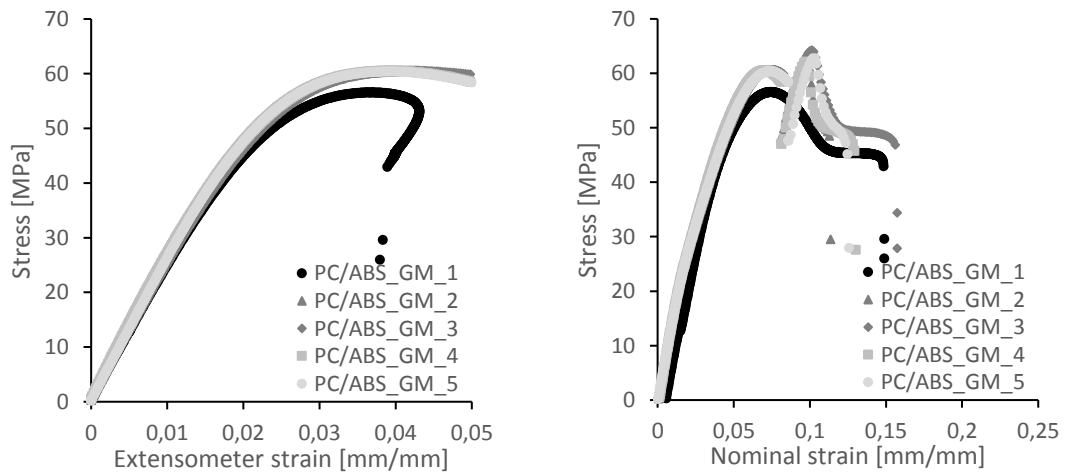


Figure D.40. Stress as a function of extensometer strain (left) and nominal strain (right) for PC/ABS with 0,5 % of GM.

ANNEX E: VIRGIN POLYMERS

Product	Polymer	Applications
Braskem [144]		
EP 440N	PP	Home appliances
SABIC [145]		
Sabic PP 412MN40	PP	Thin wall technical injection moulding articles
Sabic PP 48M10	PP	Components for the electrotechnical industry
Sabic PP 48M40	PP	Components for the electrotechnical industry
Sabic PP 512MN10	PP	Vacuum cleaner housings
Sabic PP 58MNK10	PP	Household applications
Sabic PP PHC28	PP	Electronic equipment
Sabic PP PPA20	PP	Home appliances, houseware
TotalEnergies [146]		
PPC 3650	PP	Technical parts
PPC 4640	PP	Technical parts
PPC 4660	PP	Technical parts
PPC 4663	PP	Technical parts
PPC 5660	PP	Technical parts
PPC 6742	PP	Technical parts
PPC 7712	PP	Technical parts
PPC 7810 B	PP	Technical parts
PPC 7650	PP	Technical parts
PPC 9612	PP	Technical parts
PPC 9760	PP	Technical parts
PPC 9712	PP	Technical parts
8260	PS	Appliances, fridges
3450	PS	Technical parts
6540	PS	Appliances, Housewares, Technical parts
3630	PS	Technical parts
Covestro [147]		
Bayblend FR1514	PC/ABS	Supporting material for energized parts
Bayblend FR1514 BBS073	PC/ABS	Supporting material for energized parts
Bayblend FR3005 HF BBS314	PC/ABS	Components for the electrical/electronics sector
Bayblend M301 FR	PC/ABS	Electrical and electronic devices
Bayblend M303 FR	PC/ABS	Electrical and electronic devices
Makroblend EL703	PC/ABS	Outdoor electrical enclosures
Trinseo [148]		
Emerge PC/ABS 7700	PC/ABS	Electrical housings, consumer electronics, information technology equipment
Emerge PC/ABS 7710 SK	PC/ABS	Consumer electronics, wearable devices
Emerge PC/ABS 7710	PC/ABS	Electrical housings, electrical equipment enclosures
Emerge PC/ABS 7570	PC/ABS	Electrical housing, smartphone/tablet/laptop housing/casing
Emerge PC/ABS 7700 SK	PC/ABS	Consumer electronics, wearable devices

Product	Polymer	Applications
Magnum 8391	ABS	Household appliance
Magnum 3453	ABS	Household appliances, telephones, electrical and computer equipment
Styron 634	PS	Household applications
ELIX Polymers [149]		
5120	PC/ABS	Small household appliances, electrical switches, distribution, power sets
5130	PC/ABS	Coffee machine, electrical switches, distribution boards, power sets
P2H-AT	ABS	Washing machine panel, kitchen & coffee machines, electrical switches
P2M-AT	ABS	Power toolboxes
M203	ABS	Washing machine panel, electrical switches, distribution boards, power sets
118HF	ABS	Housing big parts
M201AS	ABS	Telephones, electronic boards and housings, refrigerator door handles
P3H-AT	ABS	Lawnmowers, dishwasher panel, lids for electrical accumulators and power sets
H605	ABS	Enclosures for electric devices
E310	ABS	Refrigerator panel
E401	ABS	Refrigerator panel
Ineos Styrolution [150]		
Novodur P2H-AT	ABS	Household appliances, oven casings
Novodur P4XF	ABS	Large housings
Novodur E401	ABS	Refrigerator inliner
Novodur P2M-AT	ABS	Household appliances
Novodur P2MC	ABS	Household appliances
Novodur P3H-AT	ABS	Household appliances, washing machines
Novodur H605	ABS	Vacuum cleaner
Novodur H701	ABS	Home appliances, electrical and electronics
Terluran GP-22	ABS	Appliance housings
Terluran GP-35	ABS	Thin wall components for telecommunications
Terluran GP-35 White	ABS	Housings of electronic and entertainment devices, appliance housings
Terluran HI-10	ABS	Appliance housings
Terluran SP-6	ABS	Household appliances
Styrolution PS 165N/L	PS	Transparent parts for refrigerators
Versalis [151]		
F 332	ABS	Small appliances, electrical components
L 322	ABS	Household appliances
SK 112	ABS	Electronics
N 3380	PS	Technical items, refrigerator clear components
N 3560	PS	Injection moulding of domestic appliances, housewares, refrigerators
N 3840	PS	Glossy sheets for fridge applications, housewares

Product	Polymer	Applications
R 321P	PS	Housewares, technical items, refrigerator components
F 332	ABS	Small appliances, electrical components
L 322	ABS	Household appliances
SK 112	ABS	Electronics
Synthos [152]		
Synthos PS GP 152	PS	Drawers for storing vegetables in refrigerators
Synthos PS GP 585A	PS	Drawers for storing vegetables in refrigerators

ANNEX F: RECYCLED POLYMERS

Table F.1. * = The values were read from figures and might not be perfectly accurate. The brackets in the Polymer-cells show the polymer ratio for PC/ABS if it was available. If it was not available, it is shown as (?/?).

Polymer	Modulus (MPa)	Tensile strength (MPa)	Break strain (%)	Standard	Recycled from	Source
PP	-	26,5	-	ASTM	Electrical home appliances	[18]
PP	955,23	23,45	-	ASTM	Electronics waste from computer parts	[6]
PS	2061,2	24,3	27,2	ASTM	Waste keyboards	[16]
ABS	-	20	-	GB	Housing plastics of air conditioner	[7]
ABS	-	42,2	11	ISO	Domestic appliances	[8]
ABS	2400	39,2	12	ISO	Dismantled Volvo 700 series cars	[9]
ABS	-	39	-	GB	Lead-acid battery shells	[10]
ABS	2850 *	41 *	2,5 *	ASTM	Electronic equipment housing	[17]
ABS	2250 *	-	13,5 *	ISO	Computers	[15]
ABS	2110	32,5	7	ISO	Housings	[20]
ABS	2153	31,27	9,38	ASTM	Waste keyboards	[16]
ABS	2591	-	1,68	ISO	WEEE	[19]
PC/ABS (80/20)	2338	57,3	-	ISO	Automotive signal light production waste	[14]
PC/ABS (80/20)	-	59 *	-	GB	Shells of waste electrical appliances	[11]
PC/ABS (70/30)	-	55,1	11	ISO	CDs	[8]
PC/ABS (70/30)	2400	46,1	12	ISO	Dismantled Volvo 700 series cars	[9]
PC/ABS (?/?)	2773,7	50,41	7,16	ASTM	E-waste	[12]
PC/ABS (?/?)	2809,7	53,27	3,996	ASTM	E-waste	[12]
PC/ABS (?/?)	2753,7	48,29	5,85	ASTM	E-waste	[12]
PC/ABS (?/?)	1807	39,1	6,09	ASTM	Electronic waste plastic products	[13]
PC/ABS (?/?)	2400 *	-	21 *	ISO	Computers	[15]
PC/ABS (?/?)	2103	56	16	ISO	Housings	[20]
PC/ABS (?/?)	1830	48	18	ISO	Housings	[20]